FINAL REPORT
FDOT CONTRACT NUMBER: BDV31-977-94

REQUIREMENTS FOR USE OF FIELD-CAST, PROPRIETARY ULTRA-HIGH-PERFORMANCE CONCRETE IN FLORIDA STRUCTURAL APPLICATIONS

Submitted to
Research.Center@dot.state.fl.us
The Florida Department of Transportation Research Center
605 Suwannee Street, MS 30 Tallahassee, FL 32399

c/o Dr. Harvey DeFord, Ph.D.
Structures Materials Research Specialist
State Materials Office

Submitted by:

Dr. Kyle A. Riding (kyle.riding@essie.ufl.edu) (Principal Investigator)
Dr. Christopher C. Ferraro (Co-Principal Investigator)
Dr. H.R. Hamilton (Co-Principal Investigator)
Megan S. Voss
Raid S. Alrashidi

April 2019

Department of Civil Engineering
Engineering School of Sustainable Infrastructure and Environment
College of Engineering
University of Florida
Gainesville, Florida 32611

DISCLAIMER

The opinions, findings, and conclusions expressed in this publication are those of the authors and not necessarily those of the State of Florida Department of Transportation or the U.S. Department of Transportation.

Prepared in cooperation with the State of Florida Department of Transportation and the U.S. Department of Transportation.

APPROXIMATE CONVERSIONS TO SI UNITS (from FHWA)				
Symbol	**When You Know**	**Multiply By**	**To Find**	**Symbol**
Length				
in	inches	25.4	millimeters	mm
ft	feet	0.305	meters	m
yd	yards	0.914	meters	m
mi	miles	1.61	kilometers	km
Area				
in^2	square inches	645.2	square millimeters	mm^2
ft^2	square feet	0.093	square meters	m^2
yd^2	square yard	0.836	square meters	m^2
mi^2	square miles	2.59	square kilometers	km^2
Volume				
fl oz	fluid ounces	29.57	milliliters	mL
gal	gallons	3.785	liters	L
ft^3	cubic feet	0.028	cubic meters	m^3
yd^3	cubic yards	0.765	cubic meters	m^3
NOTE: volumes greater than 1000 L shall be shown in m^3				
Mass				
oz	ounces	28.35	grams	g
lb	pounds	0.454	kilograms	kg
Temperature (exact degrees)				
°F	Fahrenheit	5 (F-32)/9 or (F-32)/1.8	Celsius	°C
Illumination				
fc	foot-candles	10.76	lux	lx
fl	foot-Lamberts	3.426	candela/m^2	cd/m^2
Force and Pressure or Stress				
lbf	pound-force	4.45	newtons	N
lbf/in^2	pound-force per square inch	6.89	kilopascals	kPa

TECHNICAL REPORT DOCUMENTATION PAGE

1. Report No.	2. Government Accession No.	3. Recipient's Catalog No.
4. Title and Subtitle Requirements for Use of Field-Cast, Proprietary Ultra-High-Performance Concrete in Florida Structural Applications		5. Report Date January 2019
		6. Performing Organization Code
7. Author(s) Kyle A. Riding, Christopher C. Ferraro, H. R. Hamilton, Megan S. Voss, Raid S. Alrashidi		8. Performing Organization Report No.
9. Performing Organization Name and Address Department of Civil and Coastal Engineering Engineering School of Sustainable Infrastructure & Environment University of Florida 365 Weil Hall – P.O. Box 116580 Gainesville, FL 32611-6580		10. Work Unit No. 11. Contract or Grant No. BDV31-977-94
12. Sponsoring Agency Name and Address Florida Department of Transportation 605 Suwannee Street, MS 30 Tallahassee, FL 32399		13. Type of Report and Period Covered Final Report 2/18-5/19 14. Sponsoring Agency Code
15. Supplementary Notes None		

16. Abstract

Ultra-high-performance concrete (UHPC) is a groundbreaking cementitious material that has the potential for innovative structural use that makes lighter, more durable, and overall lower cost structures. Very low water-to-cementitious material ratios and high dosages of fibers are used to give UHPC high compressive strength, high tensile strength, and high toughness. Because the high tensile strength and toughness are key benefits of, and reasons to use, UHPC in Florida structures, a method to measure the UHPC tensile stress-strain relationship is needed. A specification for material acceptance and construction using field-cast, proprietary UHPC materials is also needed. Part of this study included a literature review, surveys of departments of transportation, and reviews of UHPC material specifications from other countries to help establish UHPC material and construction requirements for Florida. An experimental program was created to test UHPC flexural and tensile strengths. Based on the survey and experimental results, recommendations were made for a UHPC tensile test method, and material and construction specifications.

17. Keywords.	18. Distribution Statement
Ultra-High-Performance Concrete, Tensile Strength, Field Construction	No restrictions.

19. Security Classif. (of this report)	20. Security Classif. (of this page)	21. Pages	22. Price
Unclassified	Unclassified	194	

ACKNOWLEDGMENTS

The Florida Department of Transportation (FDOT) is acknowledged for funding this project. The assistance of Dr. H. D. DeFord, Jose Armenteros, Ghulam Mujtaba, Ivan Lasa, Patrick Upshaw, Sam Fallaha, Will Potter, and Christina Freeman is gratefully acknowledged.

EXECUTIVE SUMMARY

Background

Ultra-high-performance concrete (UHPC) is an innovative cementitious material that has the potential to considerably increase the durability and resulting service life of Florida structures. Very low water-cementitious material ratios and high dosages of fibers are used to give UHPC high compressive strength, high tensile strength, and high toughness. Because the high tensile strength and toughness are key benefits of, and reasons to use, UHPC in Florida structures, a method to measure the UHPC tensile stress-strain relationship is needed. Use of UHPC in Florida structures is currently limited to field-cast concrete using proprietary UHPC materials. A specification for material acceptance and construction using field-cast, proprietary UHPC materials is also needed.

Research Objectives

The research objective for this project was to make recommendations for (1) a test method to measure UHPC tensile stress-strength relationships, (2) material acceptance, and (3) construction requirements. Discussions with FDOT structures and materials engineers led the research team to prioritize test methods that directly measure the concrete tensile strength relationship from cast prisms instead of sawcut ones.

Main Findings

The main findings from this study are summarized as follows:

- Modifications to a concrete direct-tension test proposed by the Federal Highway Administration have been made that help prevent test failure and account for the effects of fiber alignment in cast samples.
- Responses from 32 states, Washington, D.C., and Ontario, Canada, showed differences in material and construction practices. Reasons for differences were also identified.

Recommendations

A draft Florida Test Method for UHPC direct-tension response was developed and is recommended for adoption. Recommendations for UHPC material and construction specifications have also been made, along with reasoning for each recommended requirement.

Future Work

Work performed under this contract focused on requirements for field use of proprietary UHPC in Florida structures, primarily in bridge joint and repair applications. This work recommends requiring UHPC for these applications to achieve 21,000 psi compressive strength at 28 days. UHPC could be made at lower strengths and be more cost-effective for other applications with excellent performance. Future research should investigate requirements for UHPC made with locally-available materials for different applications such as prestressed concrete members. This should include requirements for mechanical property, durability, and construction requirements for these other applications. This could result in different classes of concrete for different purposes, including different strength and durability classes. This could enable production of value-engineered UHPC for different end uses with significant cost savings over proprietary UHPC materials. Future research should also investigate non-destructive evaluation techniques and other test methods for measuring the quality of UHPC structural members, including fiber dispersion and orientation.

TABLE OF CONTENTS

LIST OF TABLES

LIST OF FIGURES

CHAPTER 1. INTRODUCTION

1.1 Background

Ultra-high-performance concrete (UHPC) is an innovative cementitious material that has the potential to considerably increase the durability and resulting service life of Florida structures. Because UHPC has a very low connected porosity, high compressive and tensile strength, and excellent durability properties, it has many potential uses. It can be used to design more efficient and lighter weight structural elements, reduce or eliminate the need for secondary reinforcing steel, repair existing structures, for harsh environmental exposures, or for structural connections with complicated loads. (Binard 2017).

There are many different definitions worldwide as to what constitutes UHPC; however, they are all based on very high compressive and tensile strength requirements. These high strengths are achieved by (a) use of particle packing theories to optimize space filling by solid materials before hydration begins, (b) very low water-to-cementitious material ratios (w/cm), typically below 0.25, and (c) large volumes of fibers (Le Hoang and Fehling 2017; Graybeal, 2016). Special knowledge, material handling, mixing procedures, and construction practices are required to produce high quality UHPC consistently.

Concrete tensile strength is typically considered zero in conventional reinforced concrete designs. The high tensile strength of UHPC provided by fibers is used to reduce cracking and reduce or eliminate the need for secondary reinforcing steel. In these cases, the concrete tensile strength and ductility are an integral part of the structural design and must be ensured through qualification and quality control testing. In order to protect the public's safety and ensure performance, UHPC tensile stress-strain response must be verified through tests. There are currently no standardized test methods available in the U.S. to measure the stress-strain response of UHPC under tension. Several methods have been proposed to either directly measure the response, or indirectly calculate it from beam-bending tests. Each of these has its own requirements and complications for material pre-qualification and quality control testing.

Several proprietary, commercially-available UHPC materials have successfully been used in precast members and in field-cast members by some U.S. departments of transportation, mostly

on a trial basis (Perry 2015; Wille and Boisvert-Cotulio 2013). The Florida Department of Transportation does not have a specification in place to allow for its use. Industry and government researchers have spent three decades developing proprietary formulations that can reliably provide the properties expected of UHPC, and the construction experience required to successfully place and cure it. Commercially-available, pre-bagged UHPC materials are ideal for field use because of the manufacturers' technical support available and the robust nature of the preblended mixtures. Currently, the high cost of proprietary UHPC and the lack of UHPC specifications severely limit its large-scale use. Utilization in a wider variety of structural products can be encouraged by the development of non-proprietary UHPC that is produced with locally-sourced raw materials to significantly reduce the cost, and by the development of specifications and guidelines to delineate its use.

1.2 Research Objectives

This project has the following research objectives:

- Document the current state-of-the-art on UHPC material, construction, and test requirements through: 1) a comprehensive literature review, 2) a survey of the usage of UHPC by other state and national transportation agencies, and 3) a review of international specifications and technical standards for UHPC.
- Develop a draft Florida Test Method for UHPC tensile testing.
- Develop a draft specification for commercially-available, prepackaged, proprietary UHPC materials.

1.3 Research Approach

In order to accomplish the project objectives, review-based and experimental activities were performed. In order to document the state-of-the-art on UHPC materials and construction, a thorough literature review was conducted. This included review of project reports, journal articles, recent conference papers, and proprietary material data sheets and literature. A comparison of sections of building codes and specifications for UHPC used by other countries was also performed. A survey of departments of transportation was conducted to determine current UHPC use and specification best practices. To develop a draft Florida Test Method for

UHPC tensile strength, a comparison of potential methods was performed at the University of Florida and Florida Department of Transportation (FDOT) State Materials Office (SMO).

CHAPTER 2. LITERATURE REVIEW

2.1 Introduction

Ultra-high-performance concrete (UHPC) is a recent class of concrete that has been developed to provide superior strength, ductility, and durability. UHPC typically contains large volumes of fiber reinforcement to increase the tensile strength and in some cases even provide strain-hardening behavior (Binard 2017). The high compressive and tensile strengths provided by UHPC open up the possibility for new highly-efficient structural shapes (Kim 2016). The durability provided by UHPC allows for it to be used selectively in problem areas such as bridge joints (Russell and Graybeal 2013; Haber et al. 2018).

2.2 UHPC Definition

UHPC is usually defined by a combination of minimum tensile and compressive strengths. Normal strength concrete (NSC) has strength ranging from 3,000-8,000 psi (ACI CT-16 ACI Concrete Terminology 2016), with a tensile strength of roughly 10% of the concrete compressive strength. The tensile strength of normal concrete however is assumed to be zero for most structural calculations. The American Concrete Institute's Building Code Requirements for Structural Concrete limits concrete's tensile strength for an uncracked prestressed section to that of $7.5(f'c)^{0.5}$ where $f'c$ is the concrete's compressive strength at 28 days. Concrete designated to be in a "transition" stage between cracked and uncracked conditions can be assigned a tensile strength of up to $12(f'c)^{0.5}$ (ACI 318-14 2014). These tensile strengths are used generally for serviceability issues and not counted on for carrying loads. In contrast to NSC, the high tensile strength and toughness of UHPC allows the tensile strength to be used in design.

UHPC has been defined differently by many different institutions, as shown in Table 2-1. While the exact threshold is not the same in every case, it is generally agreed that UHPC must have certain compressive and tensile strength requirements, even if they are measured differently.

Table 2-1: UHPC definitions

	Compressive Strength, psi (MPa)	Tensile Strength, psi (MPa)
Federal Highway Administration	21,700 (150)	720 (5)
Portland Cement Association	17,000-22,000 (120-150) (Portland Cement Association 2018)	*Flexural*: 2,200-3,600 (15-25)
American Concrete Institute	22,000 (150)	
American Society for Testing and Materials, C1856	17,000 (120) (ASTM C1856, 2017)	
French	19,000 (130) (AFNOR 2016)	1,200 (8) (Kusumawardaningsih et al. 2015)
Japanese		700 (5) (Kusumawardaningsih et al. 2015)
Swiss (Eugen Brühwiler 2017)	22,000 (150)	1,100 (7.6)
Australia	22,000-32,000 (150-220) (Gowripalan and Gilbert 2000)	
Canadian (CSA A23.3 2018)	17,000 (120) or 22,000 (150)	600 (4) or 700 (5)
Malaysia	Follows French standard	Follows French standard
Colombia (Argos n.d.)	17,000 (120) or 21,000 (150)	800 (5)

2.3 UHPC Mixture Characteristics

Although there are many different UHPC mix designs, they have several things in common. First, the maximum size of the aggregates is typically limited to about 3 mm or less. UHPC is often, though not always, made without any coarse aggregate. It often contains large quantities of silica fume, and in some cases quartz flour, in order to fill very small voids. Particle packing theory is used to ensure that a concrete with the lowest volume of voids possible is produced (Graybeal and Leonard 2017). The lack of coarse aggregate also contributes to the high strength because concrete gains strength as the maximum aggregate size decreases (Albarwary et al. 2017). In normal concrete, the weakest region of the material is the interfacial transition zone between aggregates

and paste. Due to the typical gap-graded aggregate distribution, the smaller aggregate particles and fine aggregate particles that are in contact with or close to a significantly larger aggregate particle cannot pack as densely as in the regions away from the larger particles (wall effect). This results in a higher paste content in the interfacial region, and, therefore, a higher water content. The water is consumed during hydration, producing an interfacial region with higher porosity and, consequently, lower strength. UHPC has a more continuous particle size distribution which essentially eliminates the wall effect, and particle packing density is very high relative to normal concrete. (Albarwary et al. 2017).

UHPC mixes also have a very low water-to-cementitious material ratio (w/cm) when compared to normal concrete in order to give very high strengths. Compressive strength for a given cement composition is known to be a function of the gel-space ratio, as shown in Equation 2-1 (Pichler et al. 2013; Powers 1958):

$$f_c = \beta \gamma^{\alpha} \qquad \text{Equation 2-1}$$

Where: f_c is the compressive strength in psi

β is the intrinsic strength of the gel in psi

α is a coefficient

γ is the ratio of the volume of solid products or gel to the space available for those hydration products

The gel-space ratio and, consequently, the potential strength that can be achieved are dependent on the degree of hydration of the cementitious materials and the initial amount of space not filled by solid material. Very-low w/cm is required to achieve the low gel-space ratio needed for UHPC (Pichler et al. 2013). Typical w/cm used to make UHPC are between 0.17 and 0.25 (Binard 2017). To compensate for the lack of water that can give the mix workability, large quantities of high-range water-reducing (HRWR) admixtures are used to make the concrete flow. This high amount of HRWR, along with the small average aggregate size, make the mix behave as a self-

consolidating concrete, meaning it will have a high spread value and will flow to fill the formwork into which it is placed.

When compared to normal concrete, UHPC also has an increased amount of cementitious material, often containing more cementitious material than aggregate by weight (Haber et al. 2018). Part of this increase is required because the smaller particles in the mix have a larger surface area that the paste must cover. The large amount of cementitious materials is used to obtain optimum particle packing (Haber et al. 2018). Space filled by solid material is space that does not need to be filled by water during mixing. Even with the large quantities of HRWR used in concrete, a minimum amount of water is still required to separate particles a small amount to make the concrete flow during placement. A high paste content is then needed at a low w/cm to provide the minimum amount of paste needed for flowability.

The final major UHPC mixture design component is a large volume of fibers. These fibers help to give the concrete a high tensile strength. When small cracks form in the concrete, the steel fibers can bridge the gaps and hold the concrete together. This helps the UHPC retain its strength even after it has been deformed, making it more ductile than conventional concrete. The presence of fibers also makes it possible to design UHPC with strain-hardening behaviors (Russell and Graybeal 2013). This occurs if the UHPC member has the ability to gain strength once the concrete has cracked. This happens because the strength contribution of high-strength steel fibers to the section would only occur once the fibers are placed in tension.

In addition to increased tensile and compressive strength, UHPC also offers benefits in terms of durability. The high cement content, low w/cm ratio, and well-compacted particles make UHPC almost impervious to water, and therefore, chlorides or other chemical contaminants. While there may be some voids present in the concrete, there are not enough to form a connected network, giving UHPC its impenetrability (Haber et al. 2018). In addition, the steel fibers can limit crack propagation, resulting in many small, well-distributed cracks instead of few large cracks (Rapoport et al. 2002). This limiting of crack depth helps to retain most of the concrete's impenetrability after cracking (Rapoport et al. 2002) but prior to excessive strain or failure.

2.4 Particle Packing Theory

2.4.1 Mathematical Models

In order to achieve a low w/cm, particle packing theory is used to maximize the initial amount of volume filled by solid material. This method uses information about the size distribution of particles in a granular mix to predict the packing density (de Larrard 1999). Packing density is defined as the ratio of the solid volume to the total volume in a mixture, as shown in Equation 2-2 (de Larrard 1999).

$$\phi = \frac{V_{solids}}{V_{total}} \qquad \text{Equation 2-2}$$

Where: ϕ is the packing density

V_{solids} is the volume of solids

V_{total} is the total volume

Many methods and equations have been proposed to maximize the particle packing density. Maximization of Φ is important because it corresponds to a decrease in voids. With fewer voids, the concrete is more durable and less cement is required. In addition, concrete with more efficiently-packed particles is more workable because there is more paste available to separate particles instead of having to fill space left vacant.

In order to maximize the packing density, particle interaction must be taken into account. If only one size of particles is used, the interaction between particles is consistent and predictable, and the packing density can be easily estimated. However, when different-sized particles are mixed together, their interaction can change. For example, if a coarse gravel and a fine sand are combined, the particle sizes would be different enough that they would be considered to have no interaction, such as shown in **Error! Reference source not found.**(a) and (b). The sand could fill the gaps in the gravel easily, without affecting the existing arrangement of the gravel. If the coarse gravel was mixed with a second gravel, however, the second gravel may be too large to fill existing gaps, which could result in a loosening effect as shown in **Error! Reference source not found.**(c). An important condition, called the wall effect, occurs in the interfacial region of large particles surrounded by smaller particles. The rigid surfaces of the large particles prevent the close packing

of surrounding small particles, resulting in higher void contents (**Error! Reference source not found.** (d)). The surfaces of the large particles are barriers (walls) that prevent optimum intermeshing of the smaller particles, reducing the particle packing density (de Larrard 1999).

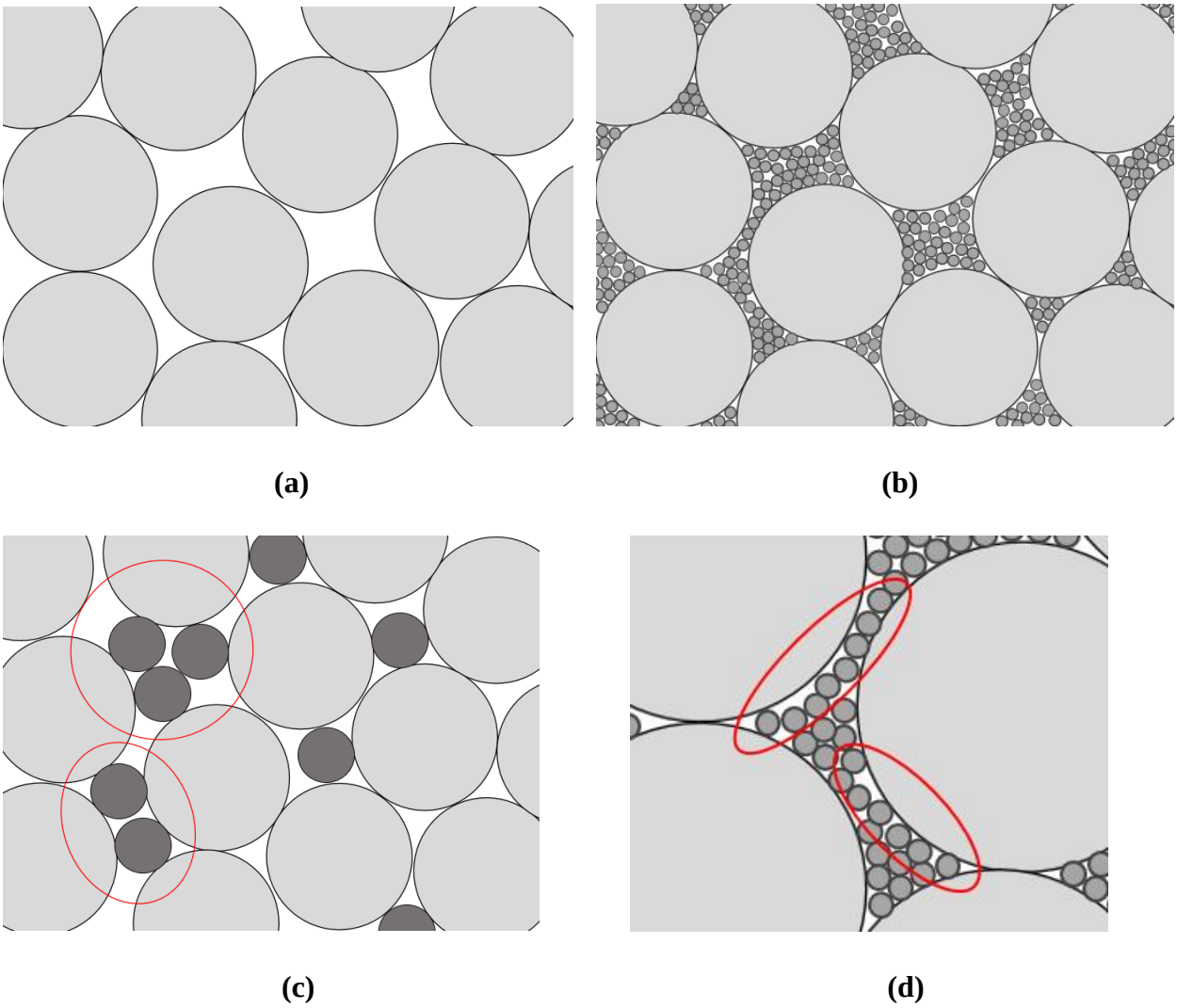

Figure 2-1: (a) Schematic of uniform particle distribution packing (b) Particle packing with particles sized d1 ≫ d2, resulting in negligible interaction between particles (c) Loosening effect (d) wall effect

One simplified mathematical approach to particle packing modeling is based on the principle of spacing average particle sizes far enough apart so no interaction exists (also called gap grading). This method is called the Apollonian model. A ratio λ is used to determine the ideal particle sizes to include in the mixture. Each particle size is multiplied by λ to find a new particle size that is

small enough so that there is relatively no interaction between particles. Theoretically, the size of the largest particles can be multiplied by λ numerous times, and the overall packing density will continue to increase with each added smaller particle size. Figure 2-2 shows how particle packing increases with each added grain size. D_1 is the size of the largest grains and D_3 is the size of the smallest. D_3 would have a size of $D_1\lambda^2$, and D_2 would have a size of $D_1\lambda$.

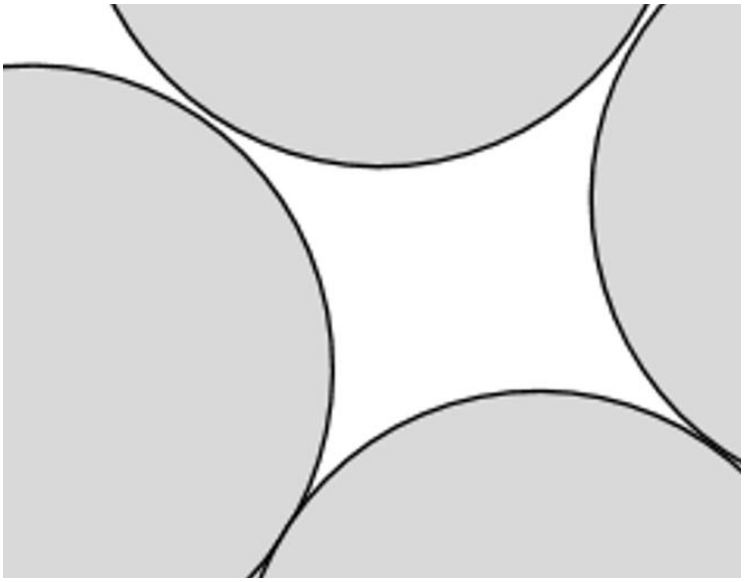

(a)

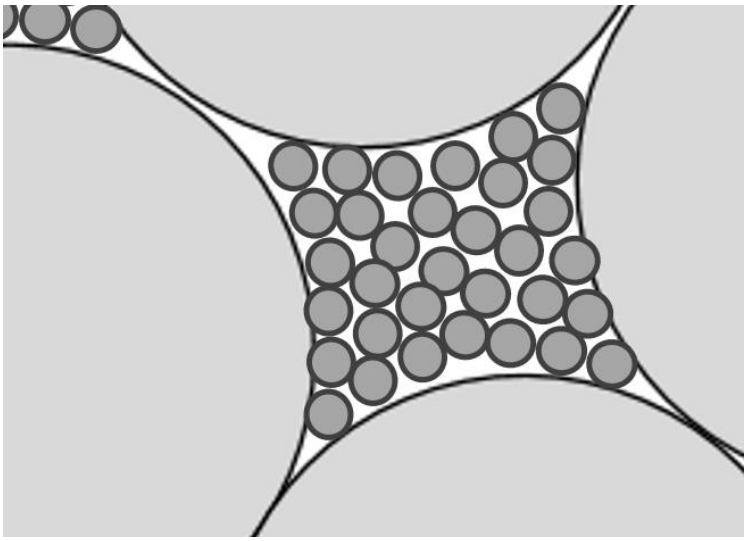

(b)

Figure 2-2: Apollonian particle packing (a) One grain size (b) Two polydisperse grain sizes (c) Three polydisperse grain sizes

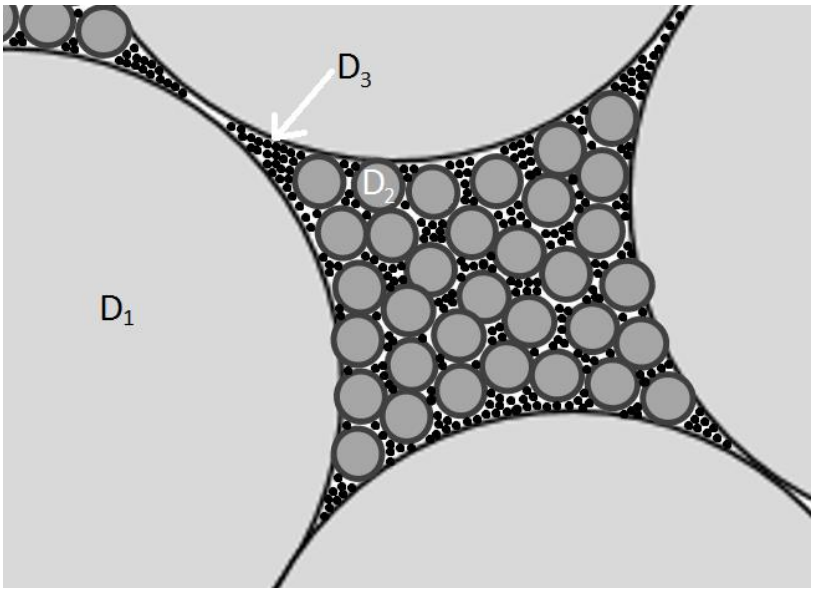

(c)

Figure 2-3: Apollonian particle packing (a) One grain size (b) Two polydisperse grain sizes (c) Three polydisperse grain sizes

There is always *some* interaction between particles, so as λ decreases, the packing density of the mixture improves. Therefore, there is no ideal value for λ. For example, de Larrard tested 6 different values ranging from 0.001 to 0.625, and the results steadily improved as the ratio decreased (de Larrard 1999). While this method provides a very simple way to design a well-packed mixture, it would be impractical to use in design because it assumes all particles are the same shape (de Larrard 1999).

Most particle packing methods used today utilize a particle size distribution, which is shown with an equation instead of a set of distinct particle sizes and quantities. The Andreasen and Andersen method is a very simple example of a distribution relationship between particle size and the percentage of particles finer in a mix. Their method is shown below in Equation 2-3 (Brouwers and Radix 2005):

$$P(D) = \frac{D^q}{D_{max}^q}$$ Equation 2-3

Where: D is the particle size

$P(D)$ is the percent finer than D

D_{max} is the maximum aggregate size used in the mix

q is the distribution modulus, which is a number between 0 and 1

Andreasen and Andersen determined that the ideal distribution modulus was between 0.33 and 0.50. They obtained a specific value of 0.37, but others have found different optimum distribution moduli. For example, Fuller determined 0.5 to be optimal (de Larrard 1999). Asphalt mixtures typically use 0.45. One factor known to affect the optimal value of q is the amount of fines present in a mix. This shows a shortcoming in the Andreasen and Andersen model, as it does not account for the lower limit of the particle diameters. Instead, it mathematically assumes an infinite continuation to smaller diameters, although eventually the percent passing would become negligible.

To account for the lower limit of particle diameters in a mix, Funk and Dinger developed Equation 2-4 (Funk and Dinger 2013):

$$P(D) = \frac{D^q - D_{min}^q}{D_{max}^q - D_{min}^q}$$ Equation 2-4

Where: D_{min} is the minimum aggregate size used in the mix

A general trend for both equations is that for mixtures with more fines, a lower q value gives a higher packing density. Because of this, guides for designing self-consolidating concrete (SCC) will often recommend an even lower number because of the relatively small particle sizes used in these concretes. For example, Brouwers used 0.28 (Brouwers 2006), and Hunger recommended a value between 0.21 and 0.25 (Wang et al. 2014). The disadvantage of a distribution modulus being too high is that there may be segregation in the mix, while a modulus that is too low can cause too much cohesion (Wang et al. 2014). Determining the best q value for a mixture may require time-consuming testing or modeling, but once it is determined, it can be applied across similar mixes.

One key factor not taken into account by the previously discussed methods is that particles have different shapes and adhesion properties (Hoang, Hadl, and Tue 2016). For example, a smooth, spherical particle of silica fume would have much different packing behavior than a rough, angular particle of metakaolin. Equation 2-3 and Equation 2-4 only take into account particle size; therefore, discrepancies between predicted and actual packing can occur.

A few models developed by de Larrard and Sedran include functions and coefficients to account for differences in particles other than a simple diameter. Unlike the simplified models in Equation 2-3 and Equation 2-4, which assume all particles of the same diameter pack in the same way, the Linear Packing Density Model (LPDM) takes into account the actual packing density of each size class. Therefore, if there are many different materials or particle shapes for a given particle diameter, the LPDM will be adjusted accordingly. The LPDM also takes into account loosening effects and wall effects caused by the interaction between differently-sized particles. It is based on Mooney's suspension viscosity model, which assumes non-reactive particles. Mooney's model describes the relationship between the solid content of a monodisperse suspension ϕ and its relative viscosity η_r as presented in Equation 2-5 (de Larrard and Sedran 1994).

$$\eta_r = \exp\left(\frac{2.5}{\frac{1}{\phi} - \frac{1}{\beta}}\right) \qquad \text{Equation 2-5}$$

Where: β is the maximum packing density

ϕ is the random packing density

One disadvantage of the Linear Packing Density Model is that it calculates only linear relationships between particle distributions and packing density, when actual relationships are curved (de Larrard and Sedran 1994). The equations for the linear packing density model, as defined by de Larrard and Sedran, are shown in Equation 2-6 -Equation 2-9:

$c = min(c(t))$ for $y(t)>0$ with

$$c(t) = \frac{\alpha(t)}{1 - \int_d^t y(x) * f\left(\frac{x}{t}\right) dx - \left(1 - \alpha(t)\right) * \int_t^D y(x) * g\left(\frac{t}{x}\right) dx} \quad \text{Equation 2-6}$$

$$f(z) = 0.7 * (1 - z) + 0.3(1 - z)^{12} \quad \text{Equation 2-7}$$

$$g(z) = (1 - z)^{1.3} \quad \text{Equation 2-8}$$

$$\int_d^D y(x)dt = 1 \quad \text{Equation 2-9}$$

Where: c is the packing density

t is the grain size

$y(t)$ = the voluminal size distribution of the grain mixture (having a unit integral as shown in Equation 2-9)

d is the minimum grain size

D is the maximum grain size

$\alpha(t)$ is the specific packing density of the t-class

$f(z)$ is the loosening effect function

$g(z)$ is the wall effect function

Adjustments to the LPDM were made to account for the non-linear relationships between particle distributions and packing density. This model, also developed by de Larrard and Sedran, is called the Solid Suspension Model (SSM). While more complex, it has proven to be much more accurate in predicting packing density near the peak packing density region (de Larrard and Sedran 1994),

which is the most important part of the curve to a researcher. Equations for the SSM are presented in Equation 2-10-Equation 2-14:

$$\eta_r^{ref} = exp\left[\int_d^D \frac{2.5y(t)}{\frac{1}{c}-\frac{1}{c(t)}}dt\right] \quad \text{Equation 2-10}$$

$$c(t) = \frac{\beta(t)}{1-\int_d^t y(x) * f\left(\frac{x}{t}\right)dx - \left(1-\beta(t)\right) * \int_t^D y(x) * g\left(\frac{t}{x}\right)dx} \quad \text{Equation 2-11}$$

$$\eta_r^{ref} = \exp\left(\frac{2.5}{\frac{1}{\alpha(t)}-\frac{1}{\beta(t)}}\right) \qquad for\ d \le t \le D \quad \text{Equation 2-12}$$

$$\sum_{i=1}^{N} y_i(t) = 1 \quad \text{Equation 2-13}$$

$$\frac{1}{\beta(t)} = \sum_{i=1}^{N} \frac{y_i(t)}{\beta_i(t)} \quad \text{Equation 2-14}$$

Where: $\beta(t)$ is the virtual specific packing density of t-sized grains

$\alpha(t)$ is the experimental specific packing density

η_r^{ref} is η_r with β=0.74 and ϕ=0.64 with Mooney's model

N is the number of different types of grains

$y_i(t)$ is the partial volume for grain type i

Mooney's model from Equation 2-5 and the associated variables also apply. Figure 2-3 shows the relative shapes of the LPDM compared with the SSM.

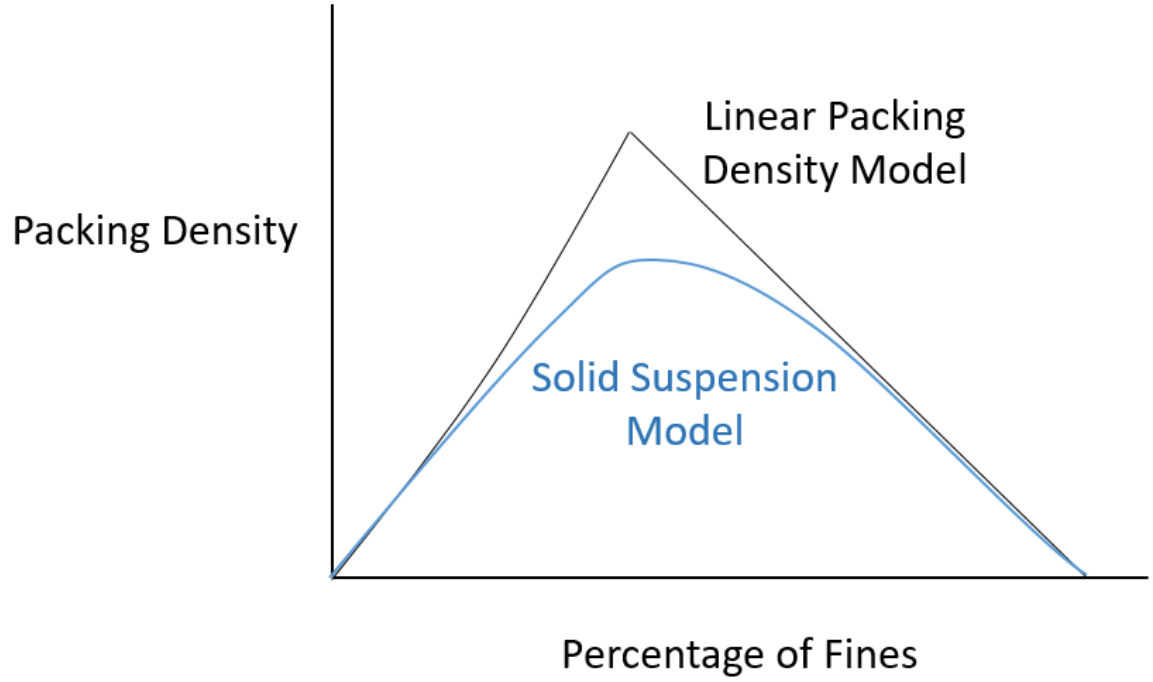

Figure 2-4: Linear Packing Density Model compared with Solid Suspension Model

The Compressive Packing Model (CPM) is like the LPDM and the SSM, but it takes into account compaction energy. Compaction energy is a function of the placing process. For example, vibration or hitting the sample with a mallet adds compaction energy to placed concrete. This stems from the observation that while particles may have a maximum density, they do not naturally orient themselves into the orderly arrangement necessary to produce this maximum density. Instead, particles have a more random orientation. This is the actual packing density, and it is lower than the maximum packing density. Therefore, a compaction index, *K* is defined to describe how close the actual packing density is to the ideal value. *K* can therefore be adjusted by the placing process (de Larrard and Sedran 2002). Equation 2-15 shows how *K* is calculated. The value for *K* would be multiplied by the ideal packing value, as obtained from a particle packing equation, to get a better prediction of the actual packing density. Equation 2-15 and Figure 2-4 show how an increase in *K* can improve packing density.

$$K = \sum_{i=1}^{n} \frac{\frac{\Phi_i}{\Phi_i^*}}{\frac{\Phi_i}{1-\Phi_i^*}}$$ Equation 2-15

Where: K is the compaction index

i denotes each class of grains in the mix

ϕ_i is the actual volume of i grains in the mix

ϕ_i^* is the maximal value of ϕ_i, if the mix was packed with an excess of i grains

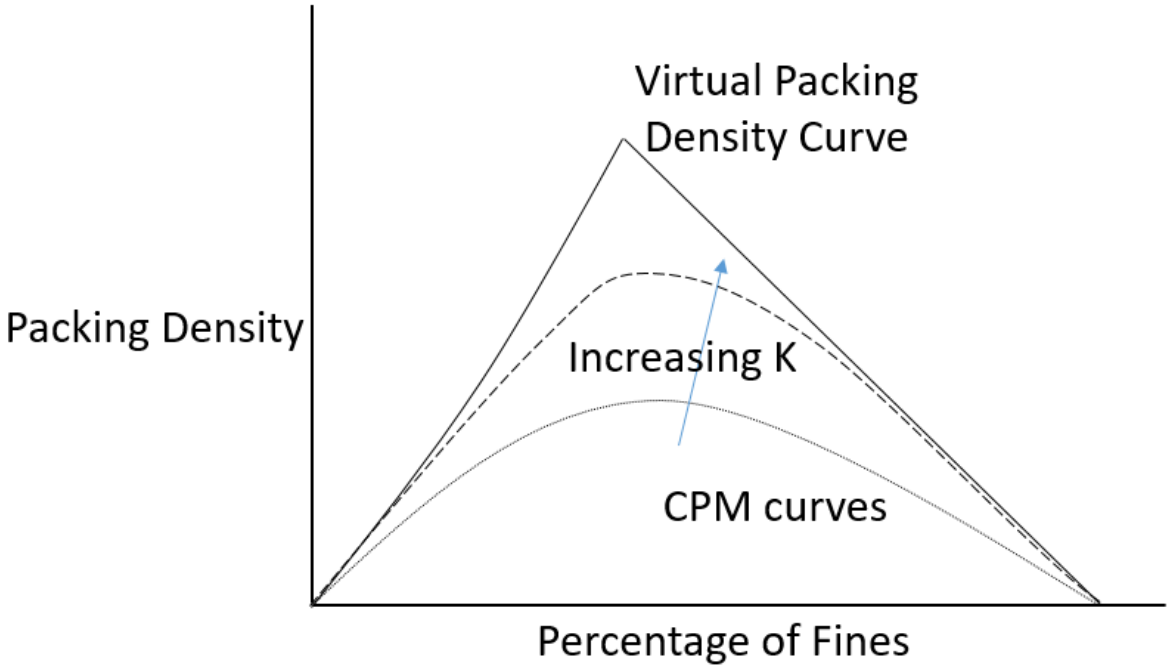

Figure 2-5: Effect of increased *K* on packing density curve with Compressive Packing Model (CPM) (De Larrard 1999)

2.4.2 ***Computer Methods***

Computer programs that simulate particle packing have been developed to allow for more complexity than can be reasonably taken into account with analytical models. While the results of these programs are not as precise as results obtained from actual tests, most computer programs will have the capacity to account for many different materials and particle sizes. In addition, the

software can easily give multiple results very quickly, where laboratory tests would be time consuming. The computer programs can calculate the void ratio of a mixture of particles so that the densest possible mix can be designed (Pade et al. 2009). Some examples of available software include MixSim, Europack (Jones et al. 2002), and 4C-Packing. The Europack program uses a database containing grain density, characteristic diameter, and an eigen-packing factor, which can be determined experimentally. The eigen-packing factor is a value from zero to one, and it is equal to the percentage of space that will be filled with particles after compaction (Pade et al. 2009). The eigen-packing factor takes into account particle characteristics, such as particle shape, that have a large influence on packing density, but have no other way to be quantified. Eigen-packing values can be easily determined by filling and compacting a sample of the particles into a container. The mass and volume of the filled container, as well as the density of the particles is measured, and the Eigen-packing factor is determined by Equation 2-16.

$$Eigenpacking = (m_1 - m_2) / (\pi (D/2)^2 h \rho) \quad \text{Equation 2-16}$$

Where: m_1 is the mass of the container with the materials

m_2 is the mass of the empty container

D is the diameter of the container

h is the height of the container

ρ is the density of the material

A downside of using an eigen-packing factor is that the method of determining the factor has a large influence on the value (Pade et al. 2009). For example, a laboratory that uses a drop table to compact a sample will have different results than a laboratory that uses vibration or rodding for the same material. There is no standard method for determining an aggregate's eigen-packing; therefore, eigen-packing factors must only be compared with factors obtained from performing the same test (Pade et al. 2009).

The Europack program was designed for normal concrete and only works for up to three components, but it can calculate packing density. This can be used to determine the minimum cement content needed (Brandt 2014). 4C Packing uses a linear packing model. Its inputs include

a grain size distribution curve, density, and eigen-packing value for each aggregate type. The model takes the loosening effect and the wall effect into account. With this information, 4C Packing can calculate packing density for given aggregate proportions, give the best proportions for a set of aggregates, or give recommended proportions to target a desired grain size distribution curve (da Silva and Ricardo n.d.). Arora et al. used a MATLAB code that virtually packed particles, starting with the largest. It could then give density values as well as information on the average spacing between particles and the average number of particles that make contact with each particle. Once particle distribution values were known for the paste materials such as cement, fly ash, slag, metakaolin, and limestone powders, many different combinations of the constituents could be tested by the MATLAB program quickly in order to select the best ones for experimental research (Arora et al. 2018).

2.4.3 ***Practical Applications***

An experimental approach can also be used to determine particle packing density instead of a mathematical model. One example is a power consumption method, which tracks the change in power consumption of a mixer set to a specific mixing speed as liquid is added to a particle mixture. As a dry mixture, a relatively low amount of energy is needed to mix the particles. As liquid is added, the surface tension created will cause an increase in power consumption from the mixer. Once the mixture is saturated (all particle voids are filled with water), the power required to mix will drop considerably. The amount of water added at this point can then be recorded. Mixtures with better packing densities will have fewer voids, therefore; this drop in energy will occur at a lower liquid amount (Hoang et al. 2016). Therefore, the optimal mix can be determined by finding the mix that requires the least amount of water to be added until power consumption drops. When applied to UHPC, the power consumption method has an advantage because it does not require any particle sizes to be determined, which can be difficult to do for fine powders. There is also no need to account for particle interactions, absorptions, or other issues by adding complications and factors to an equation because this method holistically takes these factors into account. Theoretically, fibers and admixtures could be included in this test to account for any effects they would contribute. A disadvantage may be that it is difficult to predict the behavior of an adjusted mix without running a new test.

Laskar proposed a method by which to design a high performance concrete mixture with good particle packing and characteristics (Laskar 2011). Based on the observation that concrete rheological properties are related to compressive strength, the test method begins with workability testing of trial batches. Batches that satisfy the workability criterion are then used to make samples for compressive strength testing. The suggested dose of superplasticizer is 1.5%, with a sand content of 30-40%. Based on the desired strength and the ratio of aggregate-to-paste volume in the mix, a w/cm can be determined using an empirical figure presented by Laskar (Laskar 2011). Because this method was designed for HPC and not UHPC, the w/c values range between 0.30-0.40, but a similar relationship for lower w/c values could be made. Laskar also includes provisions for determination of coarse aggregate content, but this would not apply to UHPC mixtures. Finally, the cement content of the mix is determined after all other parameters have been decided (Laskar 2011).

2.5 Mixture Components

2.5.1 ***Binder and Filler Materials***

UHPC mixtures achieve optimal particle packing by using a combination of very fine powders. One way to obtain smaller particles in the mixture is to control the size of the cement grains. Superfine cement is normal cement clinker pulverized with a ball mill, which can be used in UHPC instead of silica fume to help with particle packing. Xiao et al. tested UHPC with superfine cement and achieved strengths of around 150 MPa, but none of the mixes were compared to a mix with silica fume (Xiao et al. 2014). A low calcium aluminate content is desirable for cements in UHPC because calcium aluminate reacts quickly with water, increasing the water demand. For this reason, white cements or oil well cements are often used, but they are more expensive (Wille and Boisvert-Cotulio 2015).

Silica fume is the most common of these filler materials, and it is often used in UHPC mixes as 10-25% of the total cementitious materials by mass. Silica fume with a low carbon content is preferred for use in UHPC because the lower carbon content gives a lower water demand (Wille and Boisvert-Cotulio 2015). One problem with silica fume is that it can be expensive or scarce in certain markets (Xiao et al. 2014). For this reason, researchers have sought out alternatives that

can still achieve a high packing density without compromising strength, workability, or other important characteristics.

Metakaolin can also be used in place of silica fume to act as a filler material for small voids. Staquet and Espion found that UHPC with metakaolin instead of silica fume showed lower amounts of autogenous shrinkage when cured without heat treatment (Staquet and Espion 2004). Li reported that metakaolin can reduce mix workability and require longer mixing times. However, it does tend to speed up the hydration process to give lower initial and final set times. Rougeau and Borys tested many different filler materials, including limestone and siliceous microfillers, metakaolin, pulverized fly ash, and micronized phonolite (Li 2015). They concluded that all tested materials except for the pulverized fly ash could be used to create a concrete with a strength above 150 MPa. Of the alternative fillers, siliceous microfillers achieved the highest compressive strengths, but silica fume mix was stronger than all the other alternatives. Rougeau and Borys also found that ultrafine limestone can produce a white tint in the concrete (Rougeau and Borys 2004). This may be an aesthetic advantage because UHPC containing silica fume is usually very dark.

Replacing some of the cement used in UHPC with slag and/or fly ash can help increase strength (Xiao et al. 2014). Li concluded that a fly ash dosage between 10-25% was optimal (Li 2015). During mixing, fly ash can help with cement dispersion because of the particle size and spherical particle shape. While fly ash increases compressive strength in older concrete, it has a detrimental effect on early age strength. With regards to durability, fly ash reduced drying shrinkage and improved resistance to sulfate attack (Li 2015). Slag used in UHPC has been shown to improve both the compressive and flexural behavior of UHPC. It also improves resistance to ASR damage, chlorides, and sulfates (Eide and Hisdal 2012).

*2.5.2 **Chemical Admixtures***

Polycarboxylate ether-based superplasticizers are used to make UHPC because of their superior water-reducing abilities (Li et al. 2017) and linear dosage-retardation response. They are available in both powder and liquid suspension forms.

There are many different types of superplasticizers available, and while one may perform the best in creating a workable mix with a low w/cm, there may be side effects such as reduced early strength. Coppola et al. tested three different types of superplasticizer: acrylic polymer,

naphthalene, and melamine. They found that the acrylic polymer performed best with respect to lowering the required w/cm and 3-day compressive strength, but it was the worst performer in a 1-day compressive strength test (Coppola et al. 1997).

Often, the optimal mix involves using a combination of admixtures. UHPC mixtures typically have high volumes of silica fume, which is comprised of molecules with a large surface area that are difficult to disperse. Cement and silica fume often react differently to a given superplasticizer. Plank et al. tested methacrylate and allyl ether-based polycarboxylate ether-based superplasticizers (PCE) (Plank et al. 2009). They found that a 3:1 blend of methacrylate-based to allyl ether-based performed better than either of the two by themselves. This is because silica fume was affected more by allyl ether-based PCE, whereas the methacrylate-based PCE was shown to perform better with cement. In addition, Plank et al. used a sodium gluconate in conjunction with a PCE, which reduced the amount of PCE required. Sodium gluconate adsorbs well on to cement, so it was very successful in combination with allyl ether-based PCE, which works better with silica fume. By using these combinations of superplasticizers, the overall dosages could be reduced without compromising the workability of the mix (Plank et al. 2009).

Some chemical admixtures have shrinkage-reducing capabilities. A glycol-based agent used with a superplasticizer was tested by Sugamata et al. and was shown to reduce autogenous shrinkage strain by 15-30% and strain from drying shrinkage by 3-25% (Sugamata et al. 2006). Downsides included an increased dosage of superplasticizer required to achieve the same flow, an increase in set time, and a slight decrease in compressive strength (Sugamata et al. 2006). In order to reduce the set time required, accelerators can be used in conjunction with superplasticizers. Li (2015) studied the effect of shrinkage reducing admixture (SRA) and accelerator on the characteristics of UHPC. His results are shown in Table 2-2 (Li 2015). Percentages given for admixtures are the solid content dosages with respect to weight of cementitious material. The SRA was very effective at reducing the shrinkage, and while early strength was severely impacted, the 28-day strength was not affected. Using accelerator in conjunction with SRA reduced SRA's effect on one-day strength, but it was still significantly lower than the control mix. The drawbacks of using accelerator are the decrease in mix workability and the decrease in compressive strength.

Table 2-2: Effect of accelerator and SRA on UHPC properties (Li 2015)

	Workability	1-Day Compressive Strength	28-Day Compressive Strength	Shrinkage
Accelerator, 2%	-16%	5%	-11%	-3%
Liquid SRA, 2%	5%	-91%	-2%	-43%
Both, 2% each	-8%	-42%	-11%	-46%

Superplasticizer dosage is an important parameter to control, as a slight change can cause a large difference in mixture behavior. Li et al. (Li et al. 2016) studied four different liquid superplasticizers at different dosages and measured set time and flow diameter accordingly. Dosage was defined as a percentage of dry matter by weight of powder (Li et al. 2016). This is an important distinction because different superplasticizers may have different solids contents, making them difficult to compare side by side without normalization. With each superplasticizer tested, both the initial and final time of set increased with an increased superplasticizer dosage. In addition, flow diameter of paste increased with a larger dosage, as expected. However, the flow tended to plateau at a dosage of between 0.8%-1.2%, and in some cases, it declined between 1.6% and 2.0%. Flow diameter of UHPC was also tested at dosages of 1.0%-3.0%. Unlike the behavior for paste, flow diameter never decreased at high dosages. However, most superplasticizers still exhibited a plateau behavior at a dosage of 1.8-2.2% (Li et al. 2016). This occurs because once all the superplasticizer added has been adsorbed by the cementitious material, adding extra will no longer enhance workability properties.

Because superplasticizer can often entrain large air bubbles in the concrete mixture, a defoaming agent is sometimes used when mixing UHPC. Adding a defoaming agent at a rate of 4-6% of the superplasticizer content increased strength and greatly reduced the void ratio (Xiao et al. 2014). A mix design known as K-UHPC developed at the Korean Institute for Civil Engineering and Building Technology uses a defoaming agent at a dosage of roughly 3% of the superplasticizer content by weight ($1lb/yd^3$). It has been used in Iowa in the Hawkeye bridge. (Kim 2016)

Viscosity modifying admixture (VMA) has been used in UHPC (Haber et al. 2018). VMA was shown to decrease segregation in UHPC due to vibration for macrofibers (Ferrara and Meda 2006).

Conversely, it causes a decrease in workability (Li 2015). This relationship is intuitive as a higher viscosity material would not flow as easily as a less viscous one. In addition, VMA was also shown to reduce compressive strengths significantly, being 20% lower than mixes without VMA (Li 2015).

*2.5.3 **Fibers***

Fibers are important to the properties and behavior of UHPC because they can provide tensile strength, resistance to crack propagation, and strain hardening properties. However, the fiber type, amount, shape, size, and orientation play a critical role in obtaining high tensile strength and even strain-hardening behavior.

Many different materials have been used to create fibers for use in concrete. Among these are steel, plastic polypropylene (Topçu and Canbaz 2007), basalt, polyvinyl alcohol, glass, and carbon (Sim et al. 2005). Steel is the predominant fiber choice for UHPC applications. This is due to its high modulus of elasticity, strength, and ductility. It is also more durable in an alkaline environment like concrete than fibers made of plastic or glass (Eide and Hisdal 2012). Steel fibers used in UHPC typically have strengths of 300 ksi (2070 MPa) to 400 ksi (2,760 MPa) (Binard 2017). Steel fibers for UHPC are fabricated by drawing them to very thin diameters. In order to reduce the friction during the drawing process, they are often coated with brass. The brass coating often wears off in the mixer (Binard 2017).

In Canada, a small percentage by volume (0.2-0.3%) of polypropylene fibers is required for concrete exposed to fire (CSA A23.3 2018). This is because these fibers provide an artificial pore structure when exposed to fire, which can help reduce the buildup of hydrostatic pore pressure that can occur when concrete is exposed to fire. Without the artificial pore structure, UHPC exposed to fire has the tendency to exhibit explosive spalling (CSA A23.3 2018).

Fibers do not significantly add to the concrete tensile strength unless they are engaged in tension across a crack. The concrete first crack tensile strength is thus an important parameter and can be estimated from the tensile strength using Equation 2-17 (Graybeal 2006):

$$f_{ct} = a(f'_c)^{0.5} \qquad \text{Equation 2-17}$$

Where: f_{ct} is the concrete tensile strength at first cracking in psi

f_c' is the concrete compressive strength in psi

α is a fit parameter to account for curing method, in psi

The parameter *a* is equal to 6.7 for ambient cured UHPC, 7.8 for steam cured UHPC, and 8.3 for steam curing at 60°C or delayed steam curing of UHPC.

Fibers come in a variety of sizes, usually divided into classes of microfibers and macrofibers. Macrofibers have an equivalent diameter equal to or greater than 0.012 inches (0.3mm), while microfibers encompass everything smaller (ACI CT 2016). Most UHPC mixtures today use microfibers because macrofibers greatly reduce the workability of a mix (Rossi 2001).

The cracking mechanism of concrete can be described as follows. First, tiny microcracks form randomly and without orientation, often due to shrinkage during curing. As loads are applied, the microcracks can propagate and join together, which is referred to as localization. They continue to grow and eventually form macrocracks, which are formed based on the loading direction and stresses produced (Rossi 2001). In typical concrete, there are only a few macrocracks that form, and these propagate with additional loading. Adding fibers to the concrete alters this cracking mechanism by bridging cracks and limiting the size of the cracks that form. Added load causes new cracks to form instead of widening existing cracks. This gives many well-distributed cracks with a small width instead of one or few large cracks.

It has been found that cracks less than 0.1 mm wide do not significantly affect the concrete chloride ion transport (Aldea et al. 1999). Therefore, it is logical to assume that the ability of steel fibers to prevent cracks from expanding gives it a lower permeability and better durability after cracking than normal concrete. This was confirmed by tests from Rapoport et al.; they tested after-crack permeability of concrete with fiber volumes of 0%, 0.5%, and 1.0%. The increased fiber dosage was found to produce significantly lower concrete permeability (Rapoport et al. 2002). Because microfibers are excellent at binding microcracks, and macrofibers are better at holding together macrocracks, a combination of microfibers and macrofibers is sometimes used in UHPC mixtures (Rossi 2001).

The amount of fibers used in a UHPC mix is usually measured and recorded as a percentage of volume, denoted V_f. Producers aim to limit fiber concentration as the cost of only 1% of fibers by volume can cost more than the concrete matrix material (Park et al. 2012). However, there needs to be enough fibers in the mixture to produce a ductile failure and ideally, strain-hardening. Adding more fibers will only increase strength to a certain point, however. At higher fiber dosages, the maximum strain that can be obtained levels off to an asymptotic value. Added fibers also decrease workability severely (Fehling et al. 2008). While past UHPC mixes often used large volume percentages of steel fibers, it is now possible to obtain strain-hardening behavior with fiber contents as low as 1.5% by adjusting matrix and fiber parameters (Wille et al. 2011).

The mechanism by which fibers bond to the concrete is complex because it includes a combination of many different factors. While most of the bonding of steel reinforcement comes from mechanical factors (ribs on rebar or a twist on prestressing strand), fibers can also be bonded by chemical adhesion between the fibers and the matrix, fiber-to-fiber interlock (entanglement), and friction (Naaman and Najm 1991). The bond strength is important for UHPC because in order to provide the concrete with strain-hardening behavior, the fibers are designed to fail by means of bond slip instead of rupture. With bond slip, there is still some load transfer capability between the fiber and concrete because of friction. Strain hardening can then occur when the slipped fibers continue to carry load, and the non-slipped fibers increase their strain and corresponding stress. Steel fibers used in UHPC have very high strengths of up to 400 ksi (Park et al. 2012), and higher strength steel is less ductile than normal steel. This gives very little strain capacity that can be provided by the steel fibers alone without slip. For crimped or hooked fibers, this forces a straightening of the hooks to occur as they are pulled out of the matrix, which gives the concrete a higher energy absorption capacity (Naaman and Najm 1991). The fiber aspect ratio has a large impact on the failure behavior of fibers. A fiber's aspect ratio is defined as the length divided by the diameter. Fibers with a high aspect ratio are long and thin, while a smaller aspect ratio would define shorter and thicker fibers. The ratio of the bond strength-to-tensile strength determines whether the fiber will fail by pull-out or by rupture. The bond strength is a function of the surface area available. Higher aspect ratios increase the surface area-to-cross-sectional area ratio and increase the fiber force at failure. If the aspect ratio is too large, however, the fibers will be more likely to rupture. Steel fibers that have too low of an aspect ratio, however, do not have the

embedment length required to develop their full tensile capacity and are less likely to bridge a given crack that forms in the member, giving reduced material efficiency. Typical fiber aspect ratios in UHPC range from 40-70 (Haber et al. 2018). The Swiss UHPC code requires that fibers used in UHPC have an aspect ratio greater than 65 (Brühwiler 2017), and the Canadian code has the same requirement for polypropylene fibers used in concretes exposed to hydrocarbon fire (CSA A23.3 2018).

Preferential orientation of fibers can occur during placement, causing a reduction in tensile properties in one direction. This can be caused by multiple issues such as fiber flow, segregation, vibration, or wall factors. As shown in Figure 2-5 and Figure 2-6 the way UHPC is pumped or placed can cause fibers to align parallel to the flow of the concrete (Duque et al. 2016). Cracks that form (shown in red), do not intersect as may fibers when they form parallel to the flow of the concrete direction of placement. This preferential orientation gives the concrete an increased tensile strength if cracks form perpendicular to the fibers, but a decreased strength if cracks form parallel (Duque et al. 2016). For members that are placed into thin areas or into testing molds, narrow walls could prevent fibers (especially macrofibers) from orienting in the narrow direction. As shown in Figure 2-7, some fibers have the ability to orient in random directions, but longer fibers or fibers placed close to the edges are forced to be oriented longitudinally. Even large specimens can suffer from this wall effect, though it becomes less influential overall in a larger specimen (AFNOR 2016; Wille and Parra-Montesinos 2012). The tendency for fibers in a large specimen to align parallel near walls is depicted in **Error! Reference source not found.**Figure 2-8. This is particularly problematic for laboratory tests because small specimens are usually used for tensile testing or shrinkage tests. In order to solve this issue, specimens are often saw cut, but this requires more work and equipment. It also creates the reverse problem. Instead of preferentially aligned fibers, fibers at the edge of the specimen are now shorter than their original length, giving a lower aspect ratio and a decreased pull out strength.

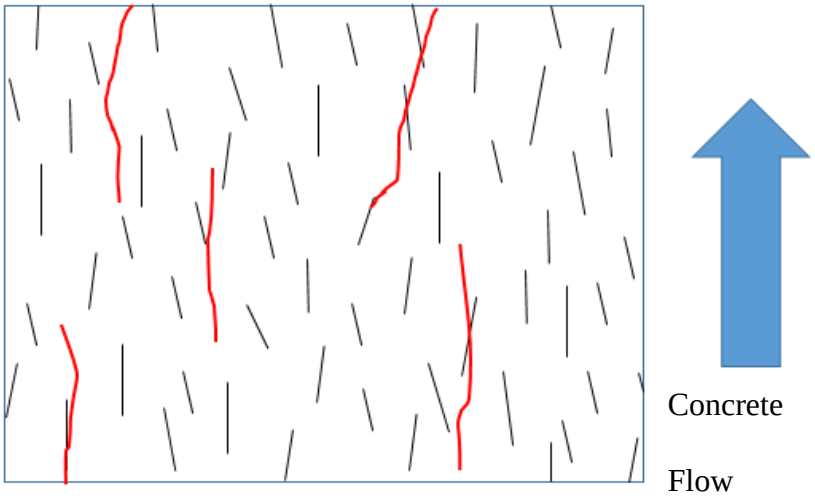

Figure 2-6: Cracks form parallel to concrete flow

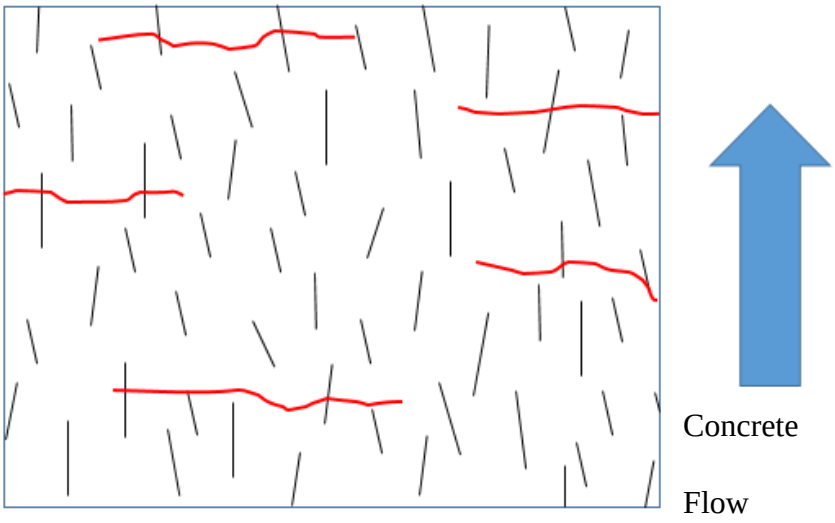

Figure 2-7: Cracks form perpendicular to concrete flow

Figure 2-8: Fiber arrangement in narrow test specimen

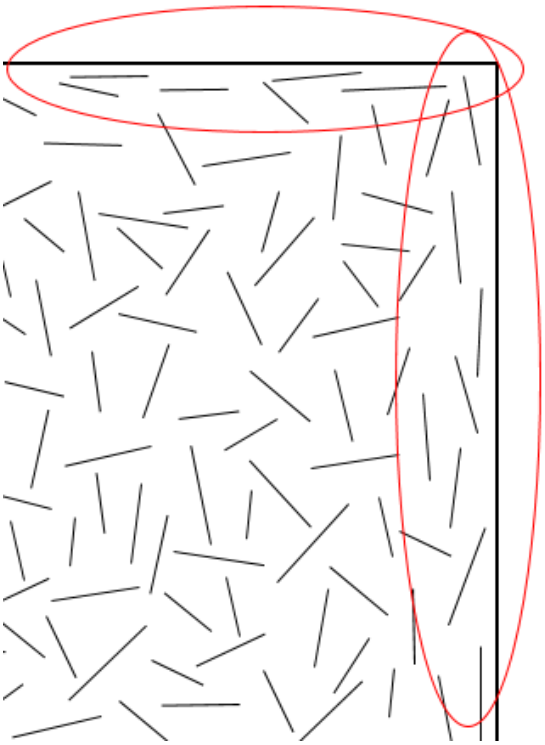

Figure 2-9: Wall effect on fiber orientation

Because UHPC members are often designed to handle loads in multiple directions, a random orientation is usually desired. A study done by Duque et al. took specimens that were saw cut from a large slab element containing 2% steel fibers. The slab element was placed from one direction so that the concrete flow would produce a preferential alignment (Duque et al.2016) as demonstrated in Figure 2-5 and Figure 2-6. The saw cut specimens were cut parallel, perpendicular, and at a 45-degree angle to the flow. They were then tested in direct tension. As expected, the tensile strengths were highest when the specimens were cut parallel to the flow (and therefore, fiber orientation), as shown in Table 2-3 (Duque et al. 2016). While most UHPC projects aim for a uniform, random fiber orientation, it may be beneficial to use preferential orientation from flow direction to maximize the effect of fibers. This would be for cases where the stresses in a member are predictable and predominantly in one direction. While fiber orientation has a large effect on tensile strength, it has not been shown to have a significant effect on compressive strength or modulus of elasticity (Graybeal 2006).

Table 2-3: Fiber orientation effects on tensile strength and strain (Duque et al. 2016)

Fiber orientation relative to tensile stress direction	First Cracking Stress, ksi (MPa)	Average Multi-cracking stress, ksi (MPa)	Strain at Localization
F0	1.4 (9.9)	1.7 (11.4)	0.006
F45	1.0 (7.0)	1.0 (7.1)	0.0027
F90	0.74 (5.1)	0.8 (5.6)	0.0029
Mold cast	1.2 (8.5)	1.5 (10.1)	0.0035

2.6 UHPC Production

2.6.1 Material Handling and Storage

Proper storage of UHPC raw materials is important to ensure the best hydration and performance. Improper storage of dry materials by exposure to moisture has been shown to cause cement balls to form in mixed UHPC (Russell and Graybeal 2013). Lafarge requires premix packages of the proprietary UHPC mix “Ductal,” to be stored in a cool, dry, well-ventilated location (Lafarge North America 2015). Sand used for UHPC mixes is often dried prior to use and then stored to

prevent any moisture ingress (Binard 2017). This is necessary because the w/cm in UHPC is so low that any variation could have a large effect on the mix consistency.

Handling of UHPC materials requires caution due to some safety risks. Proprietary UHPC mixes contain large quantities of fine particles, which can create dust as shown in Figure 2-9. Because of this, goggles and a face mask should be worn. Steel fibers also require personal protective equipment (PPE) such as gloves to be worn to prevent the thin fibers from puncturing skin. Figure 2-10 shows a worker wearing gloves and using a rod to disperse fibers to avoid contact with his hands.

Figure 2-10: Dust is created as premix is added to mixer

Figure 2-11: Workers avoid physical contact with fibers by using gloves and rods

2.6.2 ***Mixing***

UHPC requires different mixing procedures and sequences than normal concrete. The typical mixing sequence for UHPC is as follows: First, the dry ingredients are added to the mixer (Giesler et al. 2016). If dry ingredients have been measured out separately, they must be mixed together so that they are distributed uniformly. Even prepackaged UHPC dry ingredients should be mixed prior to addition of liquids because segregation can occur during transport (CSA A23.3 2018). Figure 2-9 shows the dry ingredients of a Ductal® mix being added to a portable vertical shaft mixer. After dry ingredients have been added, the liquids including water and any admixtures are added (Giesler et al. 2016). The timing of both the water and superplasticizer addition can have a

great impact on the flow characteristics of the UHPC. Hsu et al. found that adding superplasticizer in multiple stages, known as stepwise addition, improved concrete fluidity. In addition, a longer amount of time between the addition of the water and a second superplasticizer addition also increased fluidity. This also decreased the viscosity and air content of the mixture (Hsu et al. 1999). Similarly, Shihada and Arafa showed that adding 40% of the superplasticizer with the water initially and adding the rest after three minutes produced a better mix than adding the entirety of the superplasticizer later (Shihada and Arafa 2010). Ferdosian and Camões suggested a stepwise addition of water in addition to a delayed superplasticizer addition. Among many different methods tested, they found that the best system for fluidity was achieved when 70% of the water was added initially and mixed for three minutes, followed by superplasticizer addition and at least four more minutes of mixing. Finally, the remaining 30% of the water was added, and everything was mixed for an additional six minutes (Ferdosian et al. 2016). This extra six minutes of mixing time is necessary because the mixer must impart enough shear energy to transform the mix from a powdery, clumped state into a uniform, self-consolidating state.

Mixing time for UHPC is often longer than 12 minutes. Schießl et al. showed that this can be reduced by increasing mixing speed or by increasing mixer power. They also showed that mixing time is also heavily reliant upon the particle packing density and the water content of the mix. Mixtures with better particle packing required less mixing time (Schießl et al. 2007). For vertical shaft mixers like the one shown in Figure 2-9, this has been shown to require about 10 -15 minutes (Giesler et al. 2016). After the concrete matrix constituents are completely mixed, the steel fibers are added slowly to ensure their dispersion throughout the mix. One method of fiber addition is shown in Figure 2-10. Steel fibers are added after the rest of the constituents have been mixed because mixing requires much less energy after a self-consolidating state has been achieved (Calmetrix, n.d.). Fibers can greatly reduce the workability of a mix (Fehling et al. 2008), so it is best to add them at a time when power demand for mixing is lower.

The high mixing energy required to mix UHPC can increase the mixture temperature significantly. Ice is often used in place of water to keep concrete temperatures low. The Canadian UHPC specifications suggests partial substitution of mix water with ice if the concrete's internal temperature is above 77°F and complete substitution if it exceeds 86°F (CSA A23.3 2018).

The mixer shown in Figure 2-9 is a type commonly used for field mixing of UHPC. UHPC needs a high amount of mixing energy due to its low w/cm, making power output an important characteristic for a mixer. With conventional lower-energy concrete mixers, desired workability and compressive strengths can be achieved, but the mixing process takes much longer (Giesler et al. 2016). UHPC for precast members is often mixed in a conventional pan mixer or double-shaft mixer, which has a higher capacity. An example of a double-shaft mixer mixing UHPC is shown in Figure 2-11. The UHPC must then be transported to the forms for the precast elements or field use. UHPC stiffens very quickly as cement particles agglomerate together (Kim et al. 2016). This makes it much harder to place the concrete. For this reason, smaller mixers like the one in Figure 2-9 are beneficial for UHPC field use. The small batch size prevents a large amount of material from being wasted due to a delay in placement or an error in mixing.

Figure 2-12: Double-shaft mixer with UHPC Placing & Finishing

Placement of UHPC must occur quickly due to its tendency to stiffen rapidly (CSA A23.3 2018). If UHPC is transported any significant distance after mixing, it must be continually mixed during transport. If allowed to rest, the cement particles will agglomerate together (Kim et al. 2016), causing an unworkable mix. While normal concrete can be consolidated with a vibrator in case of workability loss, consolidation methods for UHPC are restricted due to the detrimental effects that

they have on fibers. Because steel is more dense than the UHPC matrix, the fibers have a propensity to settle if the mixture is agitated by vibrator or other compaction method (CSA A23.3 2018). Vibration can also cause preferential orientation. The Canadian specification for UHPC allows for external vibration to be used but prohibits internal vibration for UHPC mixes with fibers (CSA A23.3 2018).

Field placement for UHPC is often done using small wheelbarrows containing the material. An image of this is shown in Figure 2-12. It is then placed with the aid of a shovel into the desired location. This method of placement reduces the distance that the concrete must flow to reach its final destination. As UHPC flows in a specific direction, the fibers tend to align in the same direction, which would reduce the tensile strength perpendicular to the fiber alignment. The UHPC specification in Canada specifically states that UHPC should be placed as close as practicable to its final position. It also restricts drops of UHPC from more than 3.28 ft (1 m) because it may cause segregation of fibers due to shock (CSA A23.3 2018). Fiber alignment is also why pumping UHPC should be done with caution. The Canadian standard CSA A23.3 allows pumping for lengths of less than 3 meters unless the method is validated prior (CSA A23.3 2018). The UHPC recommendation from Swiss specifications state that UHPC with low fiber dosages is likely pumpable (Brühwiler 2016), but it does not specify what constitutes a low fiber dosage.

Figure 2-13: Wheelbarrow placing of UHPC in joints

UHPC placement must be done monolithically (CSA A23.3 2018), to avoid any cold joints that may occur from the formation of “elephant skin.” Elephant skin is a layer that forms quickly on the surface of UHPC (Binard 2017). It can cause problems because it does not bond well with adjacently-placed UHPC. Figure 2-13 shows a good example of two placements of UHPC that exhibit minor cold jointing due to a layer of elephant skin on the first placement. This bond is further hindered by the fact that the fibers will not bridge the interface between the two sections.

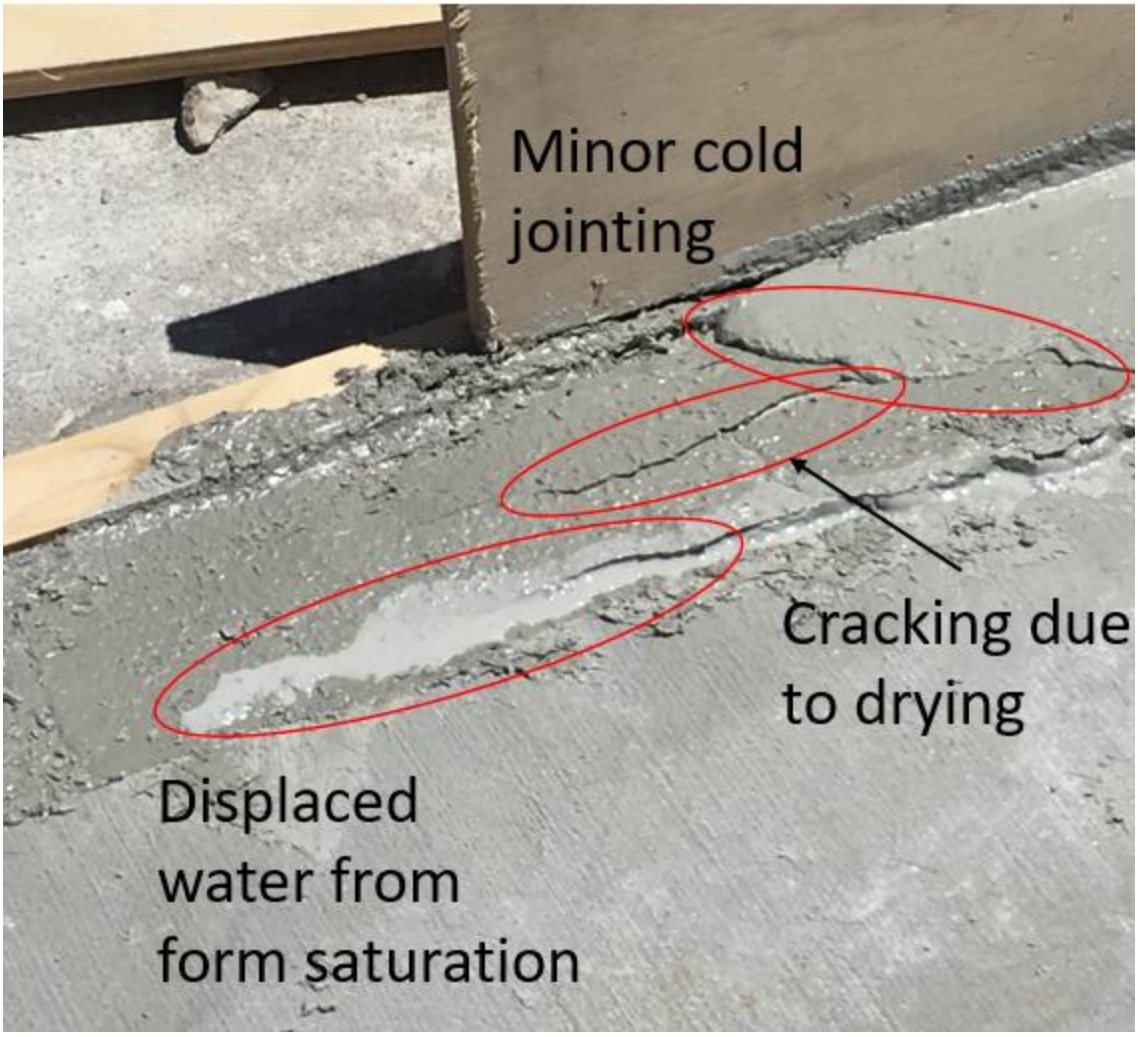

Figure 2-14: Defects in a UHPC joint due to placement procedure

The high cementitious content in UHPC can cause high amounts of shrinkage to occur early in the curing process (Binard 2017). Formwork is often overfilled and later ground to help account for the shrinkage. Another method is shown in Figure 2-14. It uses a bucket with a hole in the bottom placed on top of a UHPC joint. The UHPC joint has been covered with plywood to reduce evaporation and so that the joints will not overflow. The bucket is filled with UHPC, which flows by gravity through the holes in the bucket and the plywood to fill any voids in the formwork.

(a) (b)

Figure 2-15: Method used to ensure complete filling of formwork for joints (a) before (b) after UHPC is added to bucket

UHPC starts to dry immediately after placement and form a skin because of the low water content. Normal concrete typically has bleed water on its surface which can ensure that the concrete does not dry out. Because UHPC does not have bleed water, it should be covered immediately after finishing (Brühwiler 2016; Graybeal 2014) or it can develop plastic shrinkage cracking in a very short time, as shown in Figure 2-13 and Figure 2-15. The elephant skin formed on the surface of the UHPC makes it difficult to trowel. For this reason, joints are often ground after the UHPC has completely set.

Figure 2-16: Plastic shrinkage cracking formed approximately 20 minutes after UHPC placement

*2.6.3 **Curing***

For precast plants, the initial cure is typically accomplished by covering the concrete with plastic and/or thermal insulating blankets. For UHPC placed in the field, joints are often covered with plywood as shown in Figure 2-16**Error! Reference source not found.**. The Canadian specification for UHPC requires that curing be done with a curing compound, a waterproof plastic film, or formwork covering every surface of the UHPC (CSA A23.3 2018). The Swiss

recommendation from the Maintenance Construction Sécurite (Brühwiler 2016) prescribes use of a plastic sheet over fresh UHPC immediately after placement. For construction sites, the UHPC is to be watered daily from the end of setting and for the next 5-7 days. It also allows for verified curing compounds to be used (Brühwiler 2016).

Figure 2-17: Plywood being fastened on UHPC joint to curb water loss

As with normal concrete, the curing process can have a big impact on performance. UHPC is often cured in precast plants using a thermal curing process, where after an initial cure, the concrete is exposed to temperatures around 90°C with 100% relative humidity. This can occur either in the forms using steam or electric heaters after a short initial cure, or after removal from forms with curing in a separate chamber. This process helps to continue the hydration process in the specimen and essentially completes the hydration process for that concrete mixture in a short time period. This locks in the microstructure, virtually eliminating further strength gain, creep, autogenous shrinkage, or camber growth (CSA A23.3 2018).

The initial cure period or the length of time between specimen placement and the thermal treatment process can make a big difference in the mechanical properties. In a study performed by Ahlborn et al., the effects of the time of initial steam treatment were investigated. In all cases, the thermal treatment took place for 48 hours. Some specimens were thermally treated right after demolding (70 hours after placement), while others were delayed by 10 or 24 days. The length of time between demolding and thermal treatment did not have a significant effect on overall performance for compressive, flexural strength, or durability. However, specimens that were not thermally treated did not perform as well in these categories (Ahlborn et al. 2008). Air-cured specimens did see a continual improvement in compressive strength over the 28 days, where thermally treated specimens saw a much smaller gain after thermal treatment. This shows that steam treatment speeds up the hydration process and is a large advantage when high early strength is desired.

Graybeal et al. also compared steam-treated specimens with untreated specimens in compression, tension, and durability tests. Normal steam treatment was defined as 90°C with 95% relative humidity (RH). Tempered steam treatment was defined as 60°C with 95% RH. Both of these treatments began four hours after the specimens were demolded and took place for 48 hours. Delayed steam treatment was also carried out with the same parameters as normal steam curing, but at 15 days after the specimens were cast. All steam treatments resulted in significant improvements in compressive strength and chloride permeability, with normal steam treatment being slightly better than delayed or tempered. Tensile strength also improved over 40% with steam treatment. Steam treatment also improved the shrinkage behavior of the concrete because it forced all shrinkage to occur during steam treatment (Graybeal 2006). This could be advantageous

for precast applications because the entirety of the shrinkage could be realized by the members before they are set into place in the structure.

2.7 Material Properties

Most testing for UHPC is done with the same standard test methods from the American Standard of Testing Materials (ASTM) that are used for normal concrete. However, there are some adjustments that need to be made due to the UHPC's high strength and durability properties, as well as the fiber content and self-consolidating nature. These changes are described in ASTM C1856, "Standard Practice for Fabricating and Testing Specimens of Ultra-High Performance Concrete (ASTM C1856 2017)." The standard describes adjustments for multiple different tests used on normal concrete. It is applicable to mixes where the compressive strength is above 17,000 psi (120 MPa), the flow is between 8 and 10 inches (200-250 mm), and the maximum nominal aggregate size is ¼ in. (5 mm) (ASTM C1856 2017). For standards where a test cylinder is used, ASTM C1856 often prescribes using a 3-in. × 6-in. specimen instead of the more common 4-in. × 8-in. cylinder. There is also specific protocol for making the specimens. The molds must be filled in one layer. They are not to be vibrated, but instead must be hit with a mallet 30 times. This is to ensure fiber segregation does not occur from vibration of the molds. The specimens must be quickly covered to avoid water loss (ASTM C1856 2017).

*2.7.1 **Compressive Strength***

UHPC is tested for compressive strength using ASTM C39 with adjustments specified in ASTM C1856. In accordance with ASTM C39, a cylindrical specimen of UHPC is loaded in compression at a constant rate. The peak load sustained by the cylinder is recorded, and the peak stress is calculated and reported, along with the age of the concrete in days (ASTM C39 2018). With respect to compression testing, ASTM C1856 requires compression testing to be done only on specimens measuring 3 × 6 in. (75 × 150 mm). This smaller size helps to reduce the cost spent on testing of materials, since UHPC is much more expensive per unit volume than normal concrete. It also ensures uniformity between tests because some compression testing machines can not apply loads high enough to break a 4 × 8-in. (100- × 200-mm) cylinder of UHPC. ASTM 1856 also requires that the cylinders be ground to within 0.002 in. (0.050 mm) planeness instead of capped or placed on neoprene pads (ASTM C1856 2017). This is because the high strength of the cylinders exceeds

the strength of the capping material. ASTM C1856 also specifies that the diameter of the specimen must be determined to the nearest 0.04 in. (0.1 mm). Finally, the load rate of the specimen is increased to 145 ± 7 psi/s (1 ± 0.05 MPa/s) (ASTM C1856 2017). This is roughly four times the rate used for normal concrete, but the tolerance remains the same. The load rate is increased because the test method would take from 15-20 minutes per specimen to run if they were tested at the usual load rate (ASTM C1856 2017).

2.7.2 ***Tensile Strength***

Tensile strength is one of the most unique and potentially useful characteristics of UHPC, but it is often difficult to test. Testing for tensile strength is important, however, because it is heavily dependent not only on the mix proportions, but also on the mixing and placing methods used. This is due to the large impact that fiber dispersion and orientation plays on the tensile strength of UHPC. Because tensile strength is often used in the structural design of UHPC, any tensile strength test method used should provide an indication of the materials ductility or toughness. This is because of a UHPC with little or no fibers could be made with a high cracking strength, but no residual capacity beyond cracking. The structural designs that incorporate the tensile strength into the design depend on stress redistribution after cracking.

Splitting Tensile Test

One common method used to test tensile strength in normal concrete is the Brazilian test or splitting tensile test method ASTM C496 (ASTM C496 2017). This test method uses a cylinder with a compressive load applied along its side. This causes the cylinder to split across a rectangular area equal to the cylinder height times the width (ASTM C496 2017). The tensile strength of the cylinder is calculated using Equation 2-18 (ASTM C496 2017). A diagram of the test set-up is presented in Figure 2-17.

$$T = 2P/\pi ld \qquad \text{Equation 2-18}$$

Where: T is the splitting tensile strength (MPa or psi)

P is the maximum applied load indicated by the testing machine (N or lbf)

l is length (mm or in.)

d is diameter of the test specimen (mm or in.)

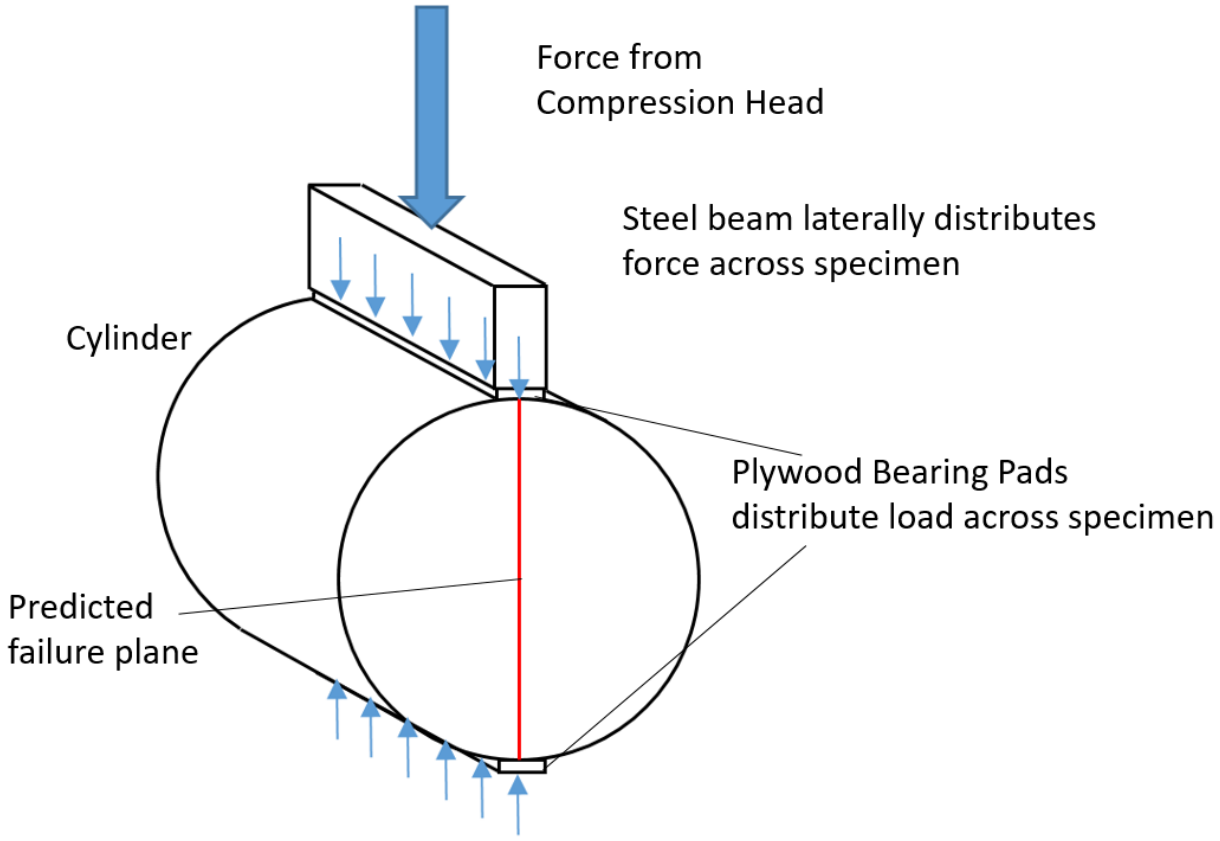

Figure 2-18: Split cylinder test set-up

While this test is useful for normal concrete, there are some issues associated with its application for fiber reinforced concrete for many reasons. The test assumes a brittle failure, as it only gives one value at the point of failure (Graybeal 2006). For normal concrete, the initial cracking occurs at the maximum tensile strength. For UHPC however, the initial cracking occurs much earlier than the maximum tensile strength. One method to overcome this barrier was used by the FHWA (Graybeal 2006). Auditory analysis was used to determine the stress at initial cracking. However, the time of first cracking determined from listening for an audible crack is somewhat subjective. Another downside to this test is that a complete stress vs. strain curve cannot be determined. The FHWA also was able to get around this issue by adding a strain measuring device across the

diameter of the specimen, perpendicular to the formation of the crack. Finally, this test tends to inflate the tensile capacity of a specimen. This is because the main mechanism by which UHPC fails is fiber pull-out, and the direction of load application in this test places the concrete confining the fibers in compression. This increases the friction preventing pull-out. Therefore, the fibers are under this bi-axial stress state are able to hold a greater load before pulling out of the concrete (Graybeal 2006).

Mortar Briquette Test

Another test method often used for tensile testing is the Mortar Briquette test AASHTO T132 (AASHTO T 132 1987). This test uses a small dogbone-shaped specimen that is 3 in. (76 mm) long and 1 in. (25 mm) thick. An example of a specimen in the test machine is shown in Figure 2-18. The thinnest width is 1 inch (25 mm) at the center, creating a failure plane of 1-inch square. The specimen shape and equipment configuration allows the specimen to rotate so that no moment or shear force is applied to the specimen during testing. This helps easily ensure that the failure is purely due to tensile forces. The mortar briquette test also has the advantage of being able to output a clear stress vs. strain diagram. However, the small size of the specimen can cause many issues with fiber alignment, likely causing fibers to align perpendicular to the failure plane. This would lead to unconservative results, which could be dangerous if used in design (Graybeal 2006).

Figure 2-19: Mortar briquette specimen in tensile test machine. Image from (Graybeal 2006).

Flexural Beam Tests

One of the most commonly used methods to test tensile strength for UHPC has been the flexural prism test. Several flexural tests have been developed over the years (AFNOR 2016; Brühwiler 2016; ASTM C1018-97 1997; Baby et al. 2013, 2012; ASTM C78 2018; ASTM C293 2016; ASTM C1609 2012; Vandewalle et al. 2003). Four-point and three-point bending tests are the most commonly used methods to obtain UHPC tensile stress-strain relationships because of the balance between test simplicity, expense of equipment required, and quality of results obtained. Among these tests are ASTM C1018 (1997), ASTM C1609 (2012), RILEM TC 162-TDF (Vandewalle et al. 2003). These tests were originally developed for fiber-reinforced concrete and fracture mechanics tests and have been adapted for use in UHPC through either specimen geometry changes or post-processing calculation. While some specimen geometry, loading, instrumentation, and calculation details may differ, conceptually the flexural prism tests have many commonalities that also bring drawbacks.

In these flexural tests, the load-deflection curve is measured, and from this relationship the curvature and tensile stress-strain relationship for the material is calculated (ASTM C1018-97 1997). In order to calculate the concrete stress-strain relationship from the test results, the inverse calculations require several assumptions that can lead to an overestimate of the strength (Graybeal 2006). There are different methods for the calculation of the stress-strain relationship depending on which flexural test is used. ASTM 1609 is a common flexural test that has a relatively simplified calculation component. This test only specifies the conversion of load applied into a stress value and does not specify a method by which to achieve a strain value from a given deflection (ASTM C1609 2012). On the contrary, the flexure test described in the French UHPC specification provides a method for obtaining a stress-strain curve, but the process is lengthy and requires many correction factors and iterations to be used (AFNOR 2016). Both of these tests and calculation methods are described in depth in this section. One major assumption that must be made for calculating a stress-strain curve is the modulus of elasticity (E) of the UHPC. This becomes difficult because the modulus of elasticity will be different for un-cracked and cracked UHPC. When un-cracked, the fibers have not begun to yield and the UHPC behavior is due to the cement matrix and particle packing, but once cracked, the tensile behavior is mainly attributed to the steel fibers (Park et al. 2012). A second assumption that must be made is the location of the neutral axis

at the point of failure, which will change as the crack propagates. The test also assumes a curvature from the deflection value, and assumes that the curvature along the length of the specimen varies with the moment diagram. However, this assumption tends to overestimate the curvature on the outer thirds of the test specimen and underestimate the curvature (and therefore, the strain), on the inner third of the specimen (Baby et al. 2013). This occurs because the majority of the cracking takes place within the inner third of the specimen, allowing it to curve more. The underestimate of the strain in the center causes an overestimate of the tensile strength of the concrete (Baby et al. 2013). Research was done by Baby, et al. to correct the error for this assumption. The same flexure set-up was used, but strain was determined with strain gauges placed in the middle third of the sample to avoid any error from calculating strain based off of a measured deflection and assumptions (Baby et al. 2012). This gave a direct measure of the strain, and the use of multiple strain gauges helped account for crack localization.

Flexural tests may be greatly affected by the type of support used for the test specimen. An ideal test set-up includes a pin and roller support underneath the prism. The roller support is modeled as having no lateral resistance, but many supports allowed for use in flexural tests can provide a friction coefficient as great as 0.4. Examples of some acceptable supports are shown in Figure 2-19. Researchers Wille and Parra-Montesinos found that specimens on high-friction supports could show a tensile strength 30% higher than that of specimens tested with low friction supports. This stresses the importance of using low friction supports in flexural testing to avoid an over-estimate of a material's tensile strength (Wille and Parra-Montesinos 2012).

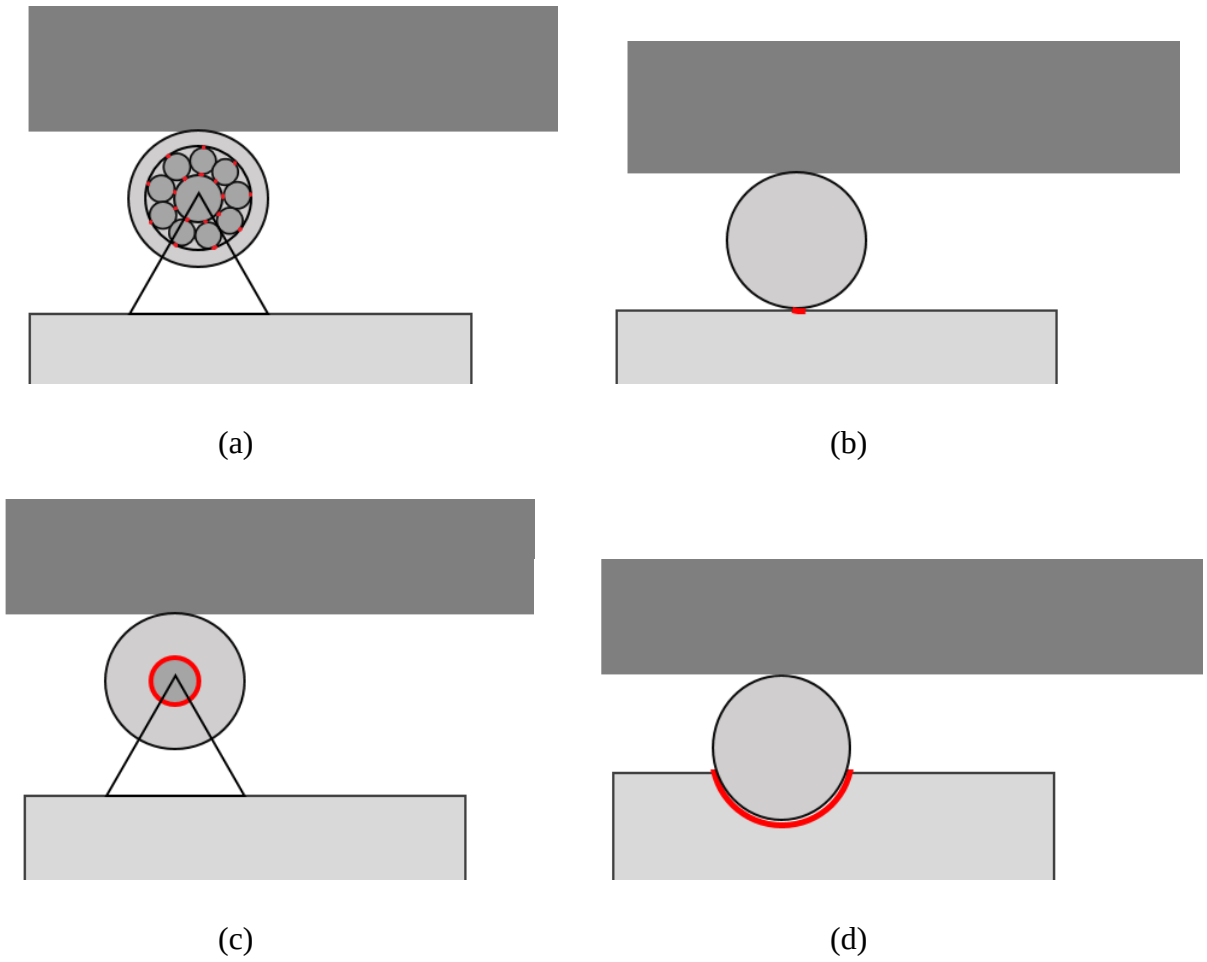

Figure 2-20: Bending test roller supports with low friction (a and b) and high friction (c and d) for lateral resistance (Wille and Parra-Montesinos 2012)

Wille and Parra-Montesinos also tested the effect of beam size, notching, and placement method on the strength results from bending tests. They found that the size did not have a large impact, but that larger beams had slightly lower bending strengths than “medium” beams. This may be attributed to the wall effect being more pronounced on a smaller beam (Wille and Parra-Montesinos 2012). It also may be due to the observation in fracture mechanics that the ductility of an object is a result of structural characteristics, not material characteristics, and that larger objects are less ductal than smaller ones (ACI 446.1R 1991). The placement methods tested by Wille and Parra-Montesinos included the procedures specified in ASTM C1609 and RILEM TC 162-TDF. The ASTM method uses a layer of UHPC to be placed with a scoop parallel to the length of the mold (ASTM C1609 2012). In the RILEM method, the UHPC is placed with a single scoop in the

middle of the specimen. The movement of the scoop in the ASTM method resulted in higher bending strengths, likely because it caused fibers to align along the length of the specimen. This theory is validated by the observation that a faster movement of the scoop further increased bending strengths (Wille and Parra-Montesinos 2012). When testing the difference between notched beams in three-point bending and un-notched beams in four-point bending, Wille and Parra-Montesinos found that notched beams exhibited a higher flexural strength. This was expected because a notch forces beam failure at a particular point, whether or not that point contains the weakest material in the specimen. On the other hand, a uniform specimen tested in four-point bending will fail at the weakest point along the central span (Wille and Parra-Montesinos 2012).

ASTM C1609 is the current flexural test suggested by ASTM C1856 to be used for UHPC (ASTM C1856 2017). This test is a four-point bending test used on a rectangular prism. The prism is loaded with a set-up similar to the one presented in Figure 2-20**Error! Reference source not found.**, except that the edge distance of *a*/2 is not specified, and the distance between supports is equal to the depth of the specimen if the depth exceeds 4 inches. Otherwise, the distance between load points is 4 inches (ASTM C1609 2012). The loading rate on the beam should be controlled so the beam reaches its first-peak deflection between 40-100 seconds after the test begins. The first-peak deflection can be estimated using Equation 2-19 (ASTM C1609 2012):

$$\delta_1 = \frac{23P_1L^3}{1296EI}\left[1 + \frac{216d^2(1+\mu)}{115L^2}\right] \qquad \text{Equation 2-19}$$

Where: δ_1 is the first peak deflection in inches (mm)

P_1 is the first peak load in lbf (N)

L is the total span length in inches (mm)

E is the estimated modulus of elasticity in psi (MPa)

I is the cross-sectional moment of inertia in in.^{4} (mm^4)

d is the average depth of the specimen at the fracture in inches (mm)

μ is Poisson's ratio

After the first peak deflection, the rate of loading can increase, but not more than eight times the original loading rate. Either the first peak strength or the peak strength can be used to find the strength of the concrete using Equation 2-20 (ASTM C1609 2012):

$$f = \frac{PL}{bd^2} \qquad \text{Equation 2-20}$$

Where: f is the strength in psi (MPa)

P is the load in lbf (N)

L is the span length in inches (mm)

d is the average depth of the specimen at the fracture in inches (mm)

b is the average width of the specimen at the fracture in inches (mm)

The strength value produced by Equation 2-20 is the modulus of rupture, or flexural strength of the concrete. This is not equal to the tensile strength because the material is not isotropic. For UHPC, the modulus of rupture will be higher than its tensile strength, so values of flexural strength and tensile strength should not be directly compared.

To determine the toughness of the material, the load vs. deflection curve can be plotted, and the area under the curve up to a net deflection of $L/150$ can be calculated to provide the toughness in 10 inch-pounds (Joules).

ASTM C1856 provides adjustments to the specimen size to be used in ASTM C1609 according to fiber length. This can help avoid the pronounced wall effect that could occur if a very small specimen was used with long fibers. The specifications on prism size based on fiber length according to ASTM C1856 are presented in Table 2-4.

Table 2-4: Prism sizes for flexural tests based on fiber length (ASTM C1856 2017)

Maximum Fiber Length in (mm)	Nominal Prism Cross Section in (mm)
< 0.60 (15)	3 × 3 (75 × 75)
0.60-0.80 (15-20)	4 × 4 (100 × 100)
0.80-1.00 (20-25)	6 × 6 (150 × 150)
> 1.00 (25)	8 × 8 (200 × 200)

ASTM C1018 was developed originally to measure the fracture toughness of fiber-reinforced concrete. The test has since been officially withdrawn without replacement as of May 2006 due to lack of interest and support for its continued use (ASTM C1018-97 1997). Nevertheless, many states still require its use for qualification of UHPC mixes. This test is run similarly to ASTM C1609, with a few exceptions. The load rate must be controlled so the first peak strength falls within 30 and 60 seconds of the beginning of the test. Instead of defining the toughness as a value in inch-pounds or Joules, ASTM C1018 uses toughness indices. These are still calculated by finding the area under the load-deflection curve, but they are unitless values because they are toughness ratios. Three indices are defined as shown in Table 2-5. Note that the term "integral" in the definition refers to the area under the load-deflection curve up to the specified point, and δ refers to the deflection at the point of the first crack.

Table 2-5: Toughness indices as defined by ASTM C1018 (ASTM C1018-97 1997)

I_5	the integral at deflection of 3δ divided by the integral at δ
I_{10}	the integral at deflection of 5.5δ divided by the integral at δ
I_{20}	the integral at deflection of 10.5δ divided by the integral at δ

The French UHPC specification NF P18-470, Annex D includes very detailed procedures for flexural tests (AFNOR 2016). Two tests use rectangular prisms with a length of four times the height. This height dimension, noted *a*, shall be between 2.8 and 7.9 inches (70 and 200 mm) and between five and seven times the length of the longest steel fibers in the UHPC. The first test is a four-point bending test, with a set-up as displayed in Figure 2-20. This test is only used for determining the linear limit for the material used. The test set-up shown in Figure 2-20 may be

altered by using an extensometer to measure the average deformation in the lower fiber instead of the deflection.

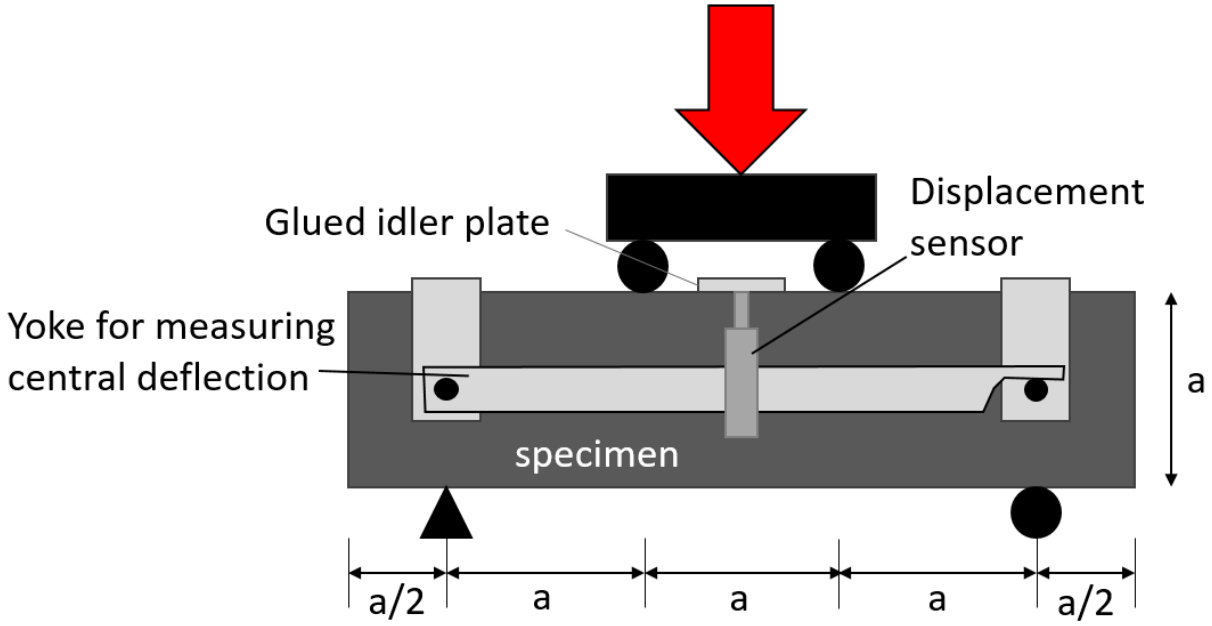

Figure 2-21: Four-point bending test schematic

As the test is run, the force-deflection or the force-extension curves shall be plotted. The value of the force corresponding to the end of the linear behavior (F_{nl}) is to be determined. From that value, the force is calculated using Equation 2-21 and adjusted for specimen size using Equation 2-22:

$$f_{ct,fl} = 3\frac{F_{nl}}{ba} \qquad \text{Equation 2-21}$$

$$f_{ct,el} = f_{ct,el}\frac{\kappa a^{0.7}}{1+\kappa a^{0.7}} \qquad \text{Equation 2-22}$$

Where: F_{nl} is the force corresponding to the loss of linearity of the behavior in Newtons

a is the distance between loading points on the specimen, which is equal to the height of the prism in mm

b is the width of the prism in mm

$f_{ct,fl}$ is the limit of elasticity in bending, in MPa

$f_{ct,el}$ is the tensile limit of elasticity

$\kappa = 0.08$, a constant that may be recalibrated for specimens with large strain-hardening characteristics

The three-point bending test as described in the French UHPC specification can be used to determine the tensile behavior of the material as well as the tensile behavior class as specified in the French code. The tensile behavior class refers to the extent of the strain hardening behavior of the material. The three-point bending test uses a specimen notched at the bottom face of the specimen and a test set-up as shown in Figure 2-21. The notch shall be sawn into the specimen at a depth equal to half the length of the longest fibers in the mix, and it should be less than 0.12 in. (3 mm) wide.

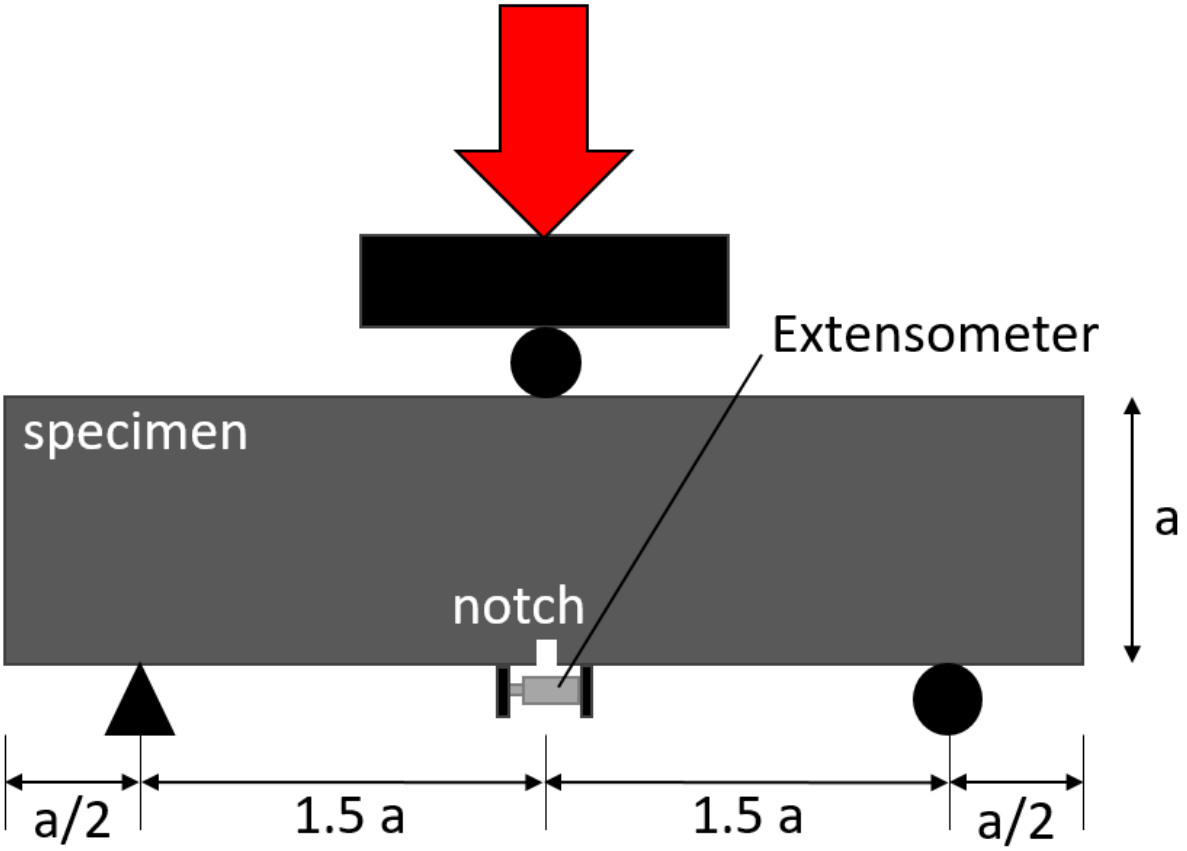

Figure 2-22: Three-point bending test set-up

The test is run with a load rate of either 0.0098 ± 0.0039 in/min (0.25 ± 0.1 mm/min) by actuator displacement control, 0.0039 ± 0.0020 in/min (0.1 ± 0.05 mm/min) by deflection control, or 0.00098 ± 0.00039 in/min (0.025 ± 0.01 mm/min) by control of the extension of the lower fiber or the crack width. The test is run until either deflection of the sample or extension of the lower fiber is equal to 0.015*a*. Data is recorded at a frequency of at least five data points per second. The data to be recorded includes the time, deflection, crack opening (or extension of the lower fiber), and the force applied on the specimen. The data is then smoothed beyond the end of the elastic region by averaging groups of data points, spanning 40 μm of crack opening at intervals of 20 μm, and plotting the average values at the center of the intervals.

The crack width, *w* is measured beginning at the end of the specimen's elastic behavior. Because of this, the cracked behavior of the UHPC can be isolated for analysis. This will result in a break in the strain curve, as shown in **Error! Reference source not found.**.

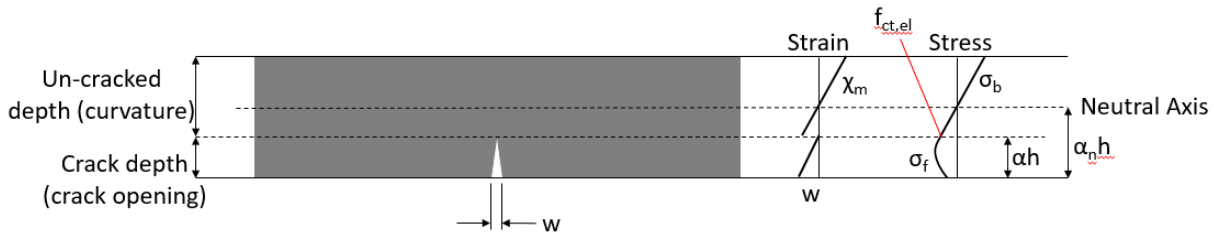

Figure 2-23: Deformations and stresses for three-point bending test after notch has progressed into a crack

Where: *h* is the height of the section after deducting the depth of the notch in m

α is the depth of the crack relative to *h* inferred by:

$$(\alpha_n - \alpha)h\chi_m E_{cm} = f_{ct,el}$$

α_n is the depth of the neutral axis relative to *h* given by:

$$\sigma_t = E_{cm}\chi_m h(\alpha - \alpha_n)$$

χ_m is the curvature of the non-cracked portion in m^{-1}

$f_{ct,el}$ is the tensile limit of elasticity (average value $f_{ctm,el}$ or characteristic value $f_{ctk,el}$, depending on the curve processed) in MPa

E_{cm} is the average value of Young's modulus in MPa

b is the width of the section in m

σ_b is the stress in the un-cracked portion of the specimen

σ_f is the stress in the fractured portion of the specimen

If the extensometer is offset from the bottom of the specimen, this shall be accounted for with Equation 2-23. If the crack width is not measured, it can be estimated from Equation 2-24.

$$w = w_{mes}\frac{\alpha h}{\alpha h + e}$$ Equation 2-23

$$w = \frac{4}{3} \times 0.9 \times (f - f_0)$$ Equation 2-24

Where: w_{mes} is the crack width as measured by the extensometer

w is the actual crack width

e is the distance by which the extensometer is offset from the bottom face of the specimen.

f is the deflection measurement

f_0 is the deflection corresponding to the end of the elastic region

The mechanical balance of the equations is shown below in Equation 2-25 through Equation 2-30. The subscript, *b* refers to the un-cracked portion of the specimen, while the subscript *f* refers to the fractured portion.

$$N_b = \frac{E_{cm}\chi_m b h^2}{2} * [(1 - \alpha_n)^2 - (\alpha - \alpha_n)^2]$$ Equation 2-25

$$N_f = \frac{\alpha h b}{w}\int_0^w \sigma_f \, d\omega$$ Equation 2-26

$$M_f = \alpha h N_f - \frac{(\alpha h)^2 b}{w^2}\int_0^w \sigma_f \omega \, d\omega$$ Equation 2-27

$$M_b = \frac{E_{cm}\chi_m b h^3}{3} * [(1 - \alpha_n)^3 - (\alpha - \alpha_n)^3] + h\alpha_n N_b$$ Equation 2-28

$$M = M_b + M_f$$ Equation 2-29

$$N = N_b + N_f = 0$$ Equation 2-30

Where: N is the normal force, equal to zero

N_b is the normal force in the uncracked section in MN

N_f is the normal force in the fractured section in MN

M is the resisting moment in MN× m

M_b is the resisting moment in the uncracked section MN× m

M_f is the resisting moment in the fractured section MN× m

The kinematic relationship between crack opening and curvature of the non-cracked part of the specimen is described in Equation 2-31.

$$w = [\chi_m + 2\chi_e]\frac{2(\alpha h)^2}{3} \qquad \text{Equation 2-31}$$

$$\chi_e = \frac{M}{E_{cm}I} \qquad \text{Equation 2-32}$$

Where: χ_e is the equivalent elastic curvature in m^{-1}

I is the moment of inertia of the rectangular cross section in m^4

The stress (σ_f) vs. crack opening curve (w) relationship that is of interest is determined by an iterative method with pairs of points (w_i, σ_{fi}). The step size of 20 μm can be used to give the stresses using a trapezoidal approximation as shown in Equation 2-33. The incremental equations for the normal force and moment in the cracked portion of the specimen are shown in Equation 2-34 and Equation 2-35.

$$\int_0^{w_{i+1}} \sigma_f \, dw = \int_0^{w_i} \sigma_f \, dw + \left(\frac{\sigma_{f_i} + \sigma_{f_{i+1}}}{2}\right)(w_{i+1} - w_i) \qquad \text{Equation 2-33}$$

$$N_{f_{i+1}} = N_{f_i}\frac{\alpha_{i+1}}{\alpha_i}\frac{w_i}{w_{i+1}} + \alpha_{i+1}bh\left(\frac{\sigma_{f_i} + \sigma_{f_{i+1}}}{2}\right)\left(1 - \frac{w_i}{w_{i+1}}\right) \qquad \text{Equation 2-34}$$

$$M_{f_{i+1}} = M_{f_i}\left[\frac{\alpha_{i+1}}{\alpha_i}\frac{w_i}{w_{i+1}}\right]^2 + \alpha_{i+1}hN_{f_{i+1}}\left(1-\frac{w_i}{w_{i+1}}\right) - \frac{(\alpha_{i+1}h)^2 b}{2}\left(1-\frac{w_i}{w_{i+1}}\right)^2\sigma_{f_{i+1}} \quad \text{Equation 2-35}$$

Equation 2-34 and Equation 2-35 can be solved to find the unknowns of crack depth and stress at step *i+1*. The iterative process must include a starting point and beginning values. The process will start at the end of the elastic region, and the beginning values for moments and normal forces in the beam are shown in Equation 2-36-Equation 2-39.

$$M_b^0 = M_{ext} = \frac{-bh^2\sigma_f^0}{6} \quad \text{Equation 2-36}$$

$$M_f^0 = 0 \quad \text{Equation 2-37}$$

$$N_b^0 = 0 \quad \text{Equation 2-38}$$

$$N_f^0 = 0 \quad \text{Equation 2-39}$$

In order to smooth the resultant curve, a correction factor is used as a moving average to adjust value *i* after the value for *i+1* has been determined. The calculation of the correction factor is shown in Equation 2-40.

$$\sigma_{fi} = \frac{2\sigma_{f_i} + \sigma_{f_{i+1}}}{3} \quad \text{Equation 2-40}$$

The equations above assume that the material is uniform throughout the specimen. This is an incorrect assumption because fibers at the edges of the specimen will have different orientation due to placement effects. Fibers in sawn specimens will also be affected because the edge fibers will be shorter than the fibers throughout the rest of the specimen. To account for this, the French standard uses correction factors for the different regions of the specimen cross section. These correction factors are applied over a width of $L_f/2$, where L_f is the length of the fibers. The correction values are used by dividing the stress value in the stress vs. strain curve by the correction coefficient weighted over the entire cross-section of the specimen. Correction factors are shown in Table 2-6.

Table 2-6: Correction factors for edge effects in flexure specimens

Location	Correction Factor
Formed edges, except for top (compression) edge	1.2
Sawn edges, except for top (compressive edge)	0.5
Edge containing notch	0
Edges not formed or sawn, compression edge, and any portion of the cross-section farther than L_f from the edge	1

Direct Tension Tests

In order to avoid the inverse calculation issues associated with flexural tests of concrete, direct tension tests have been developed. Both notched and unnotched tests have been developed. Notching of specimens helps to control the location of specimen failure, which makes it easier to measure strain or to ensure failure happens away from load transfer points. In a study done by the Federal Highway Association, 11 out of 12 notched specimens failed within the notched region (Graybeal 2006). However, stress concentrations may be caused by notching, giving results that are lower than the actual concrete strength. Kusumawardaningsih et al. used a rectangular specimen with a 1.6-in. by 1.6-in. (40-mm by 40-mm) cross section. A 0.20-in. (5 mm) square notch was included on two sides of the specimen at the center to control the location of the tensile failure. Notches were added after specimens were cured (Kusumawardaningsih et al. 2015), which would reduce error due to irregular fiber dispersion caused by a molded notch. However, a square notch would create a larger stress concentration than a curved notch, as used by the FHWA (Graybeal 2006). Figure 2-23 shows the design of the specimen used. Le Hoang and Fehling used notched specimens of the same shape but half the height, using specimens 1.6 in. (80 mm) tall instead of 6.3 in. (160 mm). The prisms were attached to the tensile testing machine by means of steel blocks on the top and bottom of the specimen. These blocks had threaded rods that attached to the tensile testing machine, and the blocks were attached to the concrete with thin steel plates epoxied to the concrete. These plates also held Linear Variable Differential Transformers (LVDTs) which could track the displacement as the specimen was loaded (Le Hoang and Fehling 2017). Because of the notching, the displacement could be assumed to be concentrated at the notch and used as a measurement of crack width.

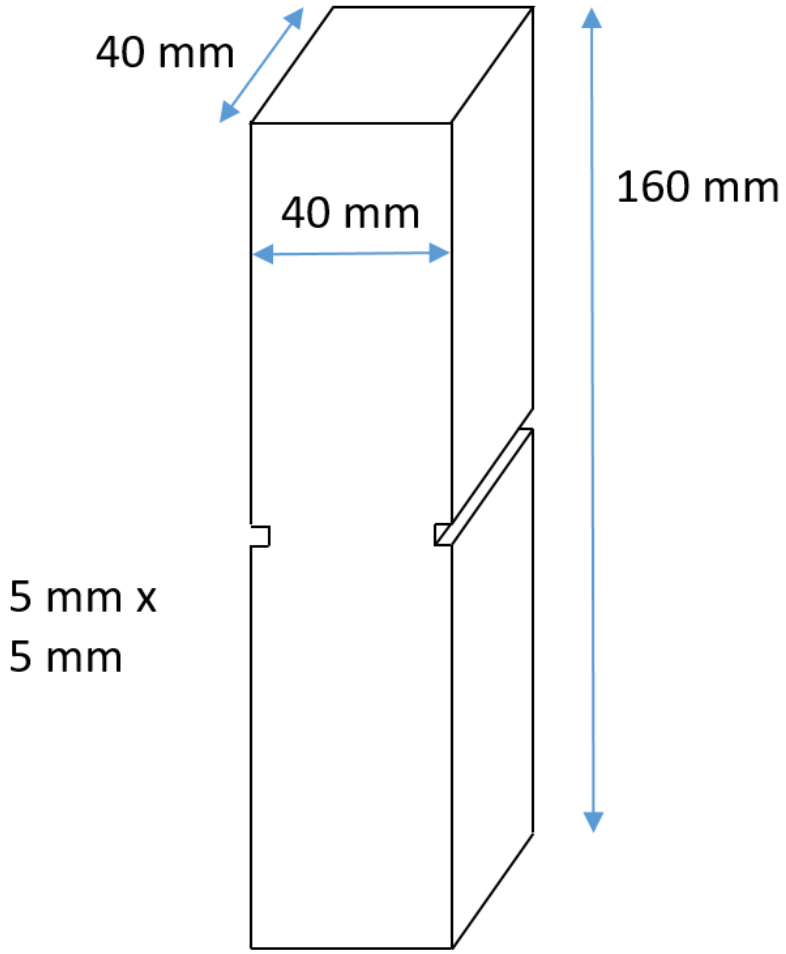

Figure 2-24: Tensile test specimen

The FWHA has used direct tensile testing of cylinders (both notched and un-notched) and rectangular prisms in past work. In 2006, the FHWA tried a direct tension test method that directly attached a UHPC concrete prism to the testing heads with high-strength epoxy, placing the epoxy in series between the specimen and test machine (Graybeal 2006). Some major drawbacks to this method were that the epoxy curing time made each test very time consuming, and a stress concentration region at the location of the epoxy caused premature failure (Graybeal and Baby 2013). The current FHWA tensile method was developed in 2013 and uses hydraulic grips to apply the tensile force to each specimen. A dog-bone shape is created by epoxying shaped aluminum plates to each side of the specimen. This can reduce local crushing at the grips and ensure that the specimen fails near the center. While a 20% increase in stress is present at the end of the aluminum

plates, this is preferred to the 60% local tensile stress increase that would be present if the plates were excluded (Graybeal and Baby 2013). A schematic of the specimen is shown in Figure 2-24. Two different specimen lengths were used in the test, so some dimensions show multiple numbers. Dimensions for the short specimen are listed first.

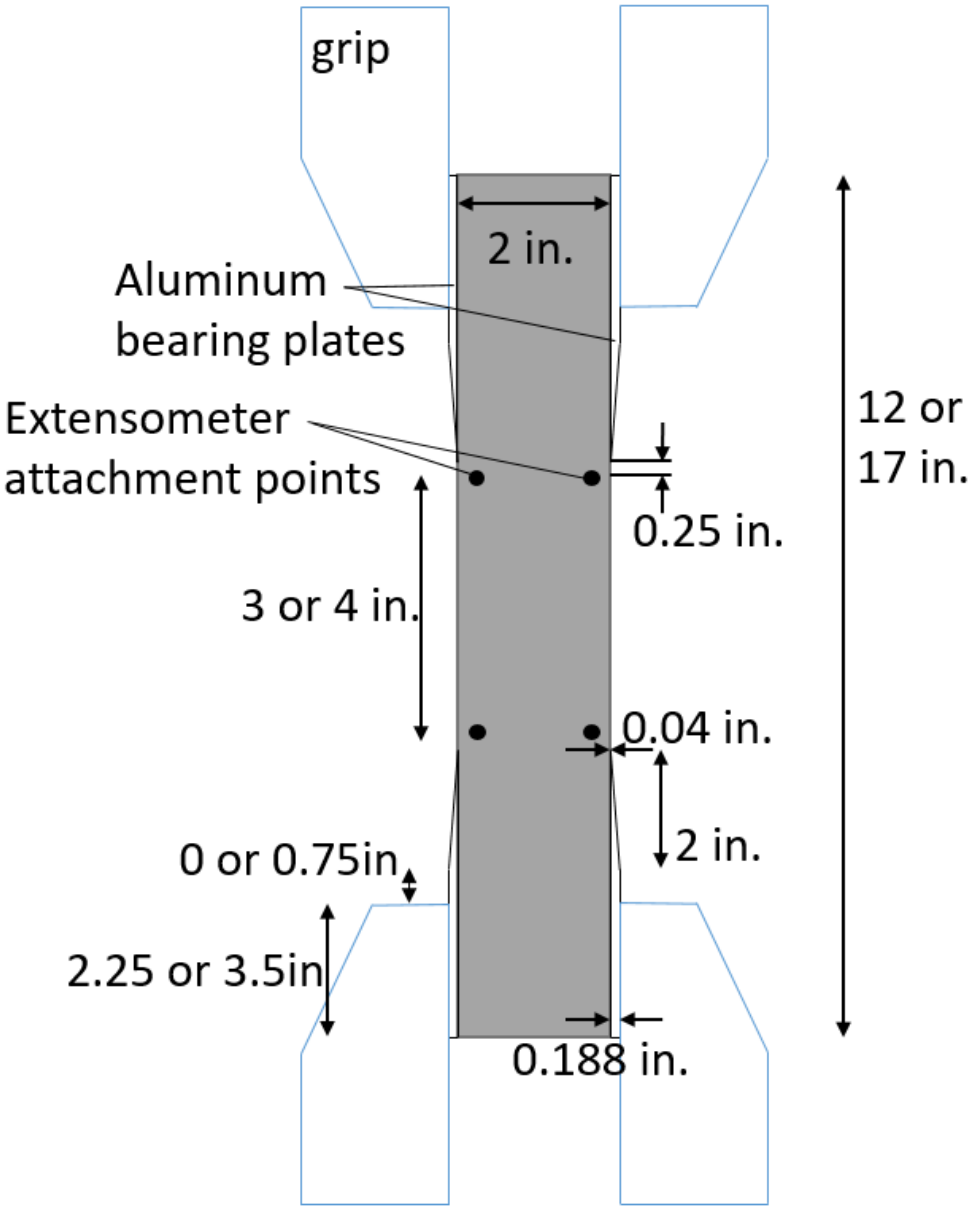

Figure 2-25: Schematic of direct tension UHPC test (Graybeal and Baby 2013)

One problem that can occur with direct tensile testing is an extra moment caused by misaligned grips. This moment will add tensile stress to one side of the specimen. This will cause strain

localization that results in artificially low tensile strength values measured. This strain localization also disrupts the cracking mechanism needed to produce a good stress vs. strain curve. An idealized stress vs. strain curve for UHPC is shown in Figure 2-25. If a specimen is affected by strain localization, it will cause only one large crack to form instead of many cracks. This is because a pure uniaxial tension test undergoes the same stress throughout the test, but a moment caused by misalignment will produce a location of maximum stress. It is recommended to use longer tensile specimens to reduce this moment, as the magnitude of the added moment due to a fixed offset distance is inversely proportional to the square of the length of the specimen (Graybeal and Baby 2013). Alignment fixtures are also available and have been used to make sure that no eccentric load is applied to the specimen (Haber et al. 2018). While the results of the direct tension test give pure tensile information and can easily provide stress vs. strain information, few laboratories can perform it because the equipment for the tensile gripping mechanism is expensive and specialized.

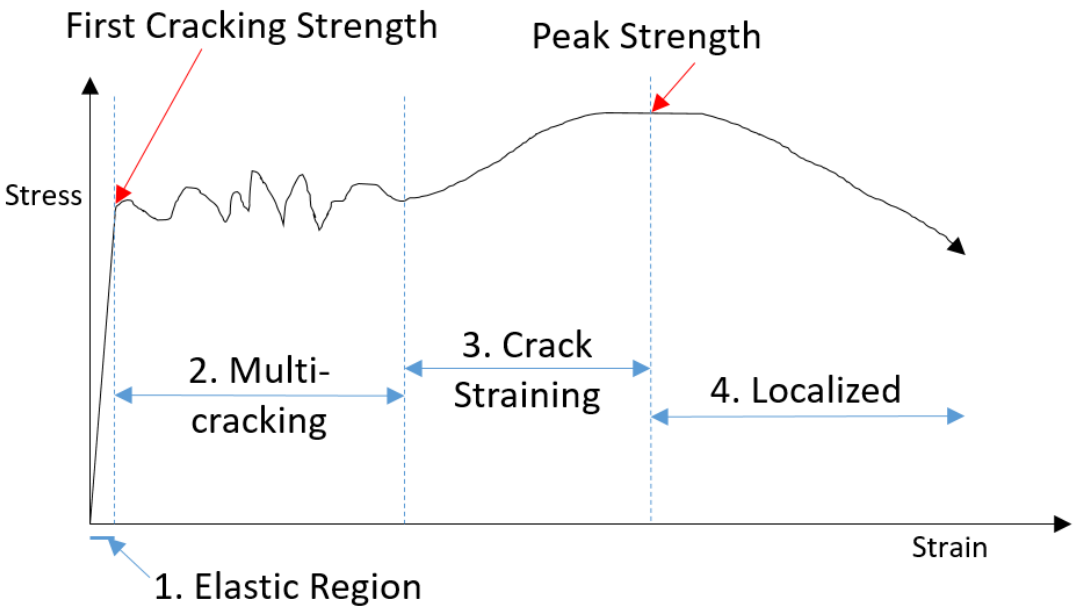

Figure 2-26: Idealized stress vs. strain curve for a UHPC direct tension test (Russell and Graybeal 2013)

While direct tension tests can eliminate many of the assumptions required by flexural bending calculations, they will still be affected by wall and size effects.

2.7.3 ***Elastic Modulus***

A material's elastic modulus, denoted *E* is defined as the amount of force applied to a material divided by the percent deformation. On a stress vs. strain diagram, it is equivalent to the slope of the line in the linear region. ASTM C469 is used to test elastic modulus and Poisson's ratio. In this test, a concrete specimen is attached with an extensometer comprising of a ring with LVDTs or dial gauges to measure strain. An image of this ring on a specimen is shown in Figure 2-26. It is then loaded in a compression testing machine to up to 40% of its compressive strength capacity, and the load vs. displacement is measured(ASTM C469 2014). The load can be translated into a stress value by dividing it by the specimen's cross-sectional area, and the strain is calculated from the displacement by dividing it by the length along which the strain is measured. ASTM 1856 adjusts this standard for use in UHPC by requiring a 3-in. x 6-in. cylinder to be used for the test and increasing the load rate to be 145 ± 7 psi/s (1 ± 0.05 MPa/s), which is the same rate used for a UHPC compression test (ASTM C1856 2017).

Figure 2-27: Concrete specimen with extensometer for modulus testing (Graybeal 2006)

Stress vs. strain results for UHPC are shown in Figure 2-27 and Figure 2-28. It is evident that the material's modulus increases with age, especially between the time periods of 24 and 48 hours. This is because at 24 hours, the concrete has not finished curing. Graybeal et al. found that the modulus of steam-cured specimens was 17-24% higher, depending on the type of steam treatment. Specimens undergoing delayed steam treatment had slightly lower moduli than those that had steam treatment immediately after demolding. Tempered steam treatment produced an average

modulus between delayed and normal steam treatment. Average values for all specimens were within the range of 40-55GPa. Additionally, it was shown that fiber orientation in a specimen did not significantly impact elastic modulus values (Graybeal 2006).

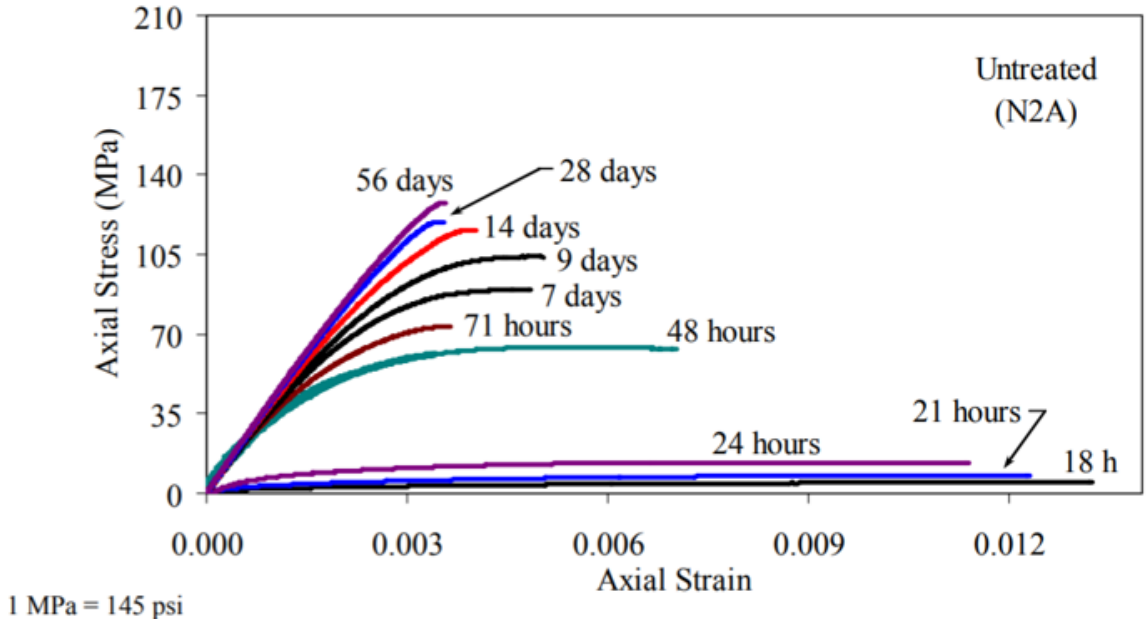

Figure 2-28: Selected stress-strain response for UHPC that was not heat treated (Graybeal 2006)

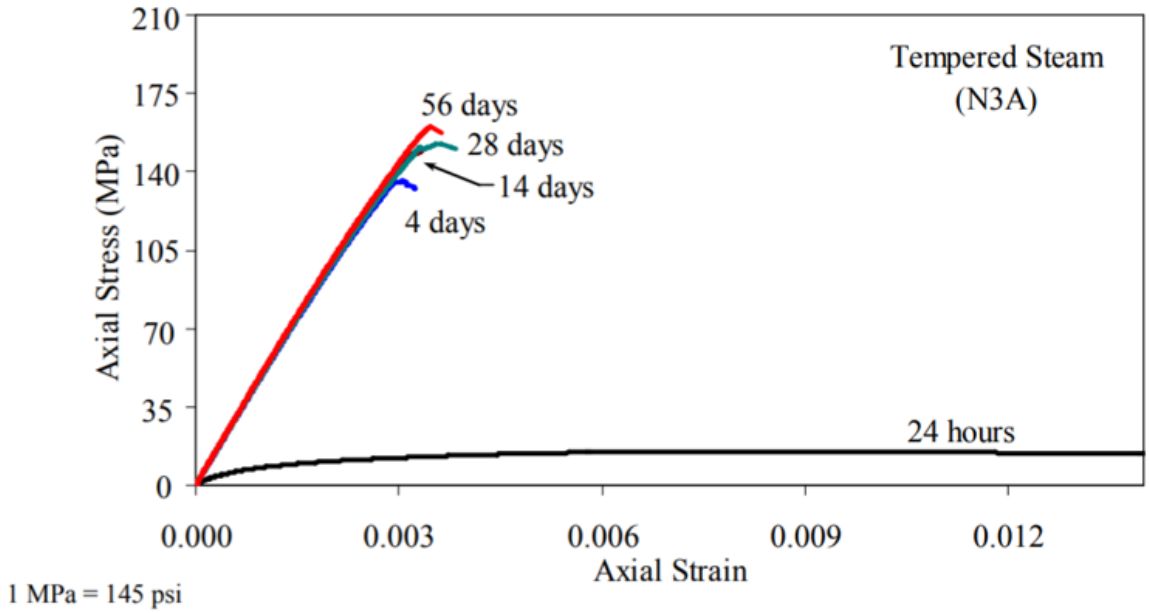

Figure 2-29: Selected stress-strain response for tempered steam-treated UHPC (Graybeal 2006)

2.7.4 ***Fiber Dispersion Testing***

Because so much of the behavior and strength of UHPC is attributed to the steel fibers, having an even fiber dispersion is important. This is difficult to test, however, because it is heavily affected by the method of placing and compacting an element. This may be difficult to reproduce in a laboratory setting, especially relating the scale and shape of the test specimen when compared to the field-cast member of interest.

One possible method was conducted by Graybeal, et al. where cylinders were placed, cured, and cut in half longitudinally. Four 1-in^2 sections were then drawn at different heights along the flat cut face. Each exposed fiber was then counted for each section and the results were compared. To analyze the effect of compaction methods on fiber dispersion, each cylinder sample underwent a different number of impacts on the flow table before curing. The results from this test were inconclusive on the effect of impacts on each cylinder. Higher fiber percentages tended to be observed at the bottom of each specimen, but it was unclear whether this was caused by the placing method or the compaction. Results were reported as fibers per square millimeter, and values ranged from 0.5 to less than 0.2, showing just how varied fiber dispersion of a single mix can be (Graybeal 2006).

Ferrara and Meda used a simple technique of taking cores from a specimen, crushing them, removing the steel fibers with a magnet, and weighing the steel (Ferrara and Meda 2006). While this is a straightforward method, it is destructive to the specimen. It also can only give information about fiber concentration and not fiber orientation. The small size of the fibers also makes it difficult to avoid losing or missing fibers in the procedure.

Electrical methods have also been used to determine dispersion and orientation of steel fibers in concrete. Impedance spectroscopy has been used for both fresh and hardened concrete, and it can give information on both fiber density and orientation (Ozyurt et al. 2004). This is because the fibers coated with concrete remain insulators at low frequencies but become conductive at high frequencies. To determine fiber orientation, measurements are taken in three directions at the same location. If fibers are aligned preferentially in the direction of the measurement, the output can be as great as three times that of randomly dispersed fibers (Ozyurt et al. 2006). Because a wide range of frequency during measurement is necessary, an alternating current must be used for the

impedance spectroscopy (Ozyurt et al. 2006). While electrical methods benefit from being nondestructive, they are heavily influenced by humidity levels and need to be calibrated accordingly. The surface connection of the testing machine to the concrete also affects the results. Finally, the equipment required is expensive, making it less desirable for use out of a laboratory setting (Ferrara et al. 2017).

In addition to their electrically conductive properties, steel fibers also have magnetic properties that can be detected to determine their concentration and orientation in concrete. Faifer et al. developed a nondestructive test method that uses inexpensive, portable equipment. The measuring device is a two-pronged probe with a wire coil connected to a computer and data acquisition system. The concentration and orientation of the fibers affects the magnetic field, which is then measured. When the probe is rotated around the same location, the signal received from measuring the magnetic field changes based on the predominant fiber orientation in that section (Faifer et al. 2013). Ferrara et al. have used this technique to verify a fluid dynamics model of flow for concrete slab elements (Ferrara et al. 2017).

X-ray analysis has been used to qualitatively examine fiber orientation in UHPC (Ferrara and Meda 2006). Through X-ray analysis, a two-dimensional image or radiograph can be produced showing fiber dispersion as well as orientation. X-ray imaging is non-destructive, but it is limited by the size of the specimen that can be tested. The maximum specimen thickness is limited by the power of the machine and the X-ray absorption capacity of the material. Radiation safety requirements and expense limit the practicality for field use of this method. The limitation to only a two-dimensional image is also a drawback because a variance in fiber dispersion across the depth of a scanned section would not be detectable (Ferrara et al. 2017).

One non-destructive method of determining fiber orientation and distribution that has successfully been used is micro-computed tomography. This technology can give a three-dimensional image of a sample based on the densities of the materials contained using X-ray imaging. While the individual sample tested is not destroyed in the testing, the sample must be small enough to fit into the machine, meaning that it cannot be used for large members or field testing. However, it can be used for models that were placed in the same way as a larger field specimen, and samples can be excised for analysis. Walsh et al. used this method to research how UHPC flow in joints affected

fiber orientation around steel reinforcement and near walls. As expected, fibers near the walls of the joint were overwhelmingly oriented parallel to the walls. In general, fiber orientation in boundary-free locations of the sample joint was typically parallel to the concrete direction of flow. Near a piece of reinforcement, the distribution of fibers was denser upstream of the reinforcement, while the area behind the reinforcement had very low fiber content, as if the rebar acted to block fibers. This caused problems with bond strength of the reinforcement because the uneven fiber distribution caused an uneven stress distribution in the concrete, with higher stresses in areas of lower fiber content (Walsh et al. 2018).

2.7.5 ***Bond to Concrete***

Because a major application of UHPC is joints between precast elements, UHPC bond to existing concrete is very important. Joints will include steel reinforcement from the precast members to improve bond, as shown in **Error! Reference source not found.** 2-29. However, if the UHPC does not bond well to the surrounding precast members, the joint will not be watertight. This could cause corrosion in the steel reinforcement and eventual degradation of the joint. UHPC has very good bond behavior when placed adjacent to normal strength concrete (NSC). It has been found that the bond between UHPC and NSC is stronger than the NSC itself (Carbonell Muñoz et al. 2014).

Figure 2-30: Steel reinforcement layout in joint between precast element and existing concrete

Multiple tests for bond are available and have been used (Li 2015). However, Austin et al. cautioned the use of values produced by these tests because the results are heavily dependent on surface conditions of the materials (Austin et al. 1999). These tests are most often used to compare surface preparation and materials used.

ASTM C882 is a commonly used bond test that tests the bond between two materials in shear (ASTM C882 2013). It has been adapted for use of UHPC instead of epoxy, for which it was

originally designed (Li 2015; Austin et al. 1999). It uses a 3 × 6-inch cylinder specimen that is half normal concrete and half the material to be tested (in this case, UHPC, but the test was designed for epoxies). The bond between the two materials is at a 30° angle with the vertical axis. The cylinder is then tested in compression according to ASTM C39, and the peak load is divided by the failure plane to determine the strength of the bond (ASTM C882 2013). Specimen size has been shown to have no significant effect on the results (Carbonell Muñoz et al. 2014). The angle at which the materials were bonded also had an effect on the results because it changed what percentage of the load acted as a shear or normal force along the bond. Therefore, it was recommended to use multiple interface angles and produce an envelope of the results (Austin et al. 1999). In general, this test gives values that are higher than the actual shear strength of a bond because of the normal force that occurs. Figure 2-30 shows how the results obtained from the slant shear test are consistently higher than those from a direct shear test when the same materials were tested multiple ways (Ferraro 2008).

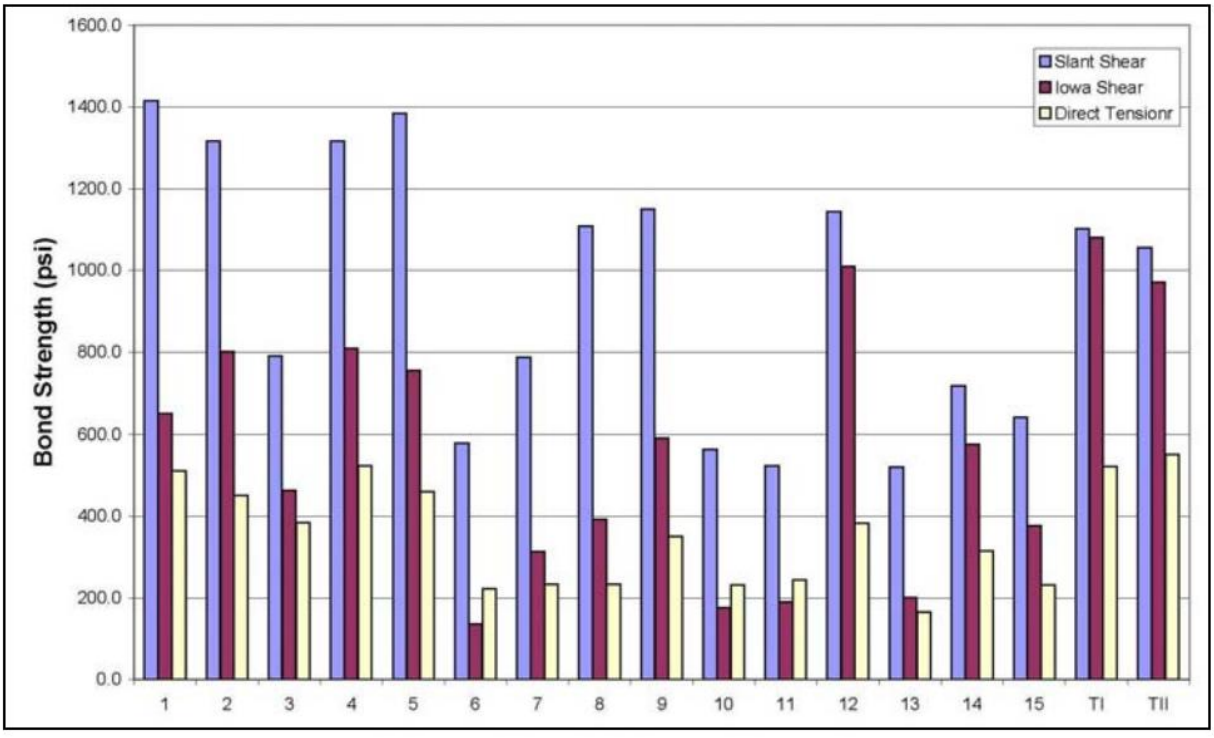

Figure 2-31: Bond strength between concretes based on test method used (Ferraro 2008)

A direct shear measurement can also be obtained from the Iowa shear test Iowa 406-C (Iowa Department of Transportation 2000). While this test has been labeled as inactive, it is a more direct measurement of the shear strength of the bond. In this test, the bonded surface is perpendicular to the vertical axis. The cylinder is tested on its side with a rig that applies a force in opposite directions for each half. This test has been shown to give consistently lower values for shear strength than ASTM C882 (Ferraro 2008), which is intuitive because the entire applied force is due to shear, as opposed to both shear and normal forces.

ASTM 1583 uses direct tension in a pull-off test for bond strength between two different materials (ASTM C1583 2013). In this test, often used for overlays, a core is taken of UHPC bonded to the underlying layer of concrete. The base of the core is left attached to the underlying concrete, and a tensile force is applied to the specimen (Carbonell Muñoz et al. 2014; ASTM C1583 2013). Because concrete has a higher shear strength than tensile strength, values for this test are predictably lower than those for bond tests in shear (Ferraro 2008). Therefore, values reported for bond strength should not be compared between test methods, and reported values should specify the test method. A comparison of multiple specimens tested with the three tests is shown in Figure 2-30.

A third-point bending test has also been used to determine bond with a flexural prism. Li used a 75 × 75-mm cross section prism with a length of 300mm, with the bond located in the center of the specimen in the vertical direction during testing (Li 2015). Li recommends this test method because although it is not commonly used or standardized, it does not require special equipment and gives reliable results (Li 2015) However, the results of his test did not agree between flexure, slant shear, and direct tension testing. Four materials were tested, and while the best mix in flexure also performed very well in the other tests, the worst flexural mix was ranked best for the slant-shear method and second best for the direct pull-off method. The slant shear and direct pull off methods seemed to have more correlation but still did not agree completely on which mix had the bests bond (Li 2015).

A very important characteristic that affects bond strength between UHPC and NSC is the surface preparation of the normal concrete. Ensuring that the existing concrete surface has a saturated surface dry (SSD) condition is the most important step in creating a good bond. This is because

the low w/cm of UHPC leaves unhydrated cement particles, and a saturated surface will help improve the hydration at the location of the bond (Carbonell Muñoz et al. 2014). Conversely, a dry surface will adsorb water from the UHPC, weakening it at that location. The Canadian code requires wetting the NSC to SSD condition before placing UHPC next to it (CSA A23.3 2018). Similarly, the Swiss code requires surface wetting for two hours prior to the placement, followed by drying of excess water on the surface (Brühwiler 2017). Excess water on the surface of the concrete will "float" to the top of the UHPC once it is placed, as previously shown in Figure 2-13. Roughening the concrete surface can also help improve bond between NSC and UHPC. Carbonell Muñoz et al. used multiple roughening methods including brushing, sandblasting, grooving, and exposing large pieces of aggregate (labeled "roughening"), and concluded that the bond was acceptable regardless of the extent of surface topography (Carbonell Muñoz et al. 2014). The Federal Highway Administration ranks bond strength as highest with exposed aggregate, less strong with sandblasting, and the weakest with an "as cast" surface (Graybeal 2014). An example of these surfaces is shown in Figure 2-31. Canada requires the aggregate in the existing concrete to be exposed and the surface cleaned before bonding (CSA A23.3 2018). Switzerland requires water jetting or shot blasting to be done to remove surface contaminants (Brühwiler 2017).

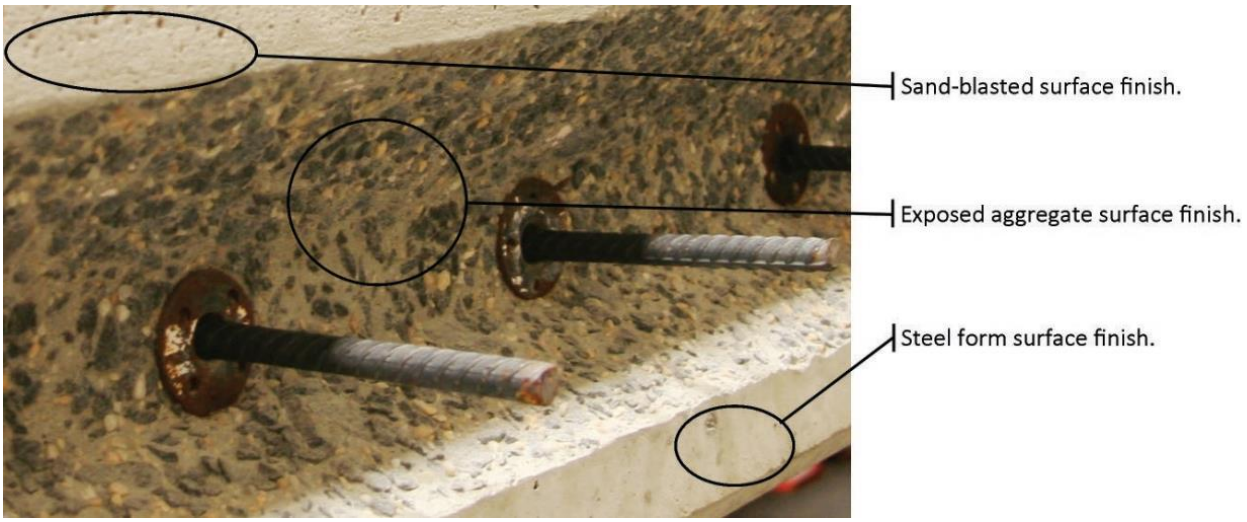

Figure 2-32: Types of surface preparation before bond of UHPC (Graybeal 2014)

UHPC typically does not bind well to hardened UHPC because there is no pore structure in UHPC to provide any interlock. To account for this, the Canadian standard requires the hardened UHPC

to be roughened until the fiber matrix is exposed, cleaned, and brought to SSD condition (CSA A23.3 2018).

2.7.6 ***Bond to Steel***

A property of UHPC that makes it desirable for use in joints is its ability to decrease rebar development lengths. While normal calculations for rebar development length do take concrete compressive strength into account (ACI 408-03 2003; ACI 318-14 2014), they do not account for the added strength from fiber reinforcement. Even in normal strength concrete, the addition of fibers can greatly increase the bond strength of steel reinforcement, as shown by Chao, et al. Fibers of different sizes, lengths, and materials were tested in concrete with compressive strengths ranging from 6-11 ksi (41 to 76 MPa), and it was discovered that the performance was superior to specimens with conventional spiral reinforcement (Chao et al. 2009). This is because the fibers can bind together cracks and prevent them from expanding enough for the reinforcement to slip. The fibers can also cause a multi-cracking failure, which is preferred to a failure with only a few large cracks. Tests performed by Saleem, et al. showed that for high-strength steel rebar embedded in UHPC, the development length can be even shorter than the value produced by the calculations in ACI 318, ACI 408, and AASHTO. They proved that development length (l_d) for a #3 bar can be as low as $12*d_b$ (where d_b is the bar diameter) and for a #7 bar as low as $18*d_b$ (Saleem et al. 2013). This is shorter than ACI's building code requirements of $16*d_b$ for bars below #7 and $20*d_b$ for bars equal to or above, as calculated for a concrete with 21,000 psi compressive strength (ACI 318-14 2014). Because ACI's requirements depend on concrete compressive strength, a normal strength concrete of 6,000 psi compressive strength would require coefficients of 30 and 38 for bars below and equal to or above a #7, respectively (ACI 318-14 2014).

An in-depth study of UHPC's strength with respect to bond with steel reinforcement was carried out by Alkaysi (2016). Numbers 4, 5, and 6 bars were tested using a direct pull-out test at different embedment lengths, coatings, fiber percentages, and fiber orientations. UHPC mixtures of 1% and 2% fibers by volume were tested. Alkaysi also normalized the data for fiber volume against the compressive strength data for the UHPC mixtures. This was done because current development length calculations for steel bars are based on the compressive strength of the concrete, and normalization ensured that the change in pull-out behavior was due solely to fiber percentage

change and not a result of an increase in compressive strength. At 8*d_b, the Number 4 bars failed due to fracture, and at 6*d_b, they failed due to fracture or to yield, slip. Fiber orientation relative to the reinforcing bar was not a statistically significant parameter (Alkaysi 2016). No. 5 bars experienced a decrease of 18% strength development with 1% fibers, and no. 6 bars had a decrease of 36%. The differences in the normalized data were similar to that of the raw data, supporting the conclusion that this change in strength was more attributed to the change in fiber content than due to an increase in the compressive strength of the concrete (Alkaysi 2016).

2.7.7 ***Creep, Shrinkage, and Prestress Loss***

Concrete creep is typically measured using ASTM C512 (ASTM C512 2015). In this test, concrete cylinders are loaded to 40% of their compressive strength, and strain is measured at various increments for a year. The stress is adjusted if needed to stay at the required 40%, and the results are plotted on a semi-log graph to solve Equation 2-41 (ASTM C512 2015).

$$\epsilon = \frac{1}{E} + F(K)\ln(t+1) \qquad \text{Equation 2-41}$$

Where: ϵ is the total strain per unit stress in MPa^{-1}

E is the instantaneous elastic modulus in MPa

$F(K)$ is the creep rate, which is equal to the slope of the line on the semi-log plot

t is the time after loading in days

When testing UHPC in creep, the adjustments per ASTM Cl856 require that the specimens loaded in compression are 3- × 6-in. specimens instead of the 6- × 12-in. specimens specified in ASTM C512 (ASTM C1856 2017). Steam-cured UHPC usually has very little creep after steam treatment (Binard 2017). This is a great advantage for prestressed concrete sections because beam camber will not increase after steam curing. A prestressed concrete producer using UHPC would be able to use heat treatment on a post-tensioning section before the prestressed force was added so that when the prestress force is added, it will not attenuate over time. Because of the pronounced effect heat treatment has on creep, the Canadian draft specification for UHPC requires creep tests to be performed only on specimens with no thermal curing and states that specimens with thermal

treatment typically have creep coefficients between 0.3 and 0.8 (CSA A23.3 2018). Lafarge lists the creep coefficient for its proprietary UHPC Ductal as being less than 0.8 without heat treatment and less than 0.2 with heat treatment (Ductal n.d.). The FHWA tested multiple UHPC mixes that were not thermally treated for both high-level and low-level load creep coefficients (Haber et al. 2018). The low-level creep coefficients ranged between 0.7 and 1.17, and the high-level load creep coefficients ranged between 0.78 and 2.47.

Shrinkage of UHPC can be tested in accordance with ASTM C157 (ASTM C157 2017). UHPC can exhibit very large shrinkage due to the high proportion of cement in the mix. Shrinkage of 500-1,000 microstrain is common for elements of UHPC (CSA A23.3 2018). However, like creep, shrinkage is negligible after steam treatment. This can be advantageous to precast concrete producers because the entirety of the shrinkage can be isolated to the period before the members are used in construction (Binard 2017). For UHPC cast in the field, it is important to account for shrinkage and to use formwork that does not cause stresses to develop in the material due to shrinkage, as this could cause cracking (CSA A23.3 2018). ASTM C1581 can be used to measure cracking caused by shrinkage restraint (ASTM C1581 2018). In this test method, a ring of concrete is cast around a steel ring and strain is measured over time. A sharp decrease in strain will show where the concrete has cracked.

2.8 UHPC Rheology

Many rheological tests have been performed on UHPC in laboratories, but the predominant method for field applications is the mini slump test (Brühwiler 2017; Choi et al. 2016). The mini-slump test for UHPC is described in ASTM C1856 (2017). It is similar to ASTM C1437 Standard Test Method for Flow of Hydraulic Cement Mortar (ASTM C1437 2015), with alterations to allow for field use. Only the mold and flow table as described in ASTM C230 are used (ASTM C230 2014). The mold shall be filled in one layer without tamping. The flow table is not dropped at all when used for UHPC (ASTM C1856 2017). The test should be performed one minute from the end of the mixing process (ASTM C1437 2015). After a two-minute period, the spread of the concrete is measured (ASTM C1856 2017). A picture of the flow table is shown in Figure 2-32. The heavy concrete pedestal and cork underneath the pedestal are not used in order to make the test portable. The UHPC is placed into the mold without consolidation. **Error! Reference source not found.**

shows the mini-slump test being performed on a batch of UHPC in the field. After the mold is removed, the mortar diameter is measured after two minutes without dropping. Figure 2-33 shows the result of the test being performed in Figure 2-34

Figure 2-33: Flow table used during UHPC field placement

Figure 2-34: Final flow of UHPC

Figure 2-35: Mini slump test performed in field

The mini slump test is used for batch approval by comparing the final spread value to a required value. However, Choi et al. showed that it is possible to get more fundamental material rheological properties out of the mini slump test by pairing it with computational fluid dynamics. By

measuring the spread over time for each test, they were able to use simple equations to give a Bingham model as an output. The results were compared with rheometer readings, and it was concluded that the mini slump test could be used to estimate the UHPC's rheological properties (Choi et al. 2016).

The small maximum aggregate size of UHPC enables the use of high-precision rheometers to quantify the concrete rheological properties without fibers. Arora et al. performed laboratory testing on different UHPC pastes using a rheometer with a vane-in-cup geometry. They were able to use a variable shear rate model to determine the yield stress more accurately than with Bingham or Herschel-Bulkley models. The plastic viscosity was also determined (Arora et al. 2018). This rheological information was paired with particle packing information from a MATLAB code to create a database of workability and strength information for a variety of mortar mixes with various supplementary cementitious materials (SCMs). This type of database could be useful for optimizing a mixture for desired characteristics. A material used for a joint with lots of steel reinforcement would need to be highly flowable and strong, whereas a mix used for a precast beam may not require the same level of workability (Arora et al. 2018). The results from the rheological and packing tests could also be weighted to aid in the decision-making process of mix selection (Arora et al. 2018).

The low w/cm of UHPC can cause problems with slump loss. Only a small amount of water loss due to evaporation can have a big impact on the consistency of the mix. Depending on the superplasticizer type and dosage used, UHPC can have an initial set time below 90 minutes (Li et al. 2016). The concrete mixture will start stiffening soon after mixing is stopped because of particle agglomeration (Ferron et al. 2013). This can cause problems if the mixing and placing process is not carried out efficiently. Higher superplasticizer dosages can increase the time before set (Li et al. 2016), but this will make the mix more expensive. In tests performed by Li et al., flow diameter was measured over time in batches using a dosage of 2.2-2.6% of four different superplasticizers. Three of the four superplasticizers tested resulted in a flow diameter reduction of about 25% in the first 90 minutes (Li et al. 2016). This reduction in workability is particularly detrimental for UHPC because using vibration as a compaction method can cause fiber segregation or preferential alignment (CSA A23.3 2018).

2.9 Durability

The excellent durability properties of UHPC can help justify the increased material cost for some applications in transportation structures. The excellent durability mainly stems from improved transport properties and material toughness.

*2.9.1 **Transport Properties***

UHPC has been found to have very low chloride ingress over a 15-year period in field trials at the Treat Island, Maine concrete exposure site. All UHPC specimens tested showed no chlorides below a depth of 10 mm, compared with chlorides up to 23 mm found in high performance concrete (HPC) (Thomas et al. 2012). This can principally be attributed to the disconnected pore structure. For a concrete with very low porosity like UHPC, the probability of pores in the interior being connected through the pore network to the surface for chloride access decreases with depth from the surface. After a few millimeters of depth, very few if any pores connect the surface, essentially stopping further ingress (Thomas et al. 2012).

Chloride diffusion can be measured using ASTM C1556 Standard Test Method for Determining the Apparent Chloride Diffusion Coefficient of Cementitious Mixtures by Bulk Diffusion (ASTM C1556-11a 2016). In this test method, concrete samples at least 3 in. thick are covered with epoxy on all but one side and soaked in a bath of 16.5% sodium chloride for at least 35 days. Afterwards, thin sections of the sample are ground and the amount of acid-soluble sodium chloride in each layer is determined by titration (ASTM C1556-11a 2016). This test requires less specialized equipment than ASTM C1202, and it does not have an electrical component, meaning that it would work even with UHPC samples containing macrofibers or high fiber percentages. A drawback to this method is that it takes much longer to run the test. While 35 days is specified by ASTM C1556, higher-quality concretes like UHPC require much longer exposure times. The Nordtest version of this standard was run by Piérard et al. with a 90-day exposure time (Piérard et al. 2012). Even with a much longer test, however, the results still showed no chlorides below a depth of 3mm. A chloride diffusion coefficient of 0.2×10^{-12} m^2/s was calculated. Similar results were found by Schydt et al. for UHPC exposed for less than four months, but chlorides were found in the sample up to 5 mm deep for UHPC exposed for 16 months (Schydt et al. 2008).

Because the test for chloride diffusion takes a long time to run, a rapid chloride migration test can be used. This test has been standardized as NT Build 492 (1999). This test method uses an electrical current to accelerate chloride migration through the concrete. A 2-in. thick concrete sample is placed in a bath such that one side of the concrete is exposed to a 10% NaCl solution, while the other side is exposed to a 0.3 N NaOH solution. Based on the initial electrical current passed through the sample, the voltage applied and length of the test is adjusted. After the electrical current is turned off, the sample is cracked open and a 0.1 N silver nitrate solution is applied to the interior surface. The distance the chlorides migrated is measured every 10 mm across the sample (NT Build 492, 1999). The flexibility afforded by the adjustable length and duration of the test allows its application to a wide range of materials. This is especially helpful for UHPC because chlorides infiltrate the dense matrix at a very slow rate under normal conditions, causing tests such as ASTM C1556 to take longer than usual to give useful information.

A common method of durability testing for normal concrete is ASTM C1202 Standard Test Method for Electrical Indication of Concrete's Ability to Resist Chloride Ion Penetration (ASTM C1202-17a 2017), or the "rapid chloride permeability test (RCPT)." In this test method, a constant voltage is applied across a vacuum-saturated 2-in. (50-mm) thick concrete specimen and the current passing through the sample is measured and recorded over time (ASTM C1202-17a 2017). A specimen with a more connected pore structure will allow a higher current to pass through, which is associated with a less durable concrete. Because UHPC is a hybrid material containing conductive steel fibers, there has been concern that an electrical test may give a misleadingly high current value as a result. ASTM C1202 states that it "is not valid for specimens containing reinforcing steel positioned longitudinally, that is, providing a continuous electrical path between the two ends of the specimen (ASTM C1202-17a 2017)." Whether ASTM C1202 is applicable to UHPC is somewhat under debate. While ASTM C1856 does not allow for the use of RCPT with steel-fiber-reinforced UHPC, Graybeal (2006) stated that fibers used in UHPC are small and randomly dispersed enough to be disconnected. Therefore, short-circuiting does not affect the results of the test (Graybeal 2006). Many codes and specifications still use this test as a durability requirement for UHPC mix approval (AFNOR 2016; Brühwiler 2017; CSA A23.3 2018). The Canadian specification on UHPC, which is designated as informative instead of mandatory, allows for a specimen tested for rapid chloride penetration to be made with or without the fibers so that a

mixture's approval will not be hindered by any adverse effects from fiber content (CSA A23.3 2018). Based on data from multiple studies, UHPC is typically categorized by this test as having negligible or very low chloride ion penetrability (Russell and Graybeal 2013; ASTM C1856 2017; Ahlborn et al. 2008; Alkaysi 2016).

*2.9.2 **Freeze-Thaw***

UHPC has been shown to work very well in aggressive freeze-thaw environments. Normal concrete mixtures contain air entrainment admixtures to provide air entrainment in the concrete, providing some protection against freeze-thaw conditions. Much of the benefit of air entrainment comes from its ability to reduce the degree of saturation of the concrete. Bulk freeze-thaw damage typically only occurs when the concrete degree of saturation is above a critical level (Li et al. 2011). Even without air entrainment, UHPC helps prevent freeze-thaw damage by keeping the degree of saturation low. UHPC experiences self-desiccation during hydration, giving a low relative humidity in the pores (Ma et al. 2003). UHPC has a microstructure tightly packed enough to prevent most water from entering into the few voids that are present and re-saturating the concrete (Graybeal 2006).

ASTM C666 (2015) is a common lab test to determine the durability of concrete under repeated freeze-thaw cycles. Damage is measured as a decrease in the concrete dynamic modulus of elasticity, mass change, and, optionally, length change. Both Ahlborn et al. and Graybeal reported a small amount of mass gain of less than 1%, which is unusual (Graybeal 2006; Ahlborn et al. 2008). This could be because the thaw cycles took place in a water bath, which could have allowed the specimens to absorb a small amount of water and potentially hydrate and therefore increase in mass instead of lose mass due to crumbling (Graybeal 2006). Piérard et al. performed a similar test on UHPC with fewer cycles and only one surface exposed to the solution. Here, very minor mass loss was recorded, which equaled about 1/6 the amount accepted for road applications while using almost four times the number of cycles (Piérard et al. 2012). UHPC samples placed at the Treat Island, Maine, concrete field exposure site demonstrated very high resistance to freeze-thaw damage. After 1,500 cycles of freezing and thawing under wet marine tidal conditions, they showed no appreciable loss in mechanical properties or visual signs of damage (Thomas et al. 2012).

2.9.3 ***Abrasion Resistance***

Abrasion resistance is commonly required for the approval of UHPC when it is used in pavement or bridge surfaces that interact with vehicle tires (AFNOR 2016; Brühwiler 2017; CSA A23.3 2018). The resistance of UHPC when in contact with snow tires is often measured according to ASTM C944 Standard Test Method for Abrasion Resistance of Concrete or Mortar Surfaces by the Rotating-Cutter Method (ASTM C944 1999). In this test method, a concrete sample is placed on a drill with rotating cutters attached to the drill head. A 44-lb weight is attached to the top of the spindle that turns the drill press, giving consistent impact of the rotating cutters on the surface of the concrete. Because of UHPC's high resistance to abrasion, the 44-lb double load on the rotary cutter is used instead of the typical 22-lb load (ASTM C1856 2017). While typical UHPC has excellent abrasion resistance (1-3 g of material loss per two-minute cycle), this can be greatly improved by heat treatment. Graybeal showed values of 0.1-0.3 g of concrete loss when the specimens had been heat treated. A delayed steam treatment did not appear to affect the results, but a tempered steam treatment showed slightly higher values of mass loss (Graybeal 2006).

2.9.4 ***Alkali-Silica Reaction***

Alkali-Silica reaction is a common problem in many concretes, however this has been reported to not be a concern with UHPC. While UHPC can have very high alkali levels per unit volume, it also contains very high amounts of SCMs such as fly ash that can mitigate ASR (Rangaraju et al. 2016). Additionally, ASR does not typically occur when the relative humidity in the concrete drops below 82% (Rust 2009). Since UHPC does such a good job of reducing water penetrability, this is usually not an issue. Piérard et al. reported no expansion or deterioration of UHPC samples immersed in a hot sodium hydroxide solution for 20 days (Piérard et al. 2013). UHPC tested by Graybeal showed expansion levels of less than 0.020%, where the standard level for "innocuous" is 0.100%. This is likely due to the fact that UHPC has no free water and is practically impermeable (Graybeal 2006).

Rangaraju et al. reported rapid expansion when testing UHPC mortar for ASR. This characteristic was observed in mixes without fly ash as the cement's alkali content increased (Rangaraju et al. 2016).

*2.9.5 **Sulfate Attack***

UHPC has excellent durability against sulfate attack. Sulfate ions have difficulty penetrating the concrete because of the very tight microstructure. One study of UHPC bars showed no expansion after 500 days of exposure to a sodium sulfate solution because of the low penetrability (Piérard et al. 2013). Li showed that using fly ash in a UHPC mix reduced the effects of sulfate attack (Li 2015). Slag has also been shown to reduce sulfate attack (Eide and Hisdal 2012).

2.10 Material Properties of Proprietary UHPCs

While UHPC is a relatively new material in the United States, there are already multiple proprietary mixes available. This is advantageous for projects because using a proprietary mix that has proven to be successful in the past makes adoption faster and usually comes with technical support from the manufacturer. Project planning is also simplified because the material proportions and mechanical properties are known. The Federal Highway Administration recently tested six different proprietary mixes from companies around the world. The brands were kept anonymous, but the mix constituents are listed in Table 2-7, along with the percentage of the mix by mass. Note that fiber content for UHPC is typically listed as a percent by volume value, and 1% of steel fibers by volume typically equals 3.1-3.3% of fibers by mass (Haber et al. 2018).

Table 2-7: Proprietary UHPC mixes available, with mass percentages (Haber et al. 2018)

	Supplier											
	A		B		C		D		E		F	
Material	Type	Mass%	Type	Mass %	Type	Mass%	Type	Mass %	Type	Mass%	Type	Mass %
Cementitious materials	Type H oil well cement	31.5	Pre-bagged powder	84	Pre-bagged powder	80.4	Pre-bagged powder	86.6	Pre-bagged powder	75.8	Pre-bagged powder	87.2
	Ground quartz	8.7										
	Silica fume	12.3										
Aggregates	Silica sand	30.5										
Chemical admixtures	High-range water reducer	0.5	High-range water reducer	1.1			High-range water reducer	0.7	High-range water reducer	1.7	High-range water reducer	1.5
							Water reducer	0.5				
							accelerator	0.9			VMA	0.035
Fibers (length, diameter)	macrofibers (1.18 in., 0.022 in.)	9.9	Short fibers (0.5 in., 0.012 in.)	2.1	Fibers (0.5, 0.012 in.)	13.7	Fibers (0.5 in., 0.008 in.)	6.2	Fibers (0.5 in., 0.008 in.)	6.2	Fibers (0.5 in., 0.008 in.)	10
			long fibers (0.79 in., 0.012 in.)	4.3								
Water	Water	6.6	Water	8.5	Water	6	Water	5.1	Water	8.9	Water	5.6

The proprietary mixes given in Table 2-7 were tested for compressive and tensile strength, along with other mechanical properties and durability properties. In addition to the recommended fiber dosage from the supplier, the mixes were also tested with fiber volume percentages of 2, 3, 4, and 4.5 percent, with the exception of UHPC-F which was tested with 3.25% fiber by volume instead of 3%, per manufacturer recommendations (Haber et al. 2018). The results of the different tests are presented in Table 2-8.

Table 2-8: Properties of proprietary UHPC mixes (Haber et al. 2018)

Concrete Properties	A	B	C	D	E	F
Static Flow (in)	5.75	10 (max)	4	7.5	7.13	5.75
Dynamic Flow, 20 drops (in)	8.36	10 (max)	7.63	9	8.75	7.75
Initial set (hours)	>9	8	4.3	5.3	>9	
Final set (hours)	<15	10.1	8	7	<24	
7 Day Compressive Strength (ksi)	17.4	15.8	17.7	19.5	14.9	
14 Day Compressive strength (ksi)	19.1	18.8	20.2	21.3	17.4	
Compressive strain at peak stress	0.0033	0.004	0.0042	0.0034	0.0047	
Poisson's ratio	0.1469	0.1451	0.1573		0.165	
Direct Tension, 2% fiber, age (days)	6	28	4	7	4	
First cracking strength (ksi)	0.7	1.10	0.76	0.36	0.89	
Ultimate cracking strength (ksi)	0.94	1.21	0.85	1.21	1.02	
Split Cylinder, age (days)	5	5	15	7	5	
Fiber content (%)	3	3.25	4.5	3	3.25	
First Cracking Strength (ksi)	1.08	0.91	1.09	1.00	0.94	
Peak Strength (ksi)	2.56	1.95	3.04	2.55	2.10	
High-level load creep coefficient	1.37	1.42	1.53	0.78	2.47	
Low-level load creep coefficient	0.7	0.9	0.71		1.17	
Autogenous shrinkage, 147 days (microstrain)	-600	-430	-720	-210	-880	-340
Drying shrinkage, 147 days	-660	-680	-770	-300	-1220	-560
Rapid Chloride Ion Penetration, 28 days (coulombs)	302	5100	425	789	470	
Rapid Chloride Ion Penetration, 56 days (coulombs)	53	2501	298	495	303	
Freeze-Thaw Resistance, RDM (%)	102	103	99	101	100	
Pull out, peak bar stress, 2% fiber volume (ksi), $l_d=8*d_b$	116	136.5	125.6	133.1	109.5	
Direct Tensile Pull-Off test (ksi)	0.339	0.482	0.217	0.417	0.371	

A downside to proprietary UHPC mixes is the high cost. While these mixes are very strong and durable, they cannot be adjusted to fit the project most efficiently. Therefore, extra expense is incurred where a weaker, less expensive concrete could also meet strength and durability requirements.

CHAPTER 3. UHPC PRACTICE SURVEY

3.1 Introduction

While UHPC has been shown to behave very well in a laboratory setting, it is important to also study its use in practical field settings. A survey was sent out to an employee from the department of transportation of each state and Ontario in Canada. The survey participants were selected from a combination of the AASHTO Committee on Materials members and online searches for state DOT employees and their roles. The employee from each state with the role most suited to concrete materials research was chosen to be a survey recipient, but each recipient had the ability to forward the survey to a different individual who may have more knowledge on the subject or more time available with which to complete the survey. Any surveys that were started but left unfinished were still submitted and recorded. If there was a discrepancy between the survey and the received specification, the specification was used.

3.2 Survey Questionnaire

Survey questions presented to each participant were varied based on previous responses so that participants were not asked questions that did not apply to their experiences. The survey began by asking states about their past use of UHPC and possible planned future use. The response to this question (Question 2) was then used to determine which other questions the participant would be asked. The survey questions are presented in Table 3-1, along with a description of which participants were asked each question. Multiple choice questions that included an optional text entry were written with a blank following the response option.

Table 3-1: Survey questions and associated logic

Number	Question	Asked to:
1	Which State DOT do you work for?	All participants
2	What is your state's history of using UHPC? (check all that apply) o Full structural elements (beam, pier…) made of UHPC have been used o UHPC has been used for connections/joints between precast elements o UHPC has been used for repair projects o UHPC has not been used but is being considered for future projects o Our state has written specifications for the use of UHPC o Our state DOT has not thought about using UHPC	All participants
3	Has your state considered (or do you already have) multiple classes of high performance concrete? (For example: HPC: 8-15ksi, Very HPC 15-21ksi, Ultra HPC 21ksi+) o Only HPC is defined o HPC and UHPC are defined without levels or tiers above or between o Multiple levels or tiers of HPC are defined _____. o Other_____.	All participants except those who have not thought about using UHPC
4	How does your state specify UHPC? Please list a numerical value and/or specific tests used for approval/qualification of UHPC, if applicable. o Compressive strength _____. o Tensile strength _____. o Flexural strength _____. o Modulus of Elasticity _____. o Durability requirements_____. o Other_____.	Participants who said their state had a written UHPC specification
5	If your state has a written specification for the use of UHPC, or if there has been a DOT project with UHPC project specifications, please upload them below if possible. [file upload]	Participants who said their state had a written UHPC specification
6	Which of the following mix designs have been used?	Participants who said their state had used UHPC

Table 3-1, continued

Number	Question	Asked to:
7	What tests were used for qualification of the mix? o Compression Test o Flexure test o Fiber dispersion test o Flow/spread test o Other _____.	Participants who said their state had used UHPC
8	If known, what kind of mixer was used for UHPC mixing (size, horsepower, brand)	Participants who said their state had used UHPC
9	What surface treatment (if any) was used between pours to eliminate cold joints?	Participants who said their state had used UHPC
10	What, if anything, would you do differently in the future?	Participants who said their state had used UHPC
11	How has UHPC performed since the casting? [The following options were presented for: Structural performance, durability, and aesthetics]. o Worse than normal concrete o Equal to normal concrete o Slightly better than normal concrete o Much better than normal concrete o Unsure/Not applicable	Participants who said their state had used UHPC
12	What reason(s) do(es) your state have for not using UHPC in DOT projects? o The cost is too high o There are no problems with our current system o Contractors do not have experience mixing and placing UHPC o The stat has no specification for the use of UHPC o Not enough is known about the behavior of UHPC o Other (please specify) _____.	Participants who said their state had not used UHPC

3.3 Survey Results

Overall, 32 responses were recorded from the survey, including 30 states, Washington, D.C., and Ontario, Canada. The results are shown in Table 3-2. The participants' answers to these questions

determined which of the remaining 12 questions they were asked to respond to, as described in **Error! Reference source not found.**. From **Error! Reference source not found.**, it can be seen that joints were the most common use of UHPC in bridge construction, while a few had experimented with bridge elements made from UHPC. A significant number of states have UHPC specifications in place, and many are actively considering its use.

Table 3-2: Question 2: What is your state's experience with respect to UHPC?

	We have not thought about using it	Not used but considering future use	Used for joints/ connections	Used for repair	Full structural elements	We have a written specification
Alabama		■				■
Arkansas	■					
Colorado		■				
Delaware			■			■
Florida			■	■		
Idaho			■		■	■
Indiana		■				
Iowa			■		■	■
Kansas	■					
Kentucky	■					
Maine			■			
Maryland						■
Michigan			■			■
Montana			■			
Nebraska			■			
Nevada		■				
New Hampshire	■					
New Jersey			■			■
New Mexico		■			■	■
New York			■			■
North Carolina	■					
North Dakota	■					
Ohio			■			
Oklahoma		■				

Table 3-2, continued

	We have not thought about using it	Not used but considering future use	Used for joints/ connections	Used for repair	Full structural elements	We have a written specification
Oregon			■			■
Tennessee	■					
Texas		■				■
Virginia		■	■		■	■
Washington		■				
West Virginia		■				■
Ontario			■			■
Washington DC			■			
Total	7	10	15	1	4	14

Respondents who reported no usage of UHPC in their state were asked for reasons as to why they have not used it, whether or not there was planned future use. The results are shown in Table 3-3.

Table 3-3: Question 12: What reason(s) do(es) your state have for not using UHPC in DOT projects?

	It is too expensive	We have no problems with our current system	Contractors lack experience	We have no specification for UHPC	Not enough is known about UHPC behavior	We have no need for UHPC/such high strength*
Alabama			■			
Arkansas		■				
Colorado	■	■	■	■		
Indiana				■	■	■
Kansas	■	■	■	■		
Kentucky		■	■	■		
Nevada			■	■	■	
New Mexico	■		■			
North Carolina		■	■	■		
North Dakota		■	■	■		
Oklahoma	■		■	■		
Tennessee	■					■
Virginia	■		■			■
Washington	■		■			
West Virginia[+]						
Total	7	6	11	8	2	3

*This response was not presented a multiple-choice option, but it was included by three states in the write-in section.

[+]West Virginia submitted a write-in response as, "Alternate construction method was used. Pending use on future projects."

It can be seen that the most common reason for a lack of UHPC use was that the contractors lacked experience working with UHPC. Only four states excluded this in their list of reasons. This is likely one of the most difficult barriers to overcome because contractors will not be able to gain experience if no UHPC projects occur in the state. Some state specifications, including those for Alabama, Iowa, New Jersey, New York, and West Virginia, require that a representative of the UHPC manufacturer is present during the mixing and pouring process. Alabama and New Jersey

specify that this representative must have at least five years of experience with UHPC. This ensures that all processes are done correctly, even if the contractors have never worked with UHPC before. While this requirement adds cost to a project, it is a good quality control measure that will help contractors gain experience and may help allow for successful projects while contractors gain the experience needed.

Many states also listed a lack of specification as a barrier to prescribing UHPC for projects. However, six respondents from Table 3-1 recorded past usage of UHPC but no state specification, showing that UHPC has been used without state specifications in place. It should be noted that in all cases of UHPC usage without a specification, UHPC usage was limited to proprietary mixes used for joints. Because proprietary UHPC providers have high standards for their material properties and often oversee the mixing and placement, it is reasonable that these materials could be used without state formal blanket specifications in place.

The third most common reason listed for not using UHPC was the high expense. Any UHPC mixture will be inherently expensive due to the materials required in the mix: large quantities of cement, supplementary cementitious materials, and admixtures. Steel fibers are also a very important component, and a lack of suppliers in the United States makes them expensive. There are also only a handful of proprietary UHPC mixes available in the United States, and they all have extremely high compressive strengths. Three states noted that UHPC was not used due to the high strengths being unnecessary for their projects. For proprietary mixes, this cannot be adjusted, but non-proprietary mixes could be designed for a particular project specification, even if the compressive strength did not reach the specified UHPC compressive strength definition. For example, Ontario lists compressive strength requirement but also allows for project-specific specifications different from what is listed. Table 3-4 shows the different strength requirements used by different states. Some states use ASTM C39, while others use AASHTO T22 to test for compressive strength.

Table 3-4: Compressive strength requirements by state or other entity, in ksi (MPa)

	24-hour	4-day	7-day	28-day	Before opening to traffic
Alabama		14 (97)		21 (145)	14 (97)
Delaware				14 (97)	
Idaho		14 (97)		20, 25 (138, 172)*	
Iowa	10 (69)				15 (103)
Maine				21 (145)	
Michigan			15 (103)		
Nebraska				21 (145)	
New Jersey	5.7 (39)	11.6 (80)		14.5 (100)	
New Mexico		14 (97)		21 (145)	
New York		12 (83)		21 (145)	
Texas		14 (97)		21 (145)	
West Virginia		12 (83)			15 (103)
Ontario		11.6 (80)		18.9 (130)	
Canada				17.4, 21.7 (120, 150)†	
France				18,850-36,300 (130-250) +	
Switzerland				17.4 (120)	
Colombia				21.7 (150)	

*Idaho requires 20 ksi for non-heat-treated and 25 ksi for heat treated concretes

†Canada uses two different compressive strength classes for UHPC

+France defines seven different strength classes within this range

Most states use a 28-day strength of 21,000 psi for their UHPC requirement. Most also have an early strength requirement. It should be noted that the respondent from New York mentioned that the state department of transportation is considering lowering the compressive strength requirement for UHPC, which could make it cheaper and more practical to use. Delaware, New Jersey, West Virginia, and Michigan have much lower requirements than average, at 14, 14.5, 15, and 15 ksi, respectively. Delaware's specification previously required a strength of 22 ksi, but it has been changed in their specification. Of all the respondents reporting that they had used UHPC, only two had used non-proprietary mixes: Michigan and New Mexico. These results are recorded in Table A-4 of the Appendix. As previously shown, Michigan has a lower compressive strength requirement than the average. The respondent from Michigan stated, "Many people prefer the

proprietary approach to the non-proprietary approach." New Mexico currently only has a specification for proprietary mixes but is working on one for non-proprietary mixes as well. This shows that different requirements may be necessary for non-proprietary mixes.

Respondents who said their states had used UHPC were asked how it performed when compared with normal concrete. The results are presented in Table 3-5. About 1/3 of respondents were unsure of how the performance compared with regular concrete. On average, structural and durability performance was ranked as better than normal concrete, and appearance was ranked as equal. The responses listed by state are presented in the Appendix in Table A-9.

Table 3-5: Question 11: How has UHPC performed compared to normal concrete?

	Unsure/Not Applicable	Worse	Same	Slightly Better	Much Better
Structural	4	0	1	1	8
Durability	6	0	1	2	5
Aesthetics	5	1	7	1	0

Table 3-6 and Table 3-7 show the mechanical properties and durability requirements by states that have UHPC specifications. Cells with an "X" denote that the state requires this property to be tested, but the minimum/maximum value is unknown. Quantities that are listed as "reported" do not need to pass a specified value but must be tested and reported.

Table 3-6: Mechanical properties required by state and country specifications

	Tensile strength ksi (MPa)	Flexural strength ksi (MPa)	Flexural Toughness ASTM C1018	Modulus	Slump Flow in. (mm)	Bond
Alabama	AASHTO T 198, 1.0 (6.9) splitting				AASHTO T347, 7-10 (180-250)	
Delaware					ASTM C1611 17-22, (430-560) no bleed water, consistent fiber distribution	
Idaho		ASTM C293, 2 (14)			ASTM C230, 7-10 (180-250)	
Iowa					ASTM C109, 7-10 (180-250)	
Michigan					7-12 (180-300)	
New Jersey			$I_{30} \geq 48$			
New Mexico					ASTM C1437, 7-10 (180-250)	
New York			$I_{30} \geq 48$			Pull-out test
Texas			$I_{30} \geq 48$			
Ontario		ASTM C1609, 2.2 (15)			ASTM C109 Within 0.59 (15) of target identified by contractor	
Canada	0.58, 0.73 (4, 5), direct tension	0.58, 0.73 (4, 5) with inverse analysis		Reported		
Colombia	1.0 (7)					
France	0.87 (6), elastic limit, direct tension	0.87 (6), elastic limit, with inverse analysis		Reported		

Table 3-6, continued

	Tensile strength ksi (MPa)	Flexural strength ksi (MPa)	Flexural Toughness ASTM C1018	Modulus	Slump Flow in. (mm)	Bond
Switzerland	1.0 (6.9) elastic limit, 1.1 (7.6) direct tension	1.0 (6.9) elastic limit, 1.1 (7.6) SIA 2052, Appendix E	X (fatigue resistance)	Reported	Reported	Pull-off test

Table 3-7: Durability properties required by state and country specifications

Property	Chloride Ion Penetrability (coulombs)	Shrinkage (microstrain)	Chloride Ion Penetrability (oz/ft^3)	Scaling Resistance	Freeze-Thaw (RDM %)	Abrasion Resistance (oz.)	Alkali-Silica Reactivity
Test Method	ASTM C1202/ AASHTO T 277	ASTM C157	AASHTO T259	ASTM C672	ASTM C666A, 600 cycles	ASTM C944, 2x weight	ASTM C1260
Alabama	≤ 250	≤ 800, AASHTO T160				< 0.026	
Delaware	≤ 250	≤ 800	<0.07, ½ in. (13 mm) depth	y < 3	> 95%		ASTM C1567, ≤ 0.08%, test at 28 days
Idaho	< 250	< 765, initial reading after set	< 0.07, $1/4^{th}$ in. (6 mm) depth	y < 3	> 96%	< 0.025, ground surface	ASTM C1567, < 0.10%, test at 28 days
New Jersey	≤ 250	≤ 800	<1.0, ½ in. (13 mm) depth	y < 3	> 96%	< 0.03	Innocuous, test at 28 days
New Mexico	≤ 360	≤ 800	<0.059, ½ in. (13 mm) depth	No scaling	> 99%, 300 cycles	< 0.026	< 0.10%, Innocuous
New York	≤ 250	≤ 800, initial reading after set	< 0.07, $1/5^{th}$ in. (5 mm) depth	y < 3	> 96%	< 0.025, ground surface	Innocuous, test at 28 days
Texas	≤ 250	≤ 800		y < 3	> 96%, 300 cycles		< 0.1%
Canada	<500, <300, <100	X (different method)		CSA A23.2-22C 0.4,0.2,0.1 kg/m^2		<5, <1, <0.5 g	
France					X	X	Non-Reactive
Switzerland	< 250	< 800	<0.07, ½ in. (13mm) depth		> 96%	< 0.025, ground surface	Innocuous, test at 28 days

As seen in Table 3-6, few states require a flexural or tensile strength test to be performed for mix approval. Iowa previously included a flexural strength requirement of at least 5 ksi, according to ASTM C78. However, Iowa recently removed this requirement from its UHPC specification. Some states use a flexural toughness test according to ASTM C1018 in place of a flexural strength test. This test is described in section 0 of this report. The value required to be reported by New Jersey, New York, and Texas is I_{30}, which is calculated by taking the area under a load vs. deflection curve up to a deflection of 15.5 × the deflection at the first peak strength, and dividing that value by the area under the curve up to the first peak strength (Reza 2018). For countries such as Canada, France, and Switzerland, tensile strength can be determined either by a direct tension test, or by inverse analysis in a flexural test (AFNOR 2016; Brühwiler 2017; CSA A23.3, 2018). France's UHPC specification describes its own detailed flexural test and calculations, as summarized in section 2.7.3. Switzerland uses the method in SIA 2025, Appendix E (Brühwiler 2016). These requirements should not be compared directly with the flexural strengths required by Idaho and Ontario. While both are strength values from a flexural test, flexural strength will be higher than tensile strength as determined by inverse analysis. ASTM C1609, as specified by Ontario, is the suggested flexural test given by ASTM 1856, and is described in section 2.7.3 in more detail (ASTM C1609 2012; ASTM C1856 2017). ASTM C293, as specified by Idaho, is a three-point flexural test designed for normal-strength concrete (ASTM C293 2016), unlike ASTM 1609, which was designed for fiber-reinforced concrete.

Flow tests are common for UHPC, but a variety of different specifications are used. ASTM 1856 describes the flow test for UHPC as being in accordance with ASTM C1437, with the flow table and mold according to ASMT C230, and adjustments such as filling the mold in one layer and avoiding tamping or table dropping. However, some states used a combination of these regulations, as seen in Table 3-6. Some states, such as New York and New Jersey, only require a flow test to be done for quality control of a mix. This is a realistic practice because flow can be easily adjusted with the addition of superplasticizer, and on-site environmental factors like temperature may have an effect on the spread value, which could not be accounted for in laboratory conditions.

New York has its own procedure for testing UHPC bond to steel, which is described in detail in their UHPC specification, according to Test Method No. NY 701-14. Steel reinforcing bars are

cast into UHPC cylinders of 12-in. (300-mm) diameter and 7.5-in. (190-mm) depth. The bars are epoxy coated. Three #4 bars are embedded 3 in. (76 mm) deep, and three #6 bars are embedded 5 in. (130 mm) deep. The material passes the test if the embedded bars yield before they are pulled out of the cylinder or the UHPC fails.

Switzerland requires a pull-off test to be performed to test the bond of UHPC to a substrate concrete. The test must be performed at seven days, and the substrate concrete and its surface texture must be representative of the material in the field. Because the Swiss specification used in this study is still in a draft state, there is not yet a specified standard by which this test must be run (Brühwiler 2017).

Durability requirements for state and country specifications are listed in Table 3-7. Typical ASTM standards for these tests are listed in the second row of the table, and adjustments are made for states specifying a different standard. The survey did not specifically ask about each of the following durability requirements, so the values in **Error! Reference source not found.** have mostly been found from specifications submitted by the states. A list of states from whom specifications were received is shown in Table A-3. Some values are taken from responses to Question 4, relating to how states specify UHPC. The responses from this question are shown in Table A-2. While Iowa, West Virginia, and Ontario all submitted specifications, no durability tests were listed. In the case of Iowa and West Virginia, this may be because they only allow for the use of Ductal concrete, which has durability values that are reported by Lafarge. Ontario's specification is also limited to a proprietary mix, but no supplier is specified.

Most of the tests listed in Table 3-7 are uniformly used throughout the states with specifications and have similar approval values. The exception is with the AASHTO T259 test for chloride ion penetrability. While similar concentrations are specified for each state (except New Jersey), the depths differ between 1/5-1/2 inch. While Iowa does have a UHPC specification, it only allows for the use of Ductal brand UHPC. Because this proprietary mix has published test values and constant mix proportions, it is reasonable that Iowa's state specification does not require any testing to be done to approve the mix.

Among the tests listed in Table 3-7, a number of other tests were described in the specifications for Canada, France, and Switzerland. Many of these tests require values to be reported, but do not necessarily have a threshold value that must be achieved.

- **Fire Resistance:** France and Switzerland require fire resistance to be tested. Switzerland does not specify how this is done. France uses the French test NF EN 13501-1+A1 to classify UHPC, and mixes containing <1% by weight or volume (whichever is lower) of organic material do not require tests. Otherwise, a full-scale test or thermochemical modeling must be performed. To determine a mix's sensitivity to spalling, it shall be experimentally tested with a representative member of the structure (AFNOR 2016). Canada requires 0.2% of polypropylene fibers by volume to be in UHPC that may be exposed to fire, and 0.3% for UHPC exposed to hydrocarbon fire (CSA A23.3 2018). France and Switzerland also city polypropylene fibers as being beneficial to prevent spalling in UHPC exposed to fibers, but do not give a required volume.
- **Water absorption:** France and Switzerland also require a water absorption/porosity test to be performed. France requires less than 9.0% water porosity according to NF P 18-459. Switzerland uses SN EN 13057, with a requirement of a mean capillarity coefficient of $\leq 100 g/m^2 h^{0.5}$ across six specimens tested at 28 days. France includes a gas permeability test according to standard XP P 18-463:2011, with provisions as specified in A.2.1 (AFNOR 2016).
- **Creep:** All three countries require creep and/or shrinkage testing to be performed, except for thermally treated specimens in Canada and France, where creep can be assumed to be

non-existent after treatment. France uses NF P 18-710:2016 and NF EN 1992-2:2006 for creep determination. Canada's creep coefficient is determined according to ASTM C512, with modifications in ASTM C1856 (CSA A23.3 2018).

- **Shrinkage:** Shrinkage in Canada is determined with CSA A23.2-21C (CSA A23.3 2018). Thermal treatment causes almost all shrinkage to occur during the steam treatment period, meaning future shrinkage will be negligible and creep coefficients will be very low.
- **Poisson's ratio:** Canada and France require a determination of the concrete Poisson's ratio, France according to NF EN 12390-13:2014, and Canada as described by ASTM C469, in accordance with ASTM C1856.
- **Slope stability:** Switzerland requires a test for slope stability, where UHPC overlays on slopes of more than 2% must be tested using a plate 3 meters long of corresponding slow and surface texture. This test is performed with visual inspection to ensure that the layer of UHPC does not undergo deformation after placement and hardening(Brühwiler 2017).
- **Sulfate Resistance:** Canada requires sulfate resistance to be tested according to CSA A3004-C8, and limits expansion to 0.05% at 12 months. Canada also includes provisions for delayed ettringite formation, saying that supplementary cementitious material shall be used for UHPC that undergoes thermal heat treatment of temperatures greater than 70°C (CSA A23.3 2018).
- **Coefficient of Thermal Expansion (CTE):** Canada requires the CTE to be tested according to AASHTO T 336. France requires the CTE to be measured according to NF EN 1770. Switzerland does not require CTE to be measured or reported, but gives a typical value for UHPC as being 5.6×10^{-6}/°F (10^{-5}/°C) (Brühwiler 2016).

While these requirements may seem to be very in-depth, these country specifications include provisions for non-proprietary mixes, which require more control and detail in testing. In Switzerland, the results for these tests only need to be redone every five years. In the U.S., where only a handful of proprietary mixes are available, it would not be difficult to run these tests for mix approval every few years.

State requirements for mix quality control are presented in Table 3-8. States were not asked about quality control in the survey, so the information in this table was gathered from the specifications

submitted by the states. The values required by the states are the same as those presented in Table 3-6 and Table 3-7.

Table 3-8: Test methods used for mix quality control

	Compression	Flexure	Flow	Other
Alabama	AASHTO T22		AASHTO T347	
Delaware	AASHTO T22		ASTM C1611	Rapid Chloride Penetration, ASTM C1202
Idaho	ASTM C39		ASTM C230	Water tight Integrity test
Iowa	ASTM C39		ASTM C109, 20 drops	
New Jersey	ASTM C39		ASTM C230	
New Mexico	ASTM C39 (C1856)		ASTM C1437 (C1856)	Temperature, AASHTO T309
New York	ASTM C39		mini-slump cone	Watertight Integrity test
Texas	ASTM C1856		ASTM C1856	Temperature
West Virginia	ASTM C39		ASTM C230, 20 drops	
Ontario	X	X	ASTM C109, 20 drops	Temperature, CSA A23.2-17C, visual test for segregation or lumps

Most states used compressive strength and flow measurements to qualify the field mix. It is likely that temperature is measured at many sites and used to determine the speed of the hydration reaction or whether ice is needed to be added to the mixture. However, it may not be used as a basis by which to accept or reject a mix. Delaware was the only state to test the field mix with a durability test, requiring ASTM C1202 to be performed. In the survey response to Question 7, as shown in Table A-5 in the Appendix, Ohio mentioned testing for fiber dispersion, but the representative was contacted for more information, and while a response was received, the representative was unsure about the details of the test. While the spread test can give a good indication of a mix's ability to keep fibers suspended in the matrix, fiber clumps could still be present as a result of mixing practice, and fiber dispersion and orientation can have a large effect on the performance of the material. Delaware mentioned using a visual inspection for mix approval along with the flow test using ASTM C1611. In addition, Ontario used visual inspection for quality control, but it was not clear whether this was for mix consistency or fiber dispersion purposes. New York and Idaho required a watertight integrity test to be performed

The survey also asked states about certain mixing and placing practices. The responses from states on the type of mixer used are presented in Table A-6 in the Appendix. Most states used a mortar mixer supplied by proprietary material supplier, which was Lafarge for all that specified a company. Virginia mentioned using a double shaft mixer for beams, which were likely placed off-site. States were also asked what precautions were taken to avoid cold joints. Their responses are presented in Table A-7, but the submitted specifications were also reviewed to find what was required. To avoid problems at the interface between placements, West Virginia, New York, Texas, and Iowa required UHPC to be placed continuously to avoid cold joints. New Mexico allows rodding to be used in the case of successive UHPC pours. For bond between UHPC and existing concrete, Delaware, New Mexico, and Canada require an exposed aggregate finish and SSD condition on the existing concrete. Idaho also requires cleaning of the surface and bringing it to an SSD condition but does not specify an aggregate finish. Canada requires that if a new placement is to be bonded to existing UHPC, the fiber matrix must be exposed.

Because UHPC has a very low water-to-cementitious material ratio, measures must be taken to limit evaporation after placement. Evaporation can cause crusting and plastic shrinkage cracking in the concrete. Canada requires all UHPC to be immediately covered and in full contact with polyethylene. In Ohio and Florida, plywood has been used to cover placed UHPC.

Survey participants were asked to share any future changes that would be made in their state's construction process. The complete responses to this question are shown in Table A-8 in the Appendix. Delaware's representative mentioned that in the future, workers would attempt to remix batches that did not meet the correct flow requirement and retest them before discarding the whole mix. Ohio's representative mentioned that stricter personal protective equipment would be required for workers handling the dry mix. The respondent from Ontario said that in the future, a mix truck would not be allowed for filling joints because the UHPC discharge was too slow.

3.4 Conclusion

UHPC has pushed the boundaries of traditional concrete performance by exhibiting extremely high compressive strengths, strain hardening tensile behavior, and consistently durable properties in harsh environments. In order to achieve these desirable properties, mixing and placing procedures must be more carefully executed. In addition, testing of UHPC must account for a behavior that is

not equal to that of conventional concrete, especially with regard to tensile testing. While the superior qualities of UHPC can allow for longer spans and lighter sections, the cost can be prohibitive, especially with respect to proprietary mixes. Therefore, UHPC use in the United States has been mostly limited to small applications such as joints between precast slabs of normal concrete. However, extensive information about mix design theory and practice is available, making it possible for non-proprietary mixes to gain popularity in the near future.

CHAPTER 4. TENSION TEST

4.1 Introduction

Ultra-High-Performance Concrete (UHPC) has the potential to be highly durable in Florida transportation infrastructure. UHPC's high tensile strength could also allow for highly efficient structural members with reduced need for embedded reinforcing steel. While this property is very useful, it cannot be utilized to its full potential unless it can be reliably measured. This research aims to find the best method to be specified in the state of Florida for determining UHPC tensile strength.

In order to determine the best method for measuring the UHPC tensile strength, the following issues were determined to be important in any method comparison:

- Does the test method provide information on the shape of the concrete tensile stress-strain curve, and not just the magnitude?
- Does the test method have a track record of producing a large percentage of invalid tests?
- How does the casting method of direct tension specimens affect the fiber orientation and therefore, the results of a direct tension test?
- Can the results of the tension test being performed with specialized equipment at the University of Florida be duplicated with the equipment at the State Materials Office?

Two candidate concrete test methods were selected for experimental analysis based on a literature review of UHPC fiber behavior, evolution of existing test method, and discussions with structural engineers at the Florida Department of Transportation and laboratory personnel at the State Materials Office (SMO). The first test method selected for evaluation was ASTM C1609 "Standard Test Method for Flexural Performance of Fiber-Reinforced Concrete (Using Beam With Third-Point Loading)" because of its history of use with fiber-reinforced concrete, comfort of the laboratory personnel at the SMO with the method, and previous use for tensile strength evaluation of UHPC (ASTM C1609 2012). The second test method selected was the concrete direct tension test developed by the Federal Highway Administration (FHWA) (Graybeal and Baby 2013).

4.2 Methods

One batch of UHPC was made at UF using an IMER Mortarman 750 mortar mixer to make flexural and direct tension samples. Flexural samples were made according to ASTM C1856 using 4×4×14 in. specimens. Direct tension samples were made using steel molds fabricated at UF. The direct tension samples were 2×2×17 in. Figure 4-1 shows a design drawing of the direct tension specimen steel mold with end plate removed to show dimensions and bolt holes, while Figure 4-2 shows a design drawing of the end plate. Each mold end plate was attached to the bottom and side mold plates using ¼ in.-20 bolts. Each bolt hole on the side and bottom plates was threaded to be compatible with the ¼ in.-20 bolts. Flexural and tensile samples were made without any vibration or rodding. Direct tension samples were made using two methods: placing the concrete using a funnel at the end of the sample and allowing the concrete to flow the length of the sample, and placing the concrete using a funnel in the middle of the sample while allowing the concrete to flow to the mold ends. These two methods were made to determine if the length of concrete flow affected the fiber orientation in the samples and sample consistency. All samples were finished with a wood float and covered with plastic. After one day of curing at lab temperature, samples were removed from the molds, labeled, and placed in an ASTM C511 moist room. Three UHPC cylinders were made for compressive strength testing according to ASTM C1856. After the concrete was placed in the cylinders, they were sealed and left to cure for 24 hours at laboratory temperature. They were then demolded, labeled, and placed in the moist room with the tension samples.

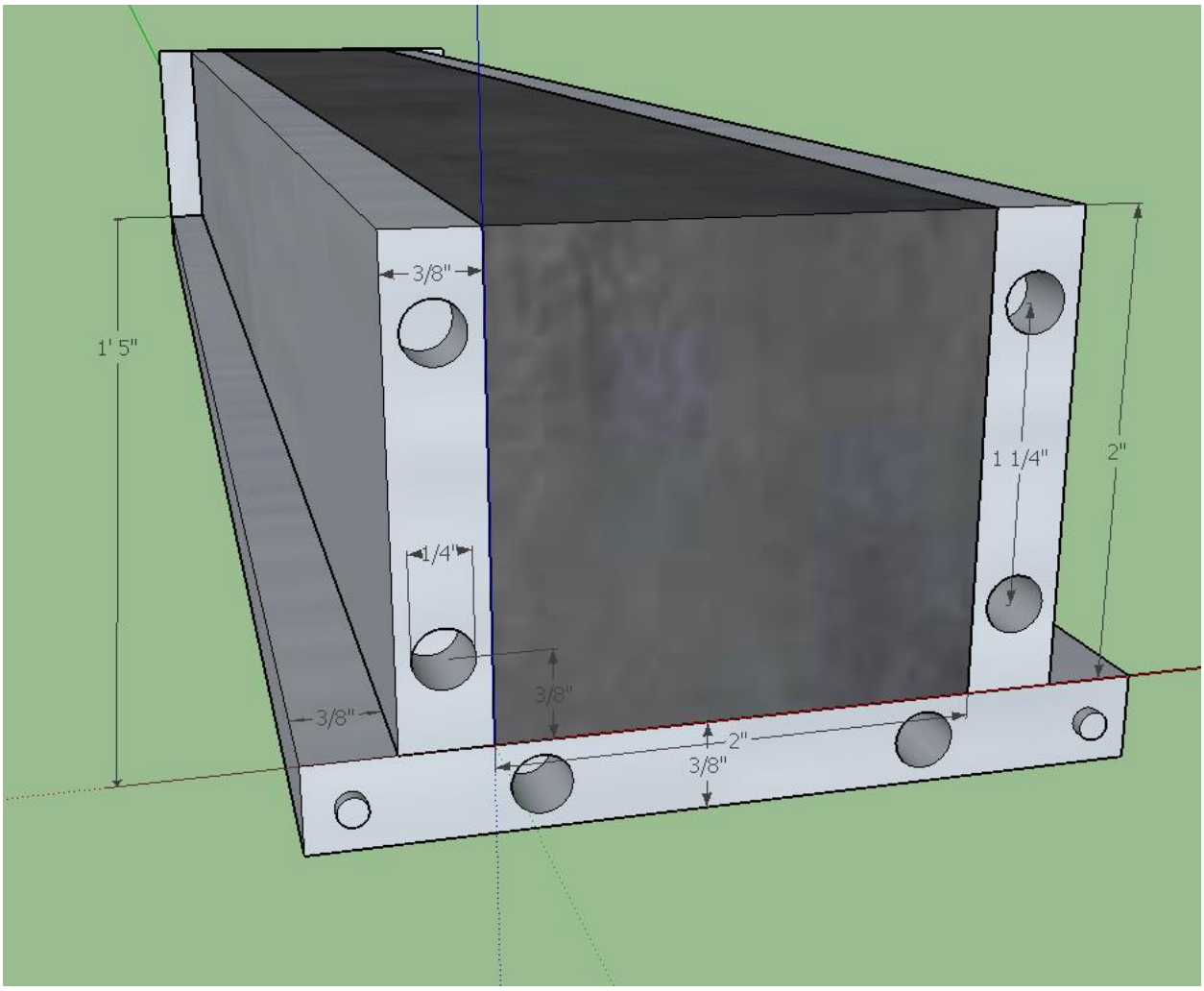

Figure 4-1: Design drawing of direct tension specimen steel mold with end plate removed to show dimensions

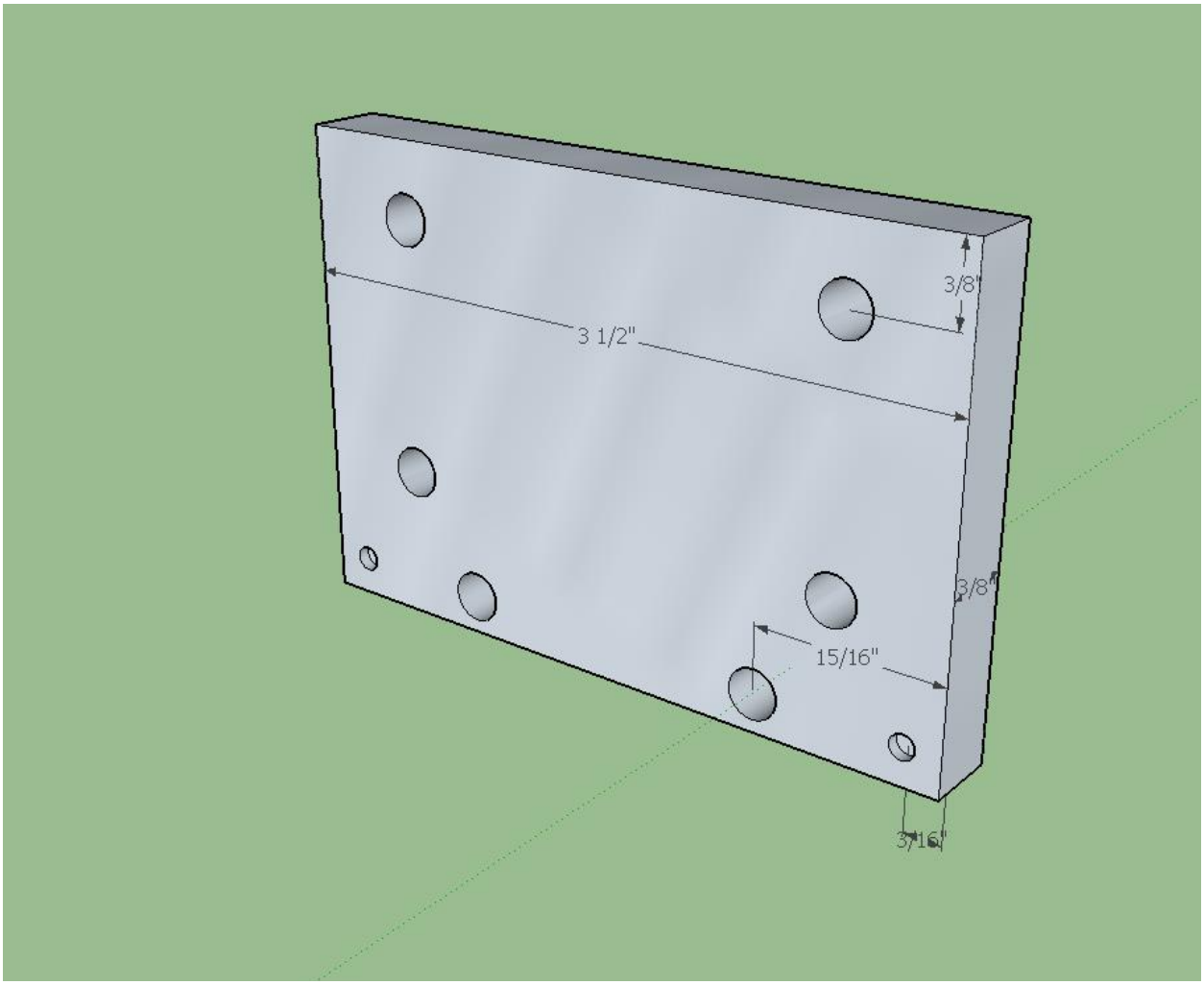

Figure 4-2: Design drawing for direct tension specimen mold end plates

An additional seven direct tension samples were made from two separate batches of UHPC using a Pheso concrete rheometer. These samples were made to test in direct tension at the SMO to determine if the Instron universal testing machine was capable of maintaining proper alignment of the test samples during loading so that valid sample breaks were obtained, indicated by cracking in the center span of the sample. Five samples were made in one batch, and two more in another batch. Those samples were made by scooping the concrete into the molds instead of placing with a funnel. They were cured in the same manner as the other direct tension concrete samples.

Before testing, two UHPC samples made for direct tension were scanned in the computed tomography machine at UF to qualitatively compare the fiber orientation resulting from concrete placement using the funnel in the middle and at the end of the samples.

*4.2.1 **Flexural Testing at SMO***

Flexural samples were tested 27 days after mixing, as specified to ASTM 1609. This is a flexure method prescribed by ASTM 1856 to be used for UHPC, and is described in detail in the Task 1 literature review submitted for this project. Its advantages are that it is simple to set up and implement for laboratories. This test is also slightly less labor intensive than the direct tension test. Disadvantages are that it does not give a direct tension value. The flexural strength value given from this test is higher than the direct tension value, and should not be used for design calculations unless reduced by a safety factor. This is because inverse calculations used to get a stress-strain curve from a tensile test are based on an assumed shape of the stress-strain relationship. An elastic-plastic relationship is typically selected (Graybeal and Baby 2013). The calculations require a modulus of elasticity to be assumed, which will change once the material has cracked and fibers are engaged in tension. In addition, the values from the flexural strength test are heavily dependent on the amount of friction in the roller supports of the sample-loading fixture (Wille and Parra-Montesinos 2012).

*4.2.2 **Direct Tension Testing at UF***

The direct tension test method has the advantage of giving direct tension strength without making assumptions or intermediate calculations. The test is slightly more labor intensive than flexural beams and requires expensive specialty equipment to grip the specimens, reducing the number of labs that have used it to date. Tensile testing conducted for this research project used the following procedures. After specimens were cured, aluminum plates, with dimensions shown in Figure 4-3, were epoxied to the ends. Sikadur®-32 Hi-Mod epoxy was used to bond the aluminum plates onto the specimens. The epoxy used by FHWA, Sikadur 31®-Hi-Mod, was also tried; however, it was found that it was easier to get a uniform epoxy thickness using the Sikadur®-32 Hi-Mod epoxy. Two clamps were used on each end of the samples to hold the aluminum plates onto the samples during curing. After curing, any epoxy on the aluminum plates in the gripping area was removed using a rotating sander to allow for a uniform grip and prevent sample misalignment due to the

presence of the epoxy. The testing machine crossheads were aligned in accordance with ASTM E1012 “Standard Practice for Verification of Testing Frame and Specimen Alignment Under Tensile and Compressive Axial Force Application” (ASTM E1012 2014) to avoid eccentric loading. Specimens were gripped 3.5 in. from either end of the specimen. An extensometer was attached to the specimen with an LVDT on each side of the specimen. The LVDTs measured the extension of the concrete as it was loaded. The loading began with a 1 ksi compressive stress, followed by a constant load increase in tension until failure was reached. Loading was performed in force-control mode. A 1.5 ± 0.5 ksi/min loading rate was used for the loading in the elastic region. Failure was defined as a drop of above 50% from the peak load. While 6 samples were loaded for each of the two placement methods, only 3 valid tests are needed. FHWA recommends testing at least 6 in case some of the tests fail in the grips or in an unacceptable manner.

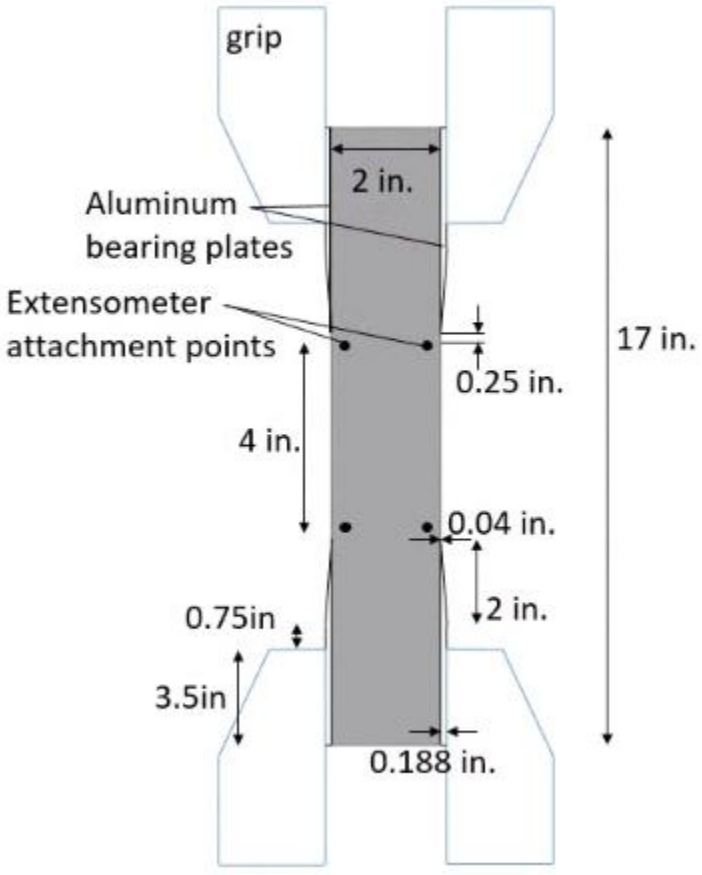

Figure 4-3: Tensile Test Specimen Dimensions

During the course of the UF direct tension testing, some problems were encountered and solved. For the first six samples tested, five of the samples failed unsatisfactorily in the same manner, giving invalid tests. The samples fractured just above where they were held in the hydraulic grips. The aluminum plates debonded from the epoxy used to attach the plates as shown in Figure 4-4. It was hypothesized that the aluminum plates were peeling away from the sample because of the compression force on one side of the plate. This reduced the shear transfer that could occur between the plates and the sample in the tapered region, leading to a failure immediately above the grips. To remedy this, two C-clamps were placed on each of the ends of the specimens on the aluminum plates in the tapered regions as shown in Figure 4-5. The C-clamps were used to apply some compressive force on the tapered regions to prevent them from bending during the gripping and allowing for shear transfer. Additionally, the gripping force was reduced from 6,000 psi to 3,000 psi. After this adjustment was made, all six samples tested failed in the middle of the sample instead of in the reinforced area, providing valid results. It is also recommended in the future to place one clamp on the tapered area and one clamp near the end of the aluminum plate to distribute the clamping force over the entire aluminum area during aluminum plate attachment.

Figure 4-4: Invalid direct tension sample after failure

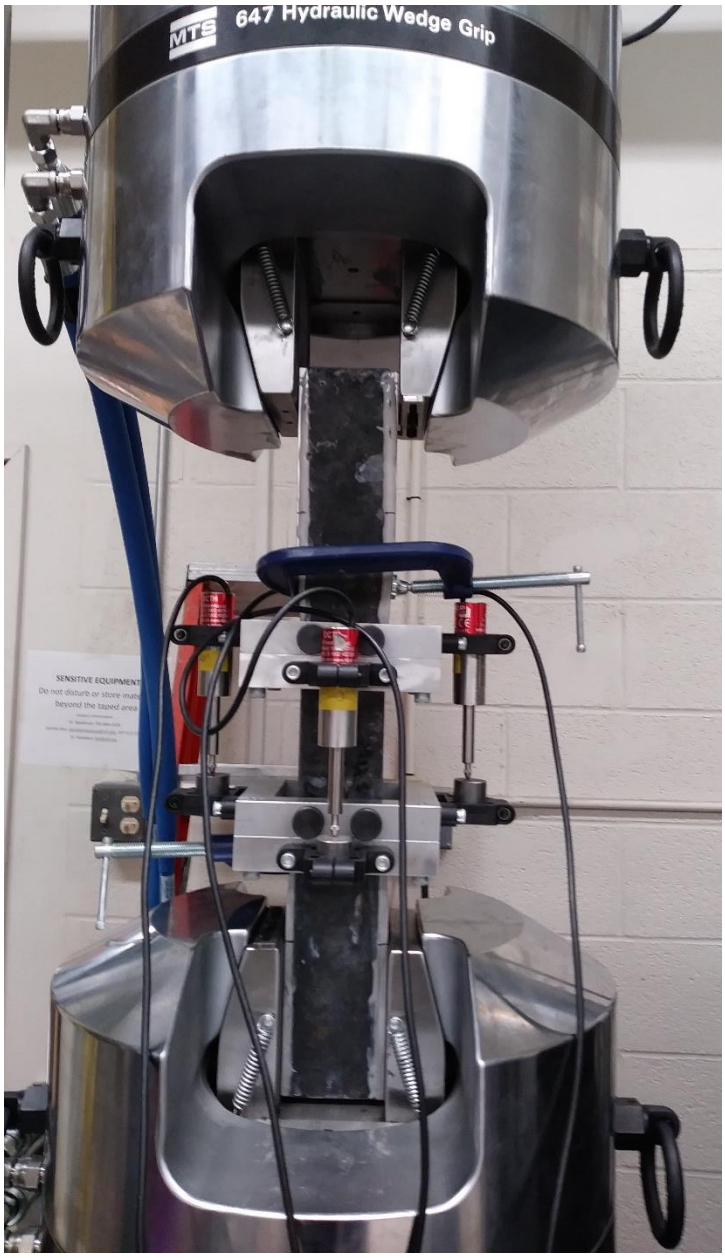

Figure 4-5: Tensile test before gripping with the C-clamps attached to prevent the aluminum plate delamination

Through experience, it was found that the aluminum plates can be re-used in order to save costs involved with tensile testing. Specimens that have been broken can be placed in an oven at 100°C. After the specimens have heated up, the bond between the epoxy will soften enough so that it is no longer bound to the aluminum, and the plates can be removed easily. This was achieved with

Sikadur®-32 Hi-Mod epoxy and an oven time of 7 hours. The plates may require some epoxy removal with a rotating sander, however this should be minimal.

*4.2.3 **Direct Tension Apparatus Alignment Measurement at SMO***

In order to get reliable tensile testing results, it is very important that no angular or rotational offsets are present. If the specimen is not in pure tension, any eccentricity will cause locations of higher force, resulting in premature failure and misleadingly low strength and toughness values. In order to check the alignment of the tensile testing system at the Department of Transportation, an aluminum specimen was fabricated. The specimen was 17 inches tall, 2 inches wide and 2.4 inches thick, to model the dimensions of a concrete specimen with aluminum plates epoxied to it. The specimen then had strain gauges placed on each of the four sides at the center, top, and bottom of the specimen. From the strain measurements, a percent bending could be calculated. This was done at the top, middle, and bottom of the specimen using Equation 4-1 through Equation 4-5 (ASTM E1012 2014).

$$a = (e_1 + e_2 + e_3 + e_4)/4 \qquad \text{Equation 4-1}$$

$$B(x) = (e_1 - e_3)/2 \qquad \text{Equation 4-2}$$

$$B(y) = (e_2 - e_4)/2 \qquad \text{Equation 4-3}$$

$$PB(x) = \frac{B(x)}{a} * 100\% \qquad \text{Equation 4-4}$$

$$PB(y) = \frac{B(y)}{a} * 100\% \qquad \text{Equation 4-5}$$

Where: e_1, e_2, e_3, and e_4 are the strain values from the LVDTs, adjusted so the zero-strain case is with a gripped specimen at zero axial load.

a is the axial strain

$B(x)$ is the bending strain in the x axis

$B(y)$ is the bending strain in the y axis

$PB(x)$ is the percent bending strain in the y axis

PB(y) is the percent bending strain in the y axis

Because the percent bending value is normalized with the total axial strain, it is expected that the percent bending would decrease with an increased load applied to the specimen. ASTM E1012 states that the force of at least three discrete loading points within the range of interest should be applied (ASTM E1012 2014). At the department of transportation, loading was increased from zero to 2,000 lb, then 4,000 lb, then 7,000 lb, and then reduced back to 4,000 lb, then 2,000 lb and finally completely unloaded. This range was chosen because a 7,000-lb load corresponds approximately to a 1,500-psi stress, which is in the upper range of tensile strength for a UHPC specimen. Each of these loads was held so that the strain measurements could be recorded. This was repeated three times, and the values are shown in Figure 4-6 through Figure 4-8.

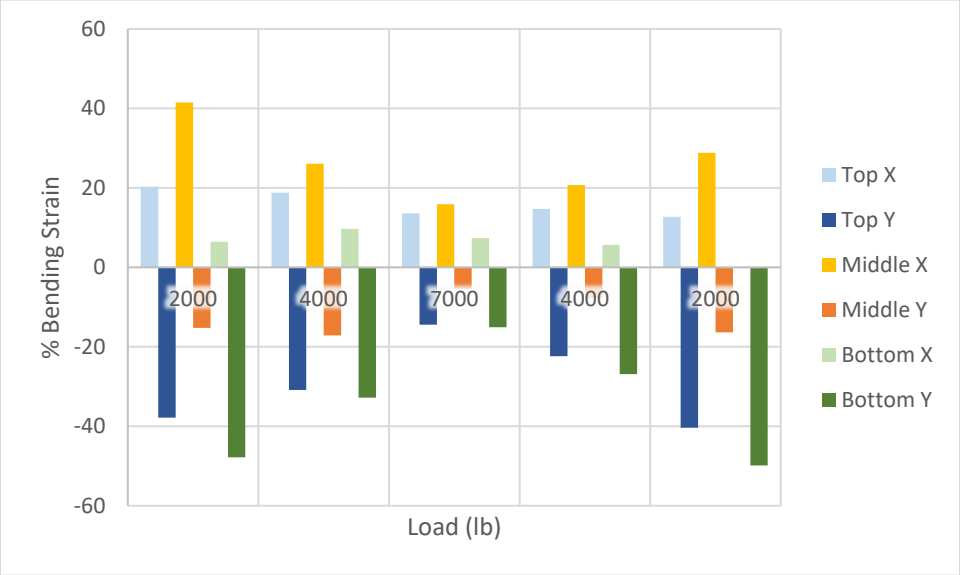

Figure 4-6: Trial 1 Percent Bending Results

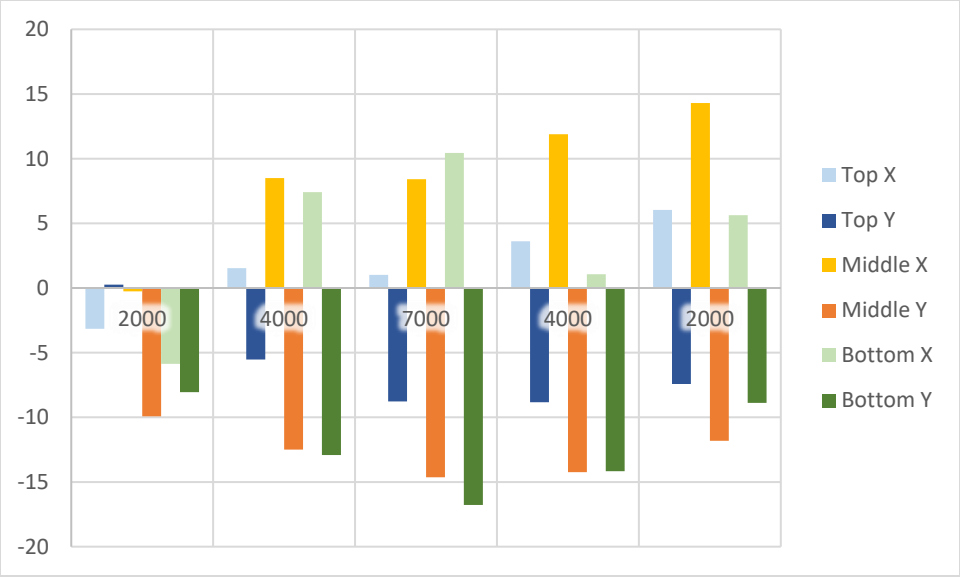

Figure 4-7: Trial 2 Percent Bending Results

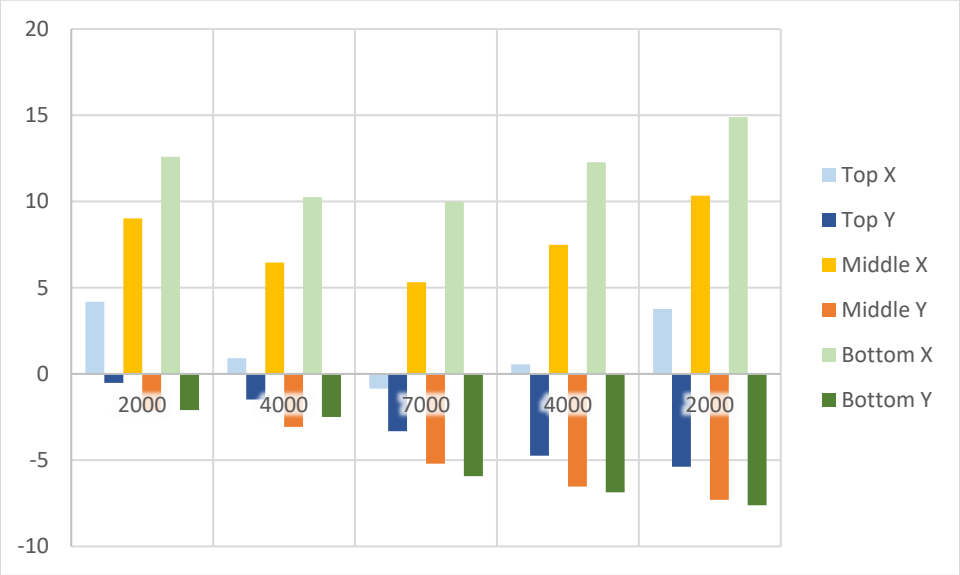

Figure 4-8: Trial 3 Percent Bending Results

According to ASTM E1012, there are three classifications of alignment verification that can be used (ASTM E1012 2014). They are denoted as 5, 8, and 10, corresponding to the limit of percent bending that the specimen must stay under throughout loading. Therefore, the most lenient classification would require that the percent bending stays below 10% for each load.

None of the above trials met the 10 Alignment Classification. Trial 3 was the best, with only 5 of the 30 measurements being over 10 percent. Trial 1 had the worst performance, with multiple strains being more than 40% misaligned. The Trial 1 values did change in an intuitive manner, however, with the percent bending decreasing as the load increased. All three trials consistently had either all positive or all negative bending on each axis (x or y). This would suggest a bending in a C shape as opposed to an S shape, which would have opposite signs on the top and bottom of the specimen.

Between Trial 1 and Trial 2, the specimen taken out of the grips and re-gripped. Between Trial 2 and Trial 3, the specimen was left in the grips, and the apparatus was taken out of the Instron testing machine and placed back inside. For all the trials, bending in the x direction was calculated from strains on the ungripped side of the specimen, and bending in the y axis was on the gripped side. The grips for this test were a series of rollers that get closer together as they near the center of the specimen. Roughened wedges are used in conjunction with the rollers to grip the specimen more tightly as it was loaded in tension. A schematic is shown in Figure 4-9 and a photograph of the setup is shown in Figure 4-10.

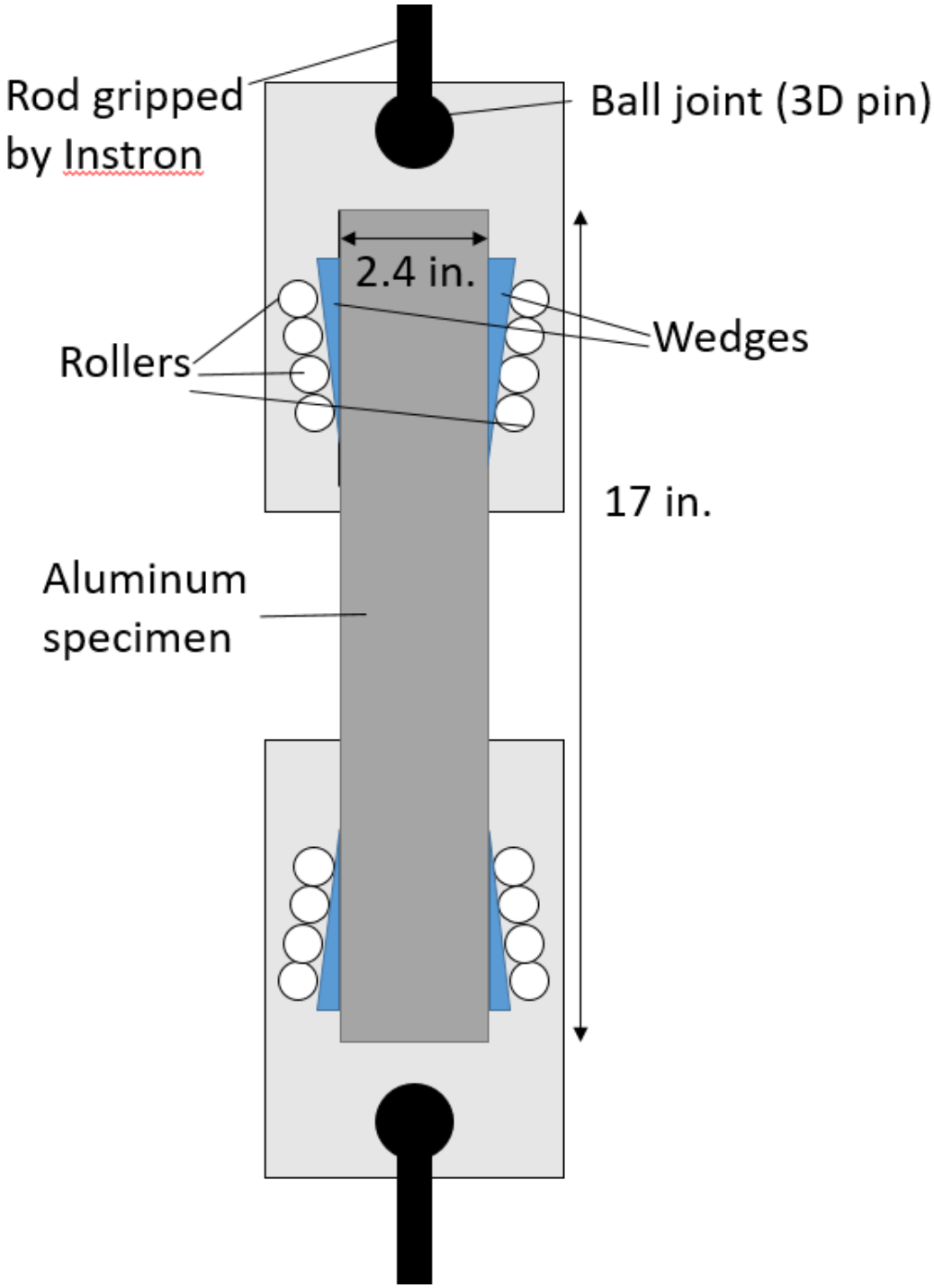

Figure 4-9: Tensile Grip Schematic

Figure 4-10: Aluminum Specimen in Tensile Grips

The ball joint on the top and bottom of the grips did a good job of making sure the entire system could release any offsets of the Instron grips. However, the gripping of the specimen within the rollers could not be controlled. If the wedges are not exactly the same size or if some wedges are pushed farther into the grips than others, the specimen can become misaligned within the roller grips. An over-exaggeration of this case is shown in **Error! Reference source not found.**. As shown, the pin joints are in-line, but the specimen itself is not. Therefore, when a tensile load is applied, there will be stress concentrations experienced by the specimen.

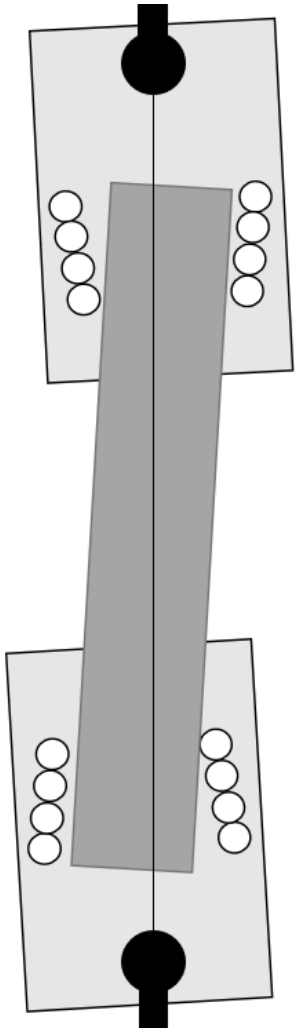

Figure 4-11: Specimen misaligned within aligned system

As seen by the variability in the percent bending results, this method produces inconsistent results each time a specimen is re-gripped. This is likely because there is a high amount of variability based on how the wedges are placed. In addition, the gripping alignment can change during loading since the rollers apart forces on the specimen as the tensile load increases. This may be why the third trial produced the best results. After the second trial, the specimen was not removed from the roller grips, meaning the grips were already pulled tight at the beginning of the third trial. However, not enough trials were done to decisively attribute the improved results to pre-loading. In addition, a concrete sample could not be preloaded to align the grips because it could not be re-used after being loaded to its maximum capacity.

While this gripping method has produced results close to the 10 percent classification, it cannot consistently produce these results. In addition, it cannot be permanently adjusted to remove eccentricities because they are caused by specimen placement instead of by an adjustable set-up. While this method can be used to determine tensile strength, it should be noted that some values may be lower than the actual concrete capacity, due to premature failure in locations of stress concentrations.

*4.2.4 **Direct Tension Testing at SMO***

Direct tension testing was performed at the SMO using samples made at UF in the Pheso concrete rheometer. Figure 4-12 shows a picture of the grips and wedge plates used at the SMO. Figure 4-13 and Figure 4-14 show pictures of the direct tension testing setup in the universal testing machine at the SMO. The wedge grips allowed the sample to be gripped in tension but not compression. The rollers in the grips were positioned at an angle so that they were closer together at the inward-facing ends. Wedges were placed between the rollers and the aluminum plates on the concrete specimen. The wedges were steel and were roughened in order to grip the specimen tightly. As the specimen was pulled in tension, the grip force would increase due to the slight movement of the specimen towards the tighter end of the rollers. A benefit of this method is that it uses perfectly pinned connections that should align the UHPC sample. The plates were attached to a ball bearing that allowed rotation in 3 dimensions. This means that no eccentricities would exist to produce stress concentrations on the specimen. A disadvantage is that the gripping mechanism relies on slippage of the grips, so crosshead displacement is much higher than the actual beam extension.

Trial and error is needed to determine the crosshead displacement required to produce an acceptable loading rate for this setup. For the tests in this study, loading was performed at a rate of 0.2 in./min of crosshead displacement. The Instron machine had the capability of logging only one LVDT at a time on the direct tension sample. This could have the effect of giving a misleading stress-strain curve for the UHPC because any slight misalignment could give more or less tensile strain on the face than the average strain across the sample. In order to use this machine in the future, strain measurements on all four faces would be needed. This could be accomplished through use of digital image correlation or LVDTs on all four faces of the samples.

Figure 4-12: SMO direct tension test grips and wedge plates

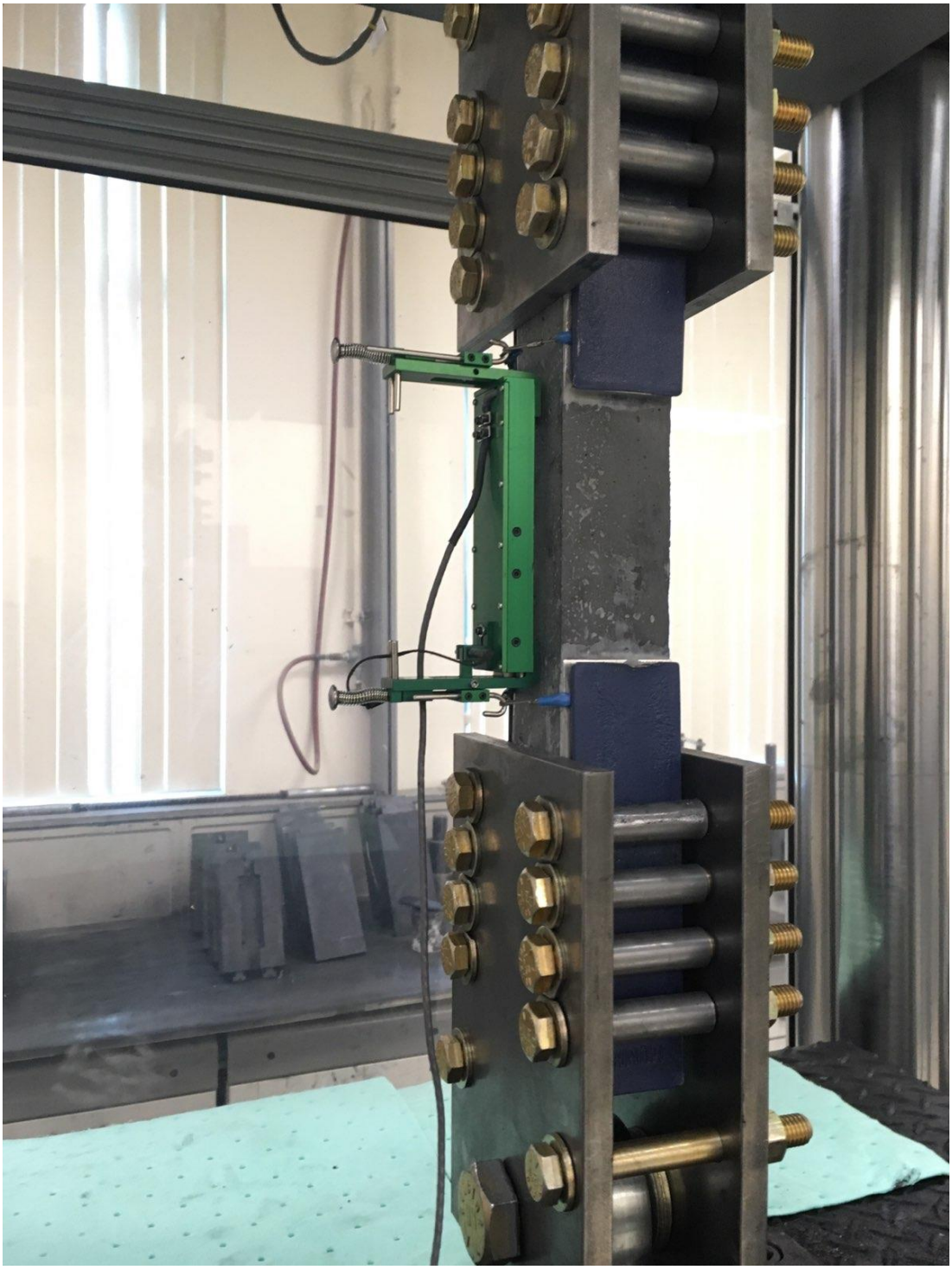

Figure 4-13: UHPC sample in SMO direct tension testing setup with extensometer in place

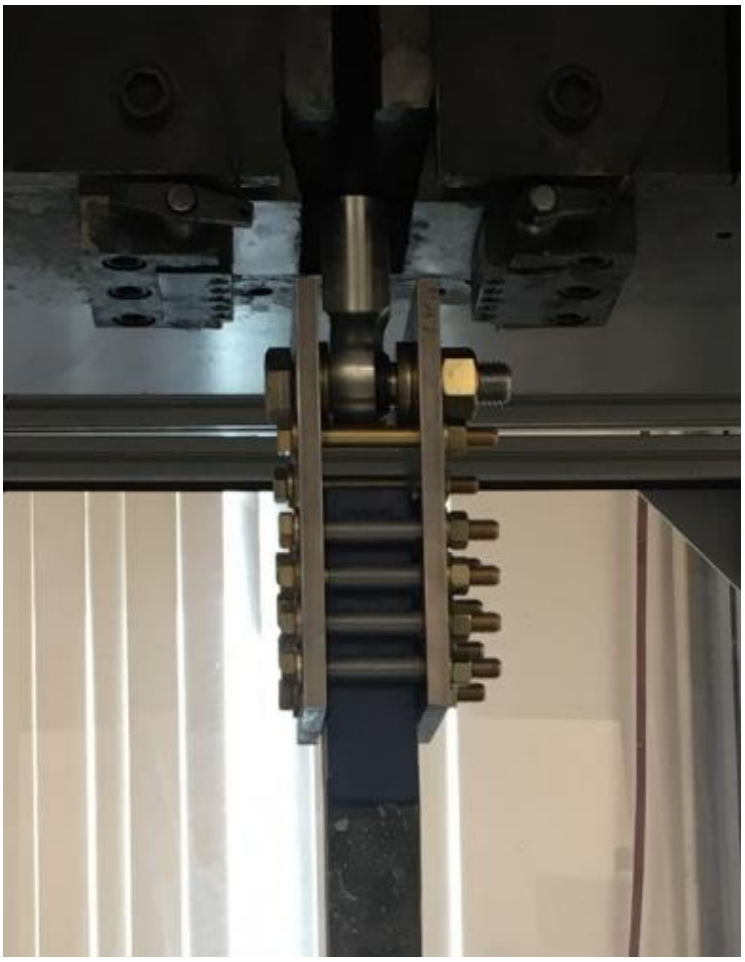

Figure 4-14: Top half of UHPC direct tension testing setup at SMO

4.3 Results

*4.3.1 **Flexural Test Results***

The force-deflection curves for the flexural tests are shown in Figure 4-15. Flexural tests conducted at the SMO were analyzed according to the procedures recommended in ASTM C1609. The first cracking strength f_1 (psi) was calculated using the equation for modulus of rupture, as shown in Equation 4-6 (ASTM C1609 2012).

$$f_1 = \frac{PL}{bd^2} \qquad \text{Equation 4-6}$$

Where P is the first-peak load, L is the span length (in.), b is the specimen width (in.), and d is the specimen depth (in.). Table 4-1 summarizes the calculated beam test parameters. The peak strength f_P was also determined using the equation for the modulus of rupture. The ratio of the peak strength-to-first-cracking strength and toughness were also calculated for each beam. The mean, standard deviation (σ), coefficient of variation (COV) of first cracking strength, peak strength, ratio of the peak strength-to-first-cracking strength, and toughness were then calculated for the six beams. A much larger variation was seen in the peak strength and toughness than for the first cracking strength. This is likely because the first-cracking strength did not depend on local variabilities in the fiber orientation and percentage. Good ductility was seen in the beam tests on average.

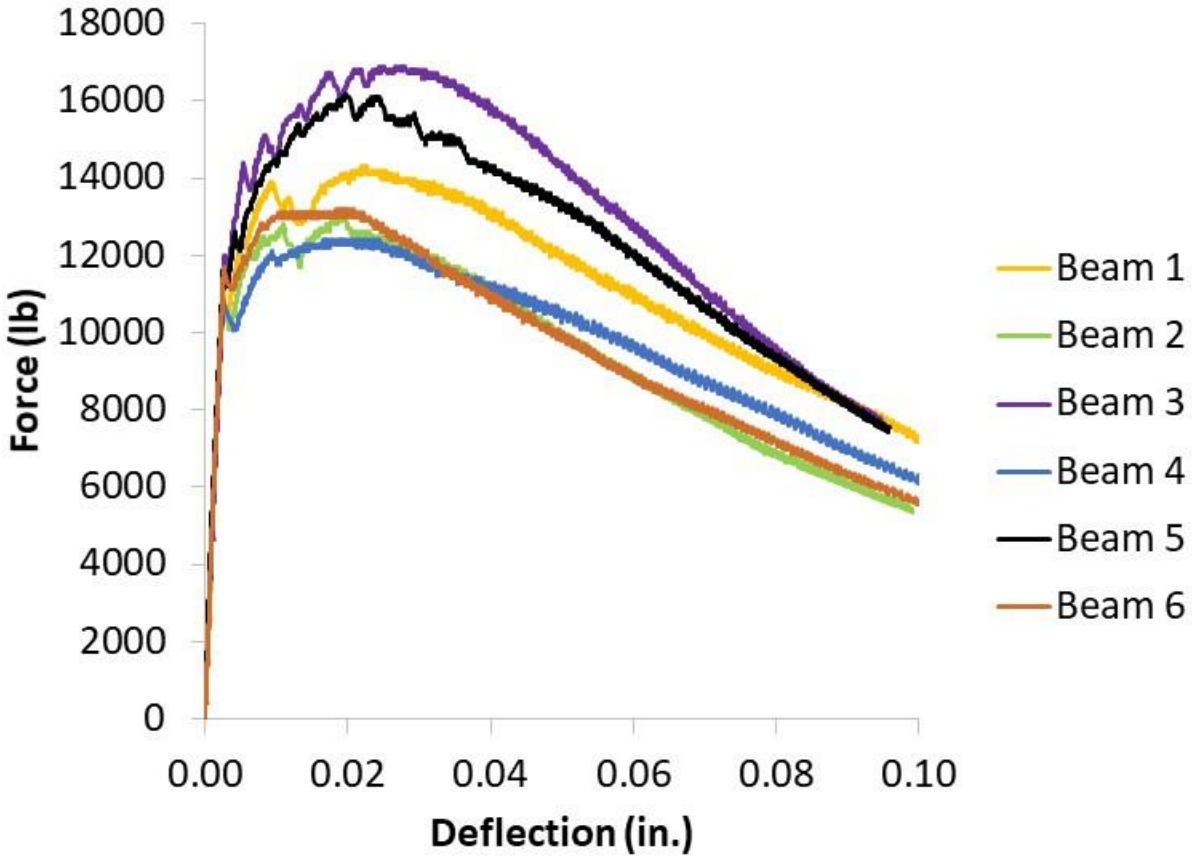

Figure 4-15: ASTM C1609 beam force-deflection curves

Table 4-1: Summary of calculated beam flexural strength and toughness parameters

Beam	f_1 (psi)	f_P (psi)	Peak-to-First Cracking Strength Ratio	Toughness (Joule)
1	2065	2680	1.30	95
2	2005	2440	1.21	82
3	2250	3170	1.41	111
4	2065	2325	1.13	83
5	2175	3040	1.40	105
6	2195	2475	1.13	83
Mean	2125	2690	1.26	93
σ	94.6	344.4	0.13	12.6
COV	4.5	12.8	10.0	13.5

*4.3.2 **Direct Tension Tests***

Direct tension tests were performed at the University of Florida for six samples placed through a funnel at the end of the specimen, and six samples placed through a funnel at the center of the specimen. The concrete stress in the test was calculated from the measured load according to Equation 4-7 (Graybeal and Baby 2013):

$$f = \frac{P}{A} \qquad \text{Equation 4-7}$$

Where f is the concrete stress (psi), P is the concrete load in direct tension (lbf), and A is the concrete gross cross-sectional area (in.^{2}). Direct tension stress-strain curves with each linear variable differential transformer for each of the 12 total specimens tested are shown in Figure 4-16**Error! Reference source not found.** through Figure 4-27**Error! Reference source not found.**. Samples Edge 2 and 3 and Center 1, 2, and 3 failed in the test grips. The average stress-strain curve for each valid specimen tested is shown in Figure 4-28 for the concrete placed at the end and Figure 4-29 for the concrete placed in the center. The concrete peak strength, strength at a strain of 0.005 in./in., compression elastic modulus measured from 0 to 500 psi, and tensile elastic modulus measured from 0 to 500 psi for the valid samples tested, are shown in Table 4-2. Table 4.3 shows the sample mean peak strength rounded to the nearest 10 psi, strength at a strain of 0.005 in./in. rounded to the nearest 10 psi, and compression and tensile moduli. The strength at a strain of 0.005 in./in. is included as a measure of the concrete ductility. A statistical analysis was performed with a two-sample T-test and 95% confidence interval to determine if there was a significant difference

between placement of concrete at the end and center of the beams. The test showed a P-value of 0.067, indicating that the sample results for placement at the edge and center were not statistically different. The coefficient of variation was slightly lower for the concrete placed at the end. The research team's experience during placement showed that placement should be done in a continuous placement using a funnel to avoid problems with cold joints and layers forming.

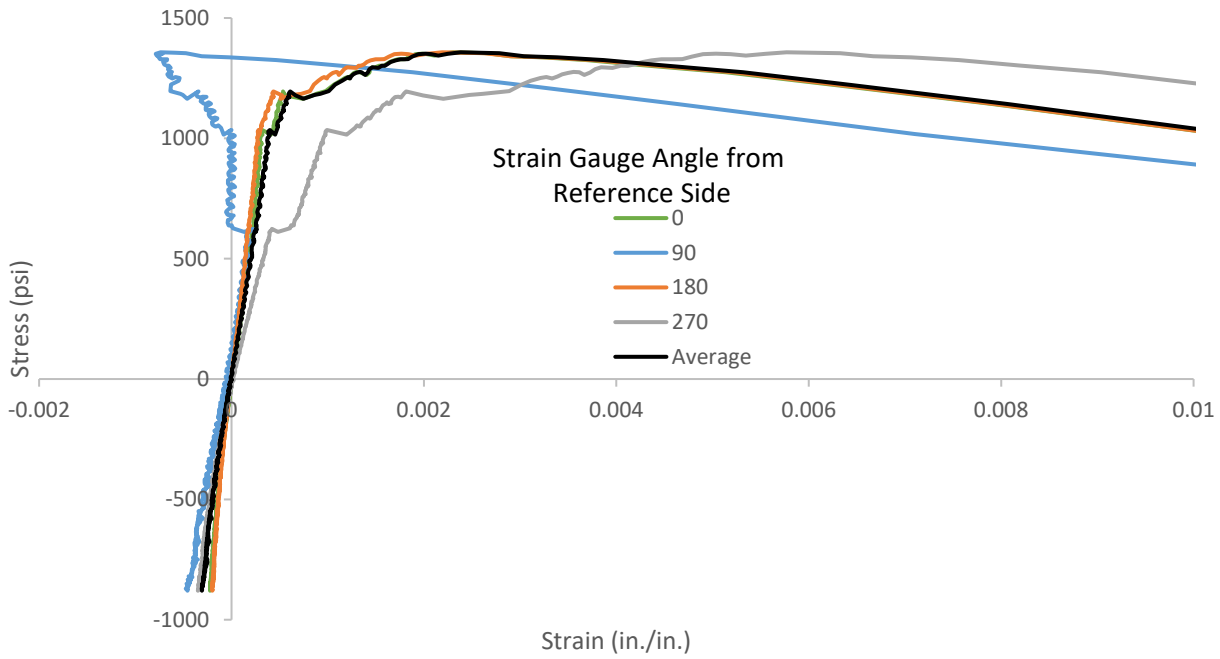

Figure 4-16: Direct tension results for sample 1 placed at the end

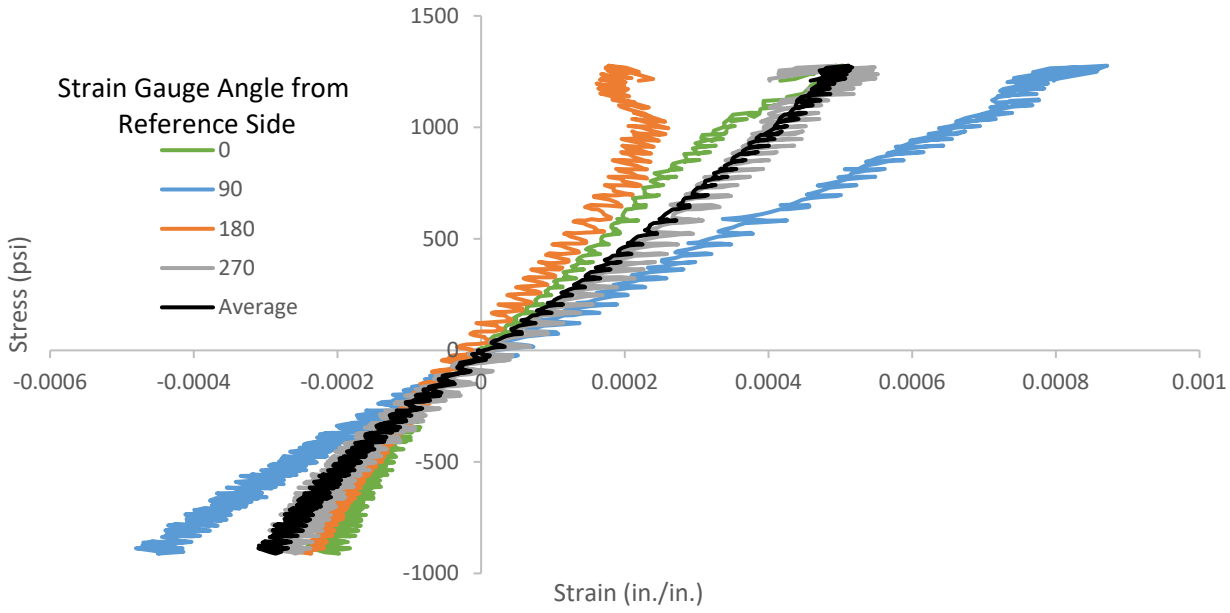

Figure 4-17: Direct tension results for sample 2 placed at the end

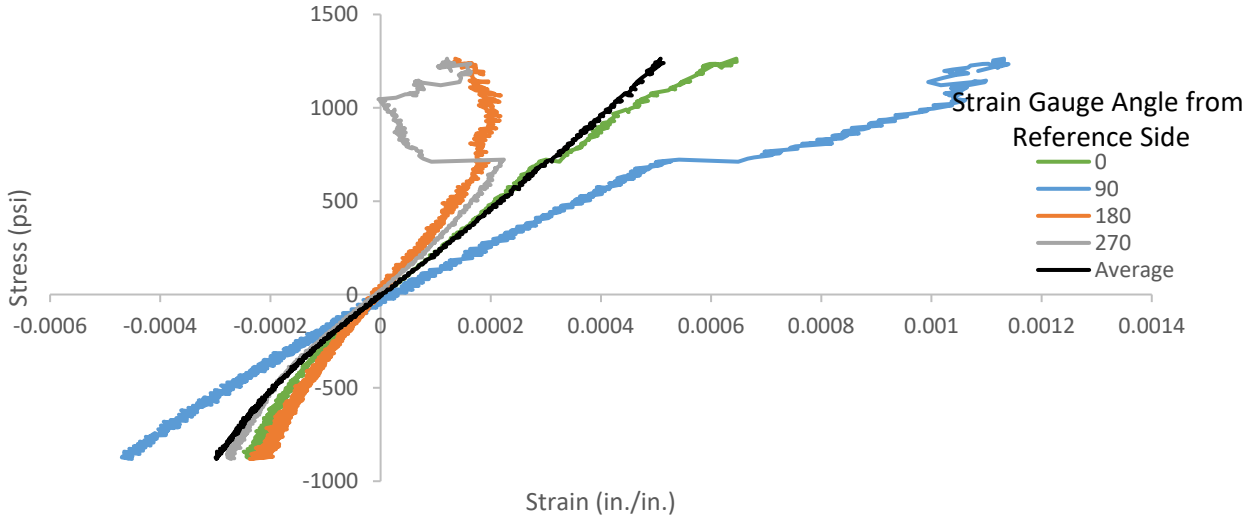

Figure 4-18: Direct tension results for sample 3 placed at the end

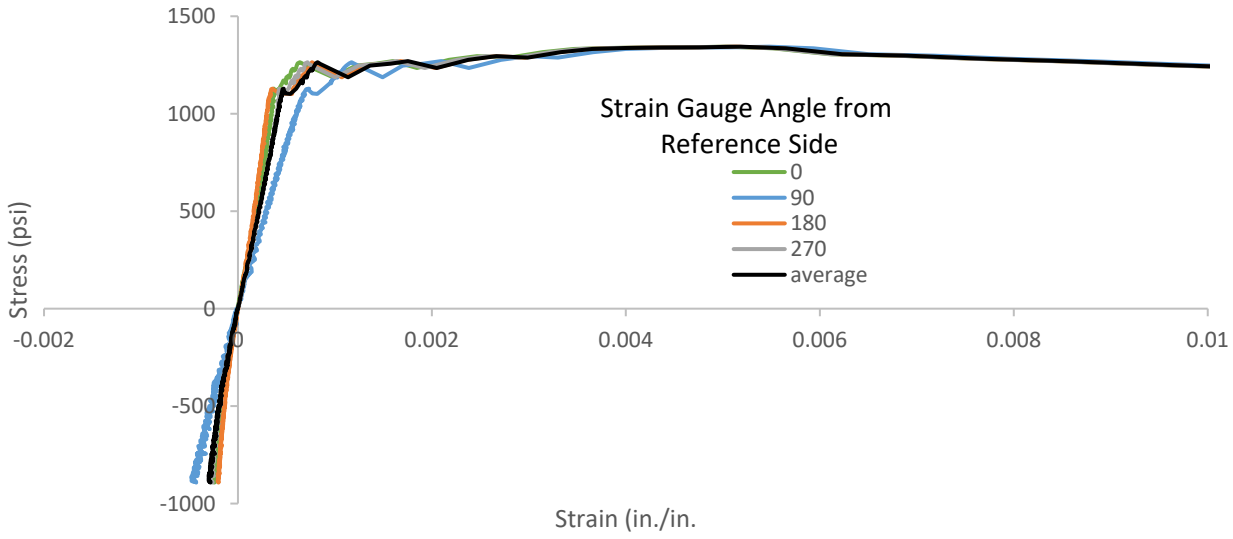

Figure 4-19: Direct tension results for sample 4 placed at the end

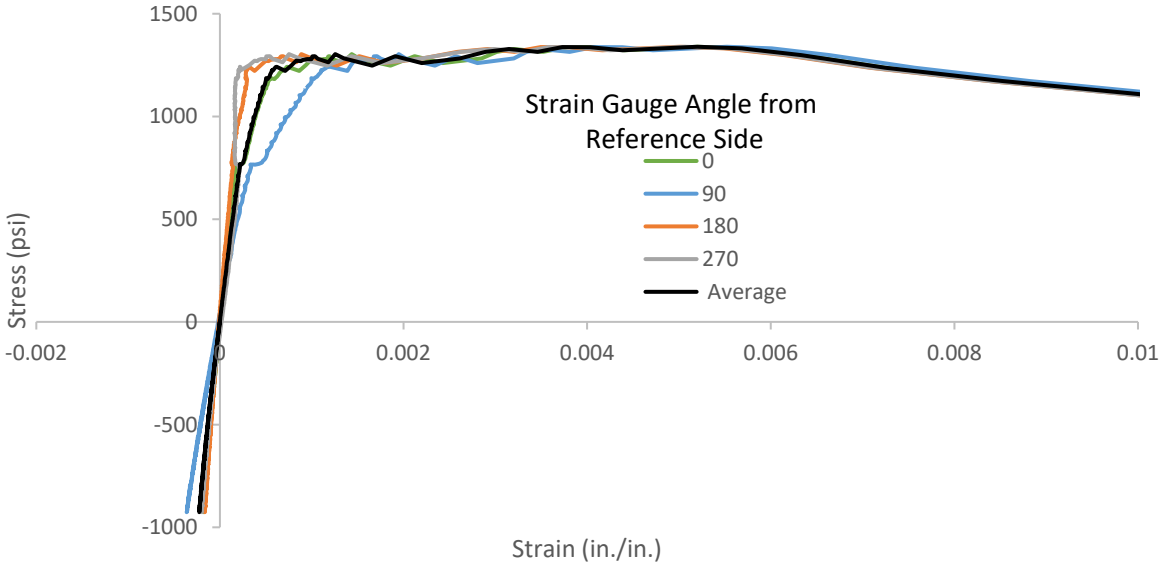

Figure 4-20: Direct tension results for sample 5 placed at the end

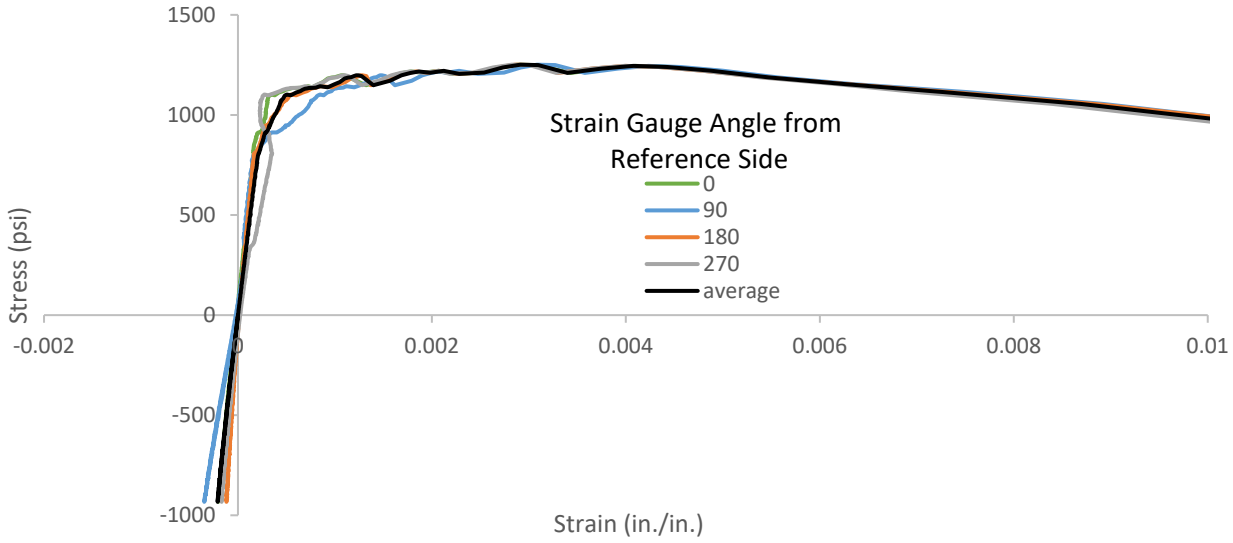

Figure 4-21: Direct tension results for sample 6 placed at the end

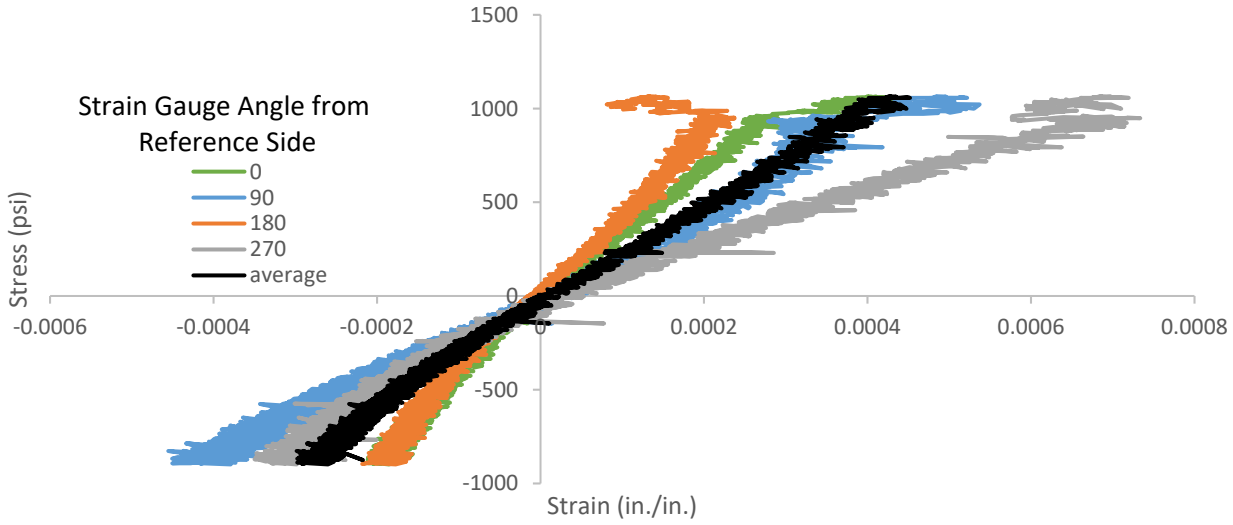

Figure 4-22: Direct tension results for sample 1 placed at the center

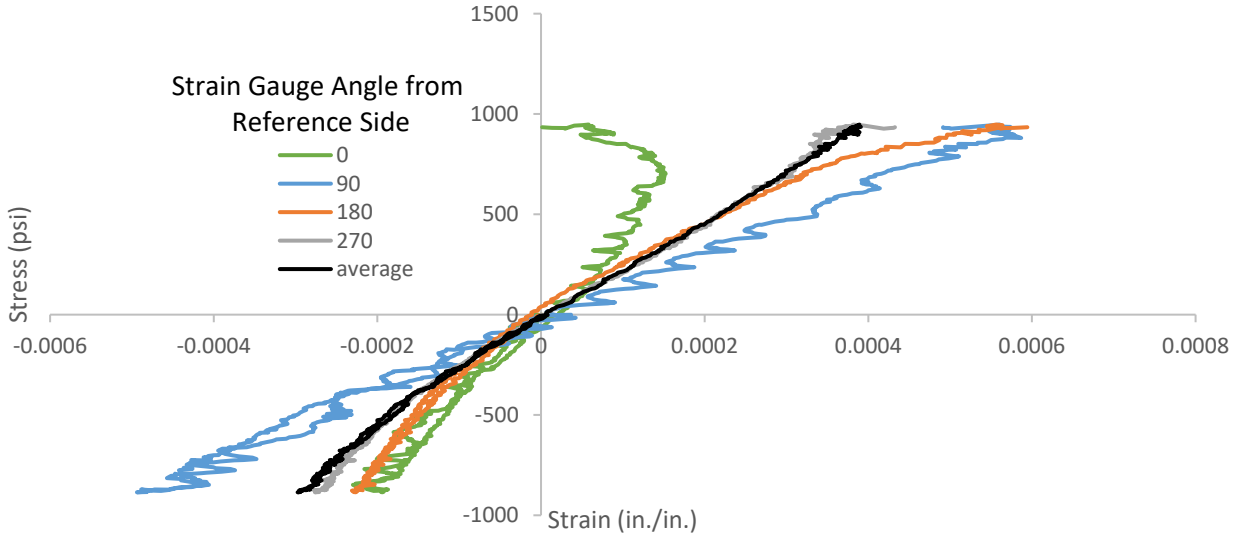

Figure 4-23: Direct tension results for sample 2 placed at the center

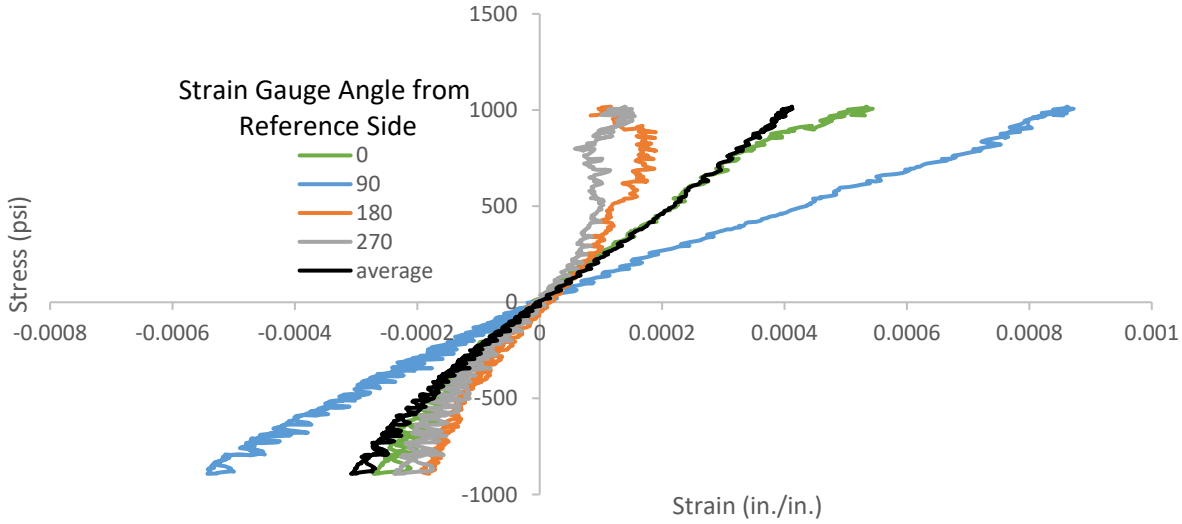

Figure 4-24: Direct tension results for sample 3 placed at the center

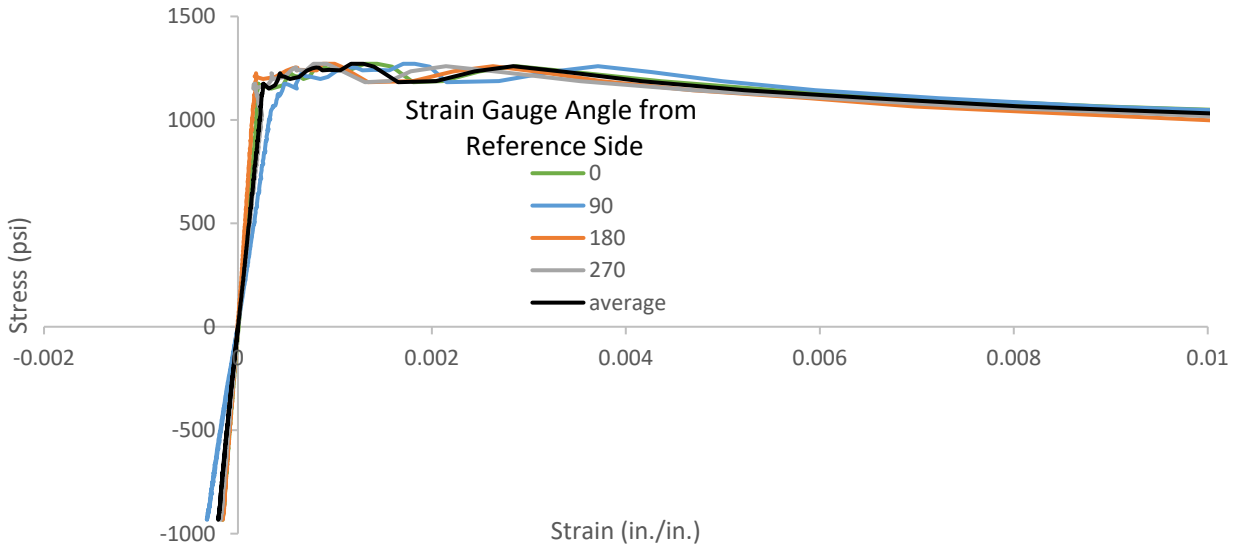

Figure 4-25: Direct tension results for sample 4 placed at the center

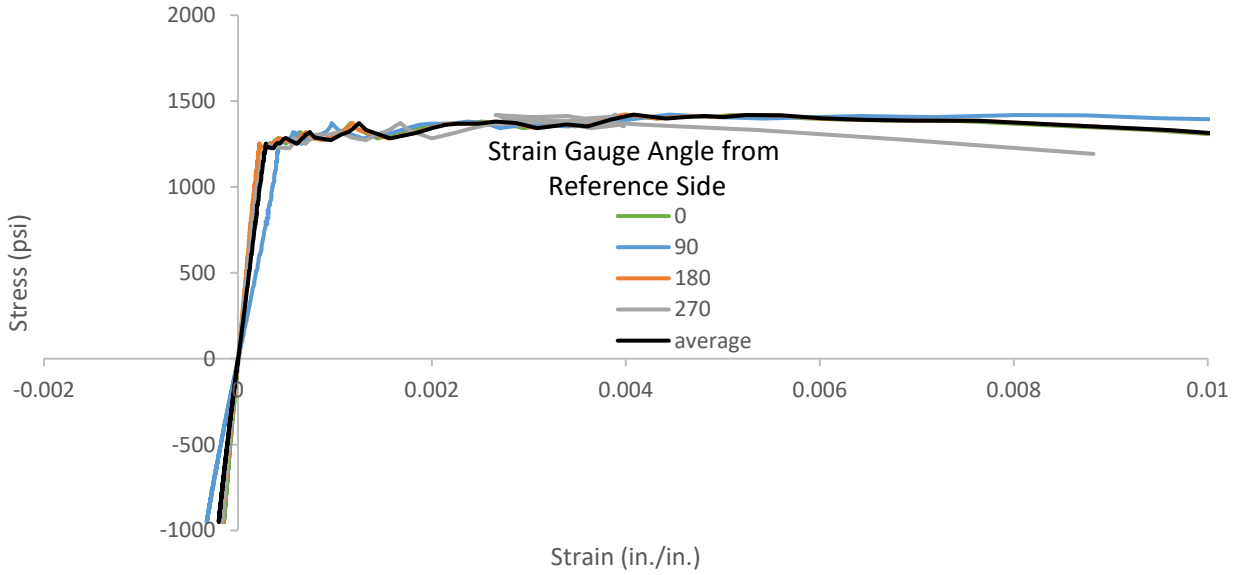

Figure 4-26: Direct tension results for sample 5 placed at the center

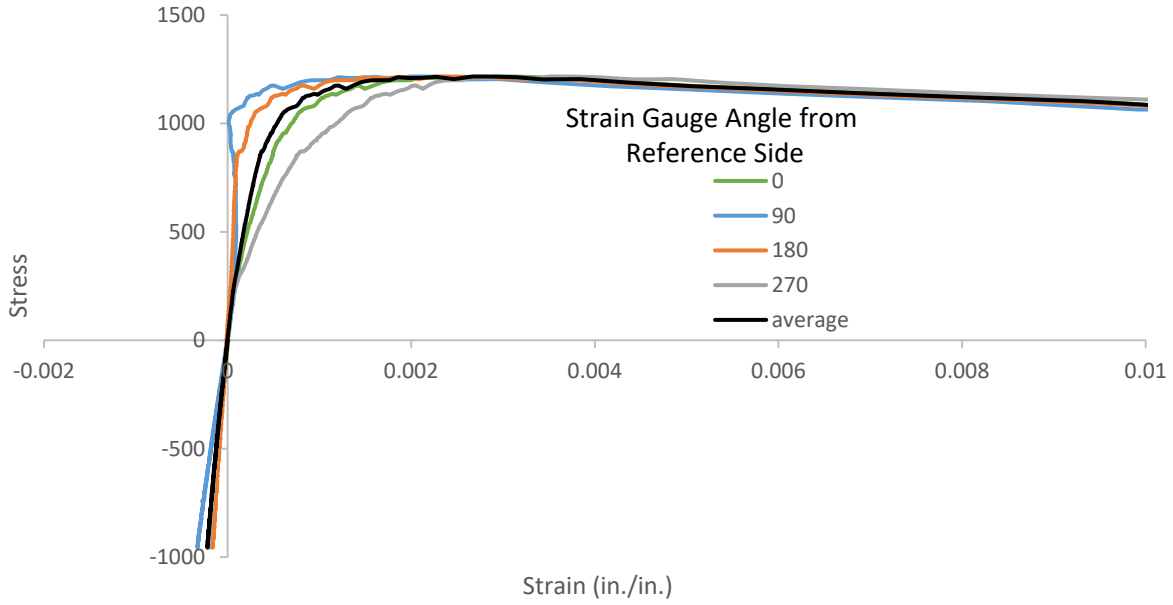

Figure 4-27: Direct tension results for sample 6 placed at the center

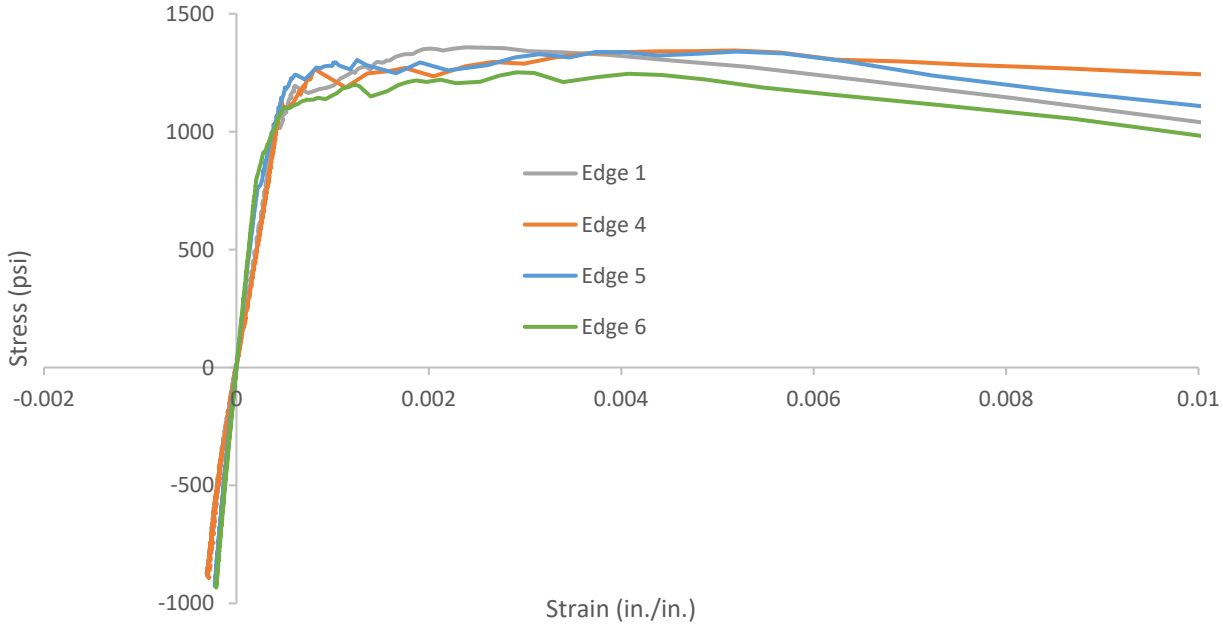

Figure 4-28: Comparison of sample direct tension test results for samples placed at the edge

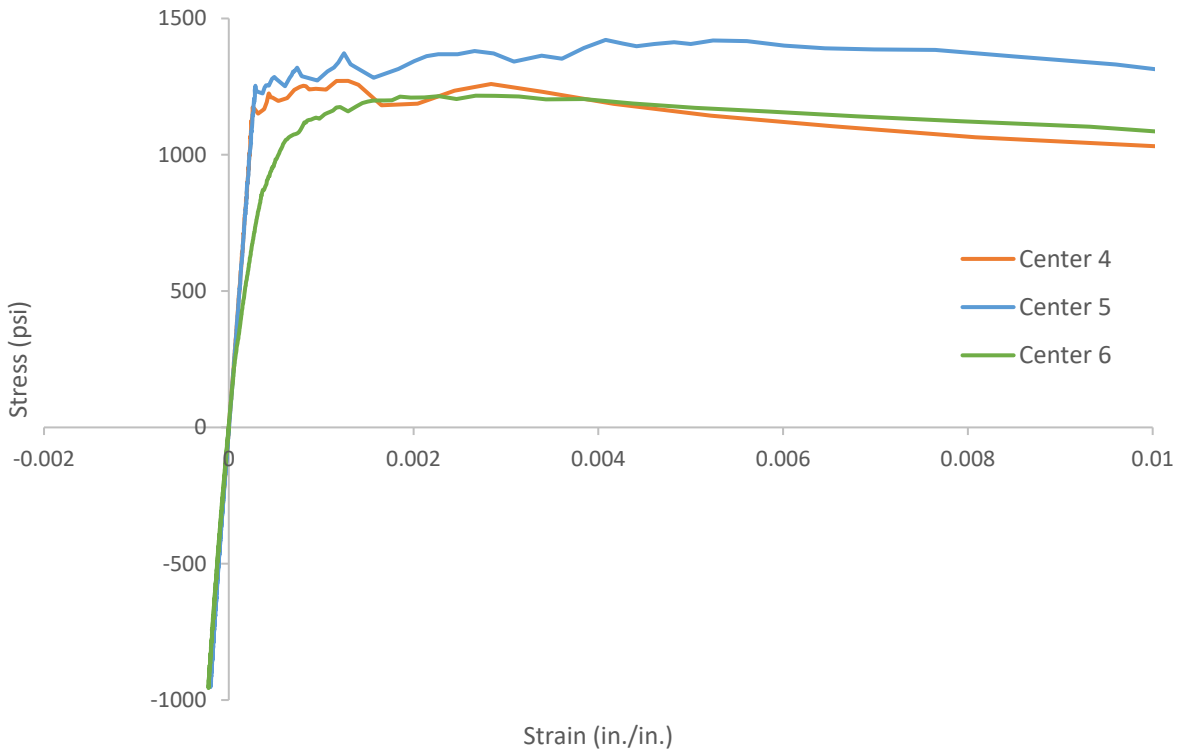

Figure 4-29: Comparison of sample direct tension test results for samples placed at the center

Table 4-2: Summary of strength and modulus results from direct tension testing

Sample	Peak Strength (psi)	Strength at 0.005 strain (psi)	Tension Modulus (million psi)	Compression Modulus (million psi)
Edge 1	1,357	1,302	2.5	2.4
Edge 4	1,344	1,341	2.3	2.5
Edge 5	1,339	1,330	3.7	3.7
Edge 6	1,251	1,221	3.9	4.2
Center 4	1,271	1,187	4.3	4.3
Center 5	1,421	1,407	4.2	4.4
Center 6	1,217	1,188	3.1	2.6

Table 4-3: Direct tension results mean by placement location

	Placement Location	
Mean Results	Edge	Center
Peak Strength (psi)	1,320	1,300
Peak Strength Standard Deviation (psi)	48	106
Peak Strength Coefficient of Variation (%)	3.7%	8.1%
Strength at 0.005 Strain (psi)	1,300	1,260
Tensile Modulus (million psi)	3.1	3.9
Compression Modulus (million psi)	3.2	3.8

The tests performed under load control at UF showed a more rapid pullout after cracking than desired. While the MTS machine and data acquisition equipment were still able to record valid stress-strain curves for the samples tested, it is believed that a switch from force-control to displacement control, like that used at the SMO, will result in less strain localization and possibly less variability. A discussion with Mr. Richard DeLorenzo from the SMO also leads the research team to believe that this will make the test easier for other laboratories to perform the test. It is recommended to use the crosshead displacement to control the testing rate, with the crosshead displacement adjusted to give 1.5 ± 0.5 ksi/min of loading during the compression portion of the test and during the initial elastic portion of the tension loading. This is the same loading rate recommended by FHWA.

Direct tension testing performed at the SMO showed that a system for aligning the grips is needed to prevent sample eccentricities. A data acquisition system to capture the strain on all sides is also needed. The use of wedge grips instead of hydraulic grips precludes the use of a pre-compression loading; however, this should not be required to perform the direct tension test. Of the 7 samples tested, 3 fractured in the middle and 4 in the grips. The SMO did not have the capability of measuring the concrete strain on all four sides of the samples. Without this data, it is not possible to get the full stress-strain curve or the stress at a strain of 0.005 in./in. The UHPC samples tested at the SMO had effective strengths of 1,260, 1,270, and 1,460 psi, giving an average effective strength of 1,330 psi.

4.3.3 ***Fiber Alignment***

Computed tomography scans were made of the middle section of one sample fabricated by placing the concrete in the center of the mold using a funnel and the middle section of another sample at the end using a funnel. Figure 4-30 shows longitudinal (flow direction) cross-sectional views of the CT scan from the middle 5-in. section near the edge of a UHPC direct tension sample with concrete placed at the end. Figure 4-31 shows cross-sectional views of the CT scan from the middle 5-in. section near the center of a UHPC direct tension sample with concrete placed at the end. Figure 4-32 shows cross-sectional views of the CT scan from the middle 5-in. section near the edge of a UHPC direct tension sample with concrete placed at the center. Figure 4-33 shows cross-sectional views of the CT scan from the middle 5-in. section near the center of a UHPC direct tension sample with concrete placed at the center. Green color in the CT scan images represents the cementitious matrix, greenish-yellow pixels represent steel fibers, and dark colors represent air voids. As expected, fibers were aligned more in the longitudinal direction near the edge than in the center for both samples scanned because of the wall effect. No qualitative difference in fibers was seen between the samples placed at the ends and center. A more rigorous quantitative analysis of fiber alignment direction would be needed to determine if a statistically valid difference in fiber preferential orientation was present between the samples placed at the end and center. There were many more entrapped air bubbles seen in the concrete samples than expected. This could explain the low compressive strength of 16,140 psi measured.

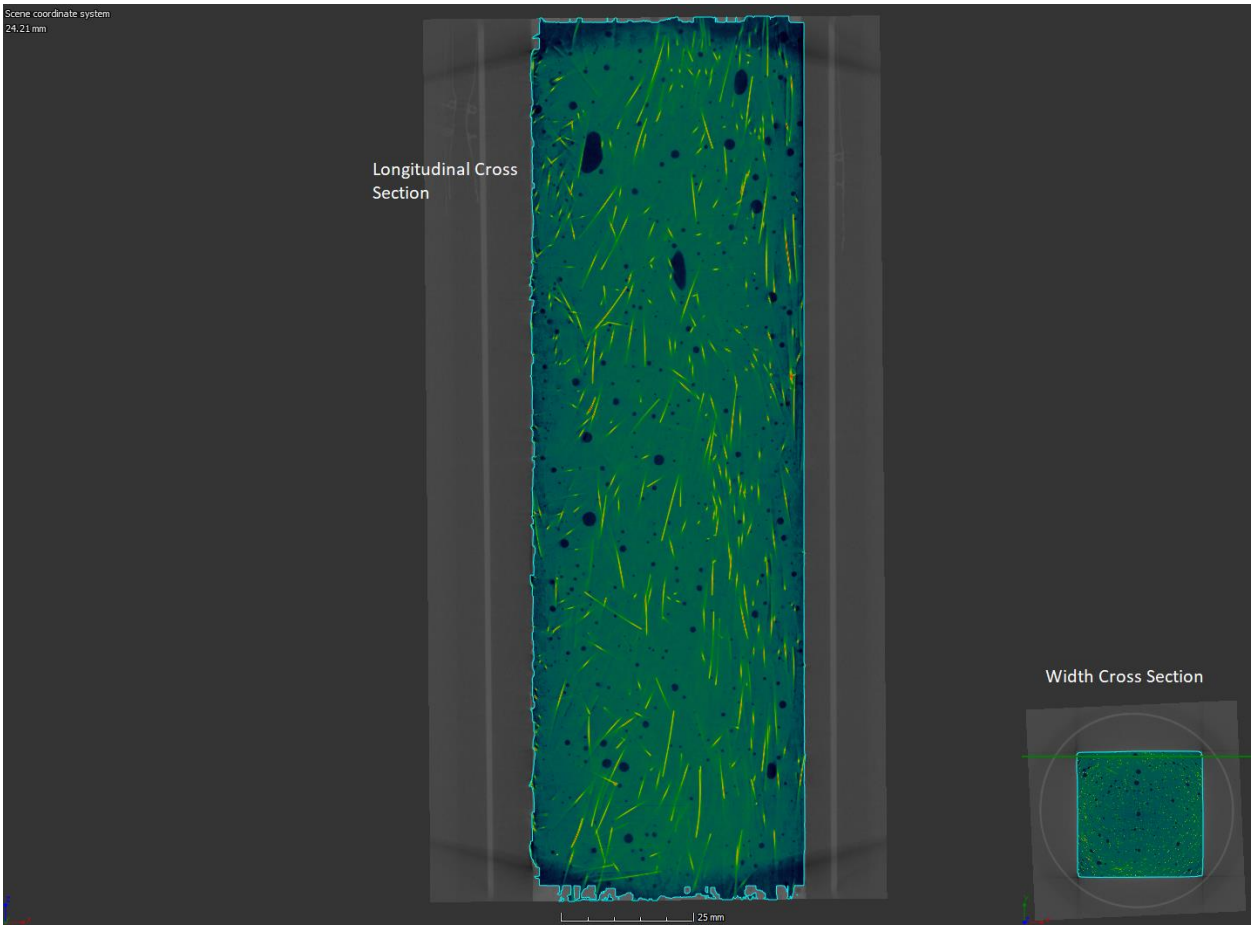

Figure 4-30: CT scan of middle 5 in. and near edge of UHPC direct tension sample for concrete placed at the end

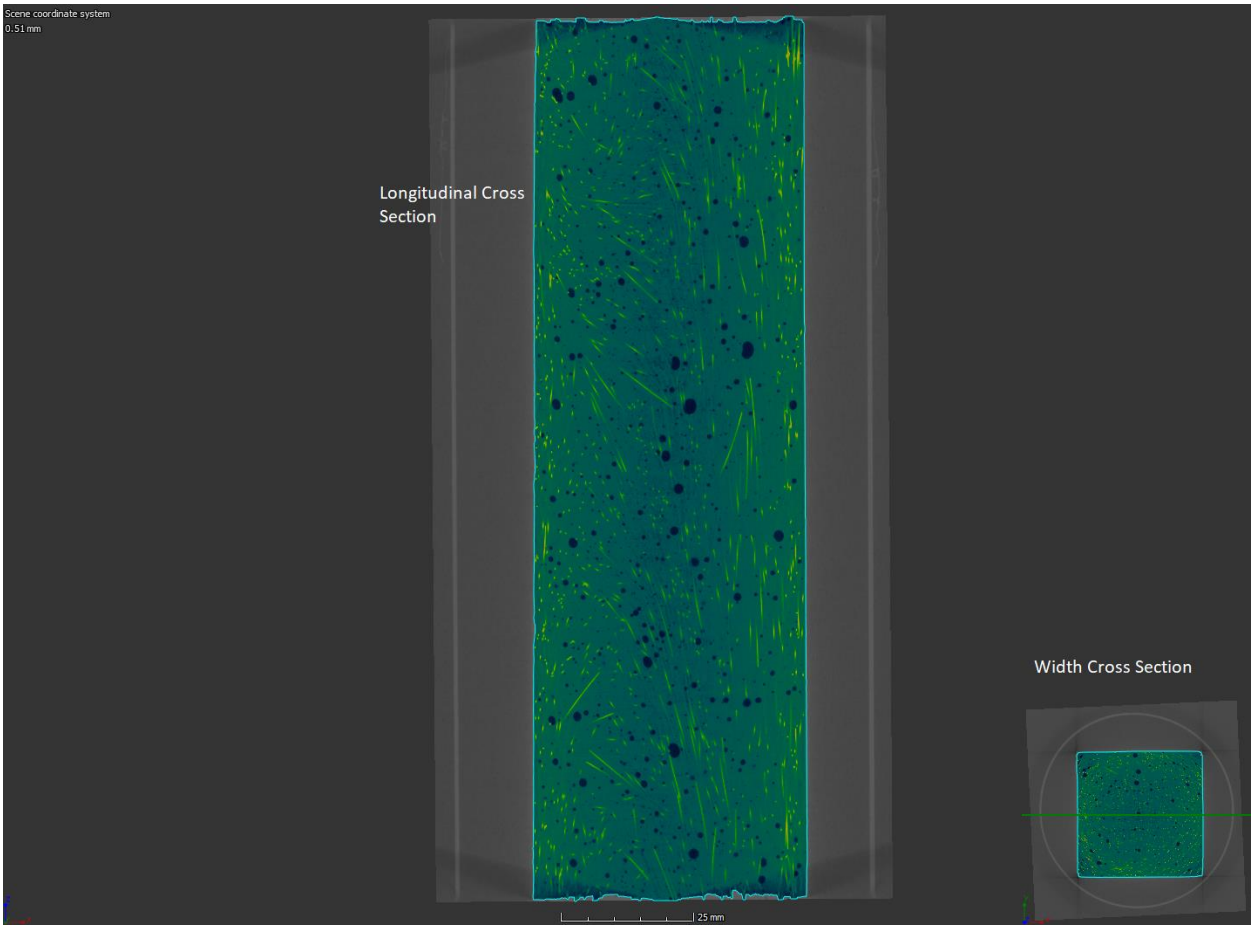

Figure 4-31: CT scan of middle 5 in. and center of UHPC direct tension sample for concrete placed at the end

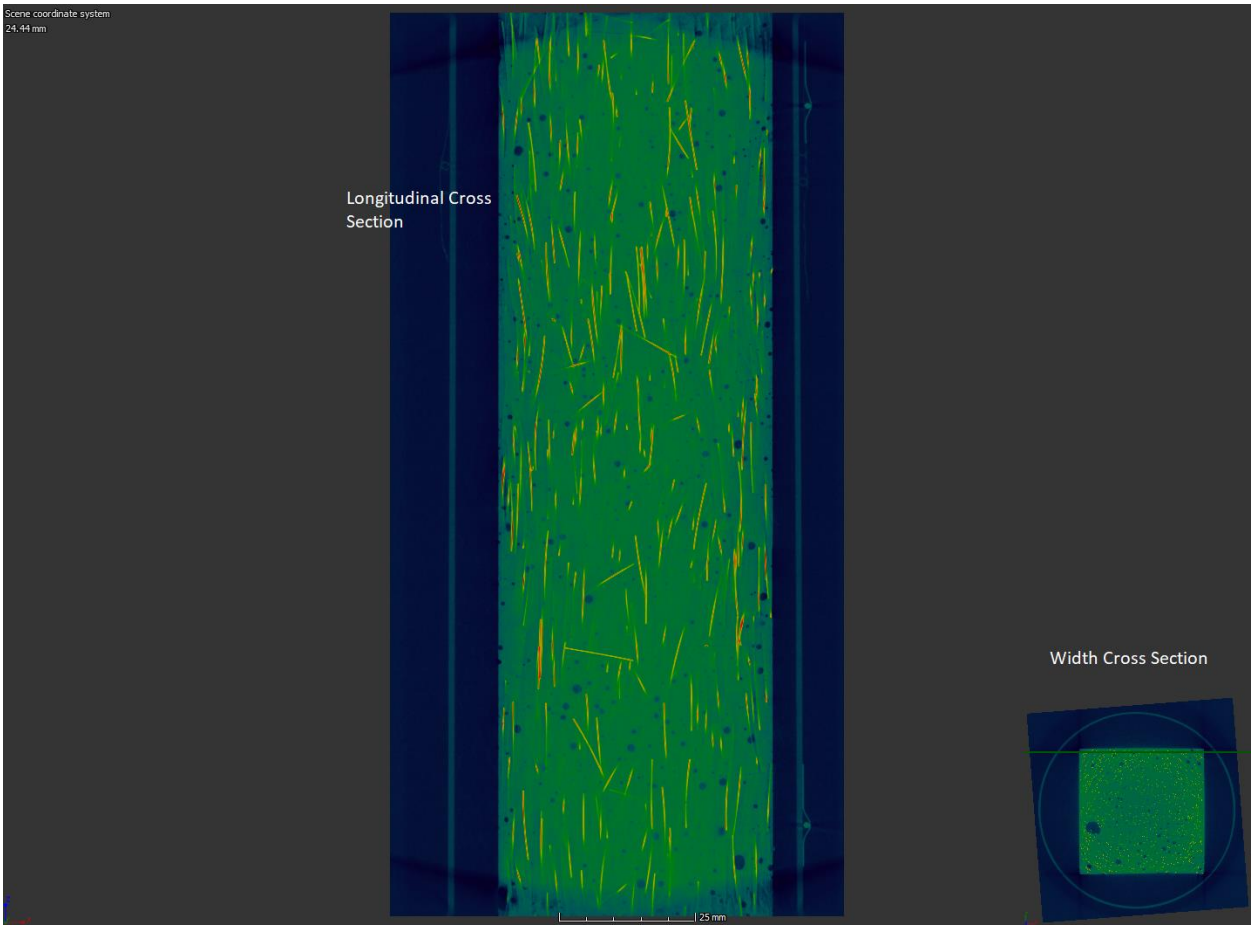

Figure 4-32: CT scan of middle 5 in. and near edge of UHPC direct tension sample for concrete placed at the center

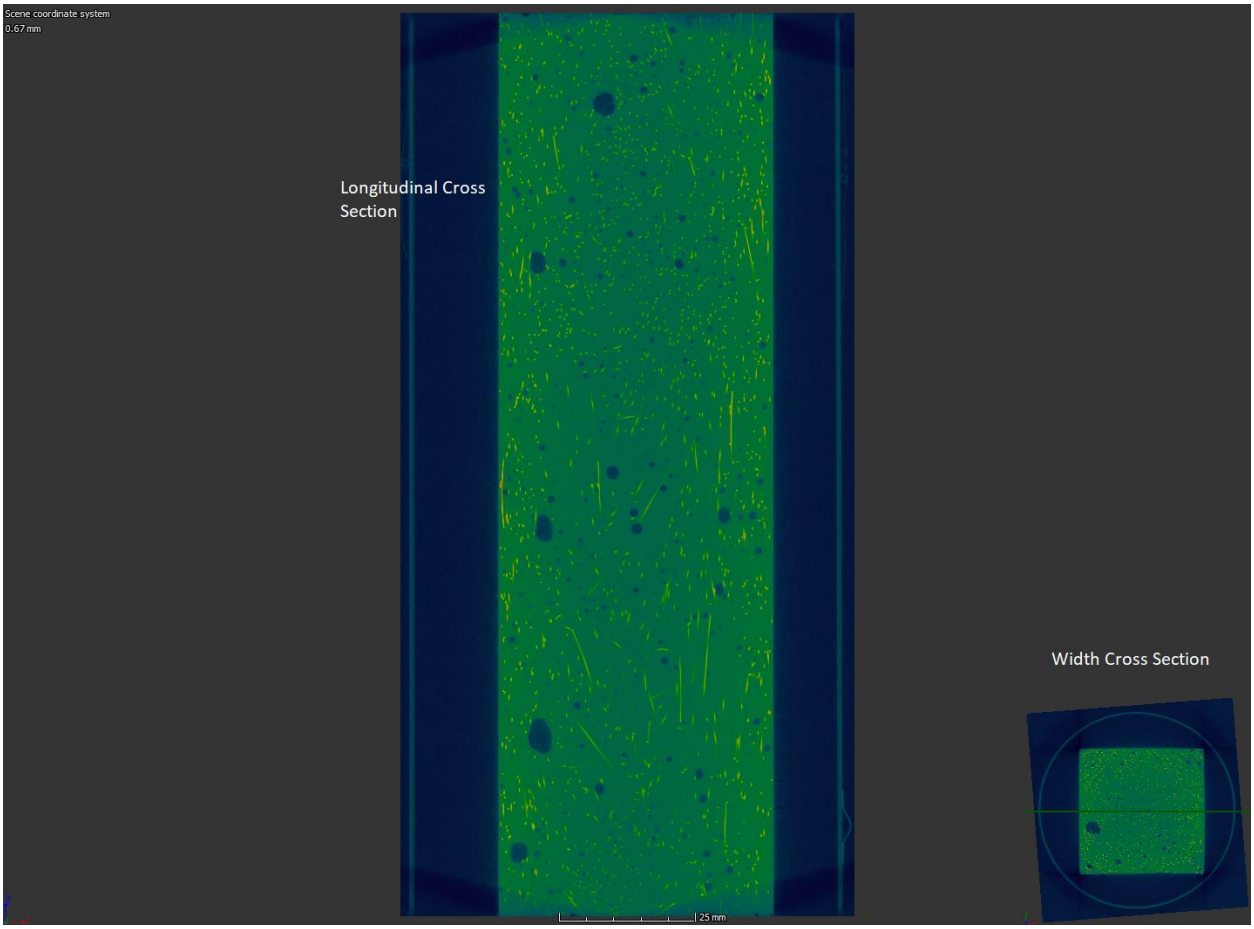

Figure 4-33: CT scan of middle 5 in. and center of UHPC direct tension sample for concrete placed at the center

The computed tomography results demonstrate that the preferential fiber alignment near the edge because of the wall effect could inflate the tensile strength results in a slightly non-conservative manner. This can be accounted for using an effective cross-sectional area term in Equation 4-7 using the method developed for the French UHPC specification NF P18-470, Annex D (AFNOR 2016). In this method, concrete near a boundary should be adjusted for this effect by an area correction factor. A formed surface causes fibers to preferentially align in a manner that would increase the measured tensile strength, while sawcutting a surface would eliminate the development of fibers to the side of the fiber that was removed, reducing the measured concrete strength. Concrete at a distance of half the fiber length would be affected by these effects. The concrete area in this affected region is multiplied by a correction factor as described in Table 4-4. For the concrete made in this study, three sides were formed, while the top surface was not. This

would result in concrete correction of the areas shown in Figure 4-34. The cross-section equivalent area, A_e, for the sample type shown in Figure 4-34 can be calculated using Equation 4-8:

$$\mathrm{A}_e = wd + \frac{l_f}{2}\left[\left(w - \frac{l_f}{2}\right)(C_f - 1) + \left(d - \frac{l_f}{2}\right)(2C_f - 2)\right] \qquad \text{Equation 4-8}$$

Where w and d are sample dimensions (in.) as shown in Figure 4-34, C_f is the edge type correction factor for formed surfaces as described in Table 4-4, and l_f is the average fiber length (in.). For a 2-× 2-in. cross-section and a fiber length of ½ in. with three sides formed, A_e is equal to 4.2625 in.^{2}. A_e should be used in Equation 4-2 instead of the gross cross-sectional area for all calculations except those used to calculate the UHPC elastic modulus. The gross cross-sectional area should be used to calculate the UHPC elastic modulus because fiber orientation is unlikely to have a significant effect on the UHPC stiffness before cracking. For a sample with all four sides sawn, a 2×2 in. cross-section, and a fiber length of ½ in., A_e would be 2.875 in.^{2}. For the samples tested in this study with three molded sides and average results shown in Table 4-3, it resulted in an average overestimation of the strength by 6.1%. Table 4-5 shows the average tensile strength corrected for the fiber alignment provided by the mold wall effect.

Table 4-4: Correction factors for edge effects in flexure specimens (AFNOR 2016)

Location	Correction Factor, C_f
Formed edges	1.2
Sawn edges	0.5
Edges not formed or sawn, and any portion of the cross-section farther than L_f from the edge	1

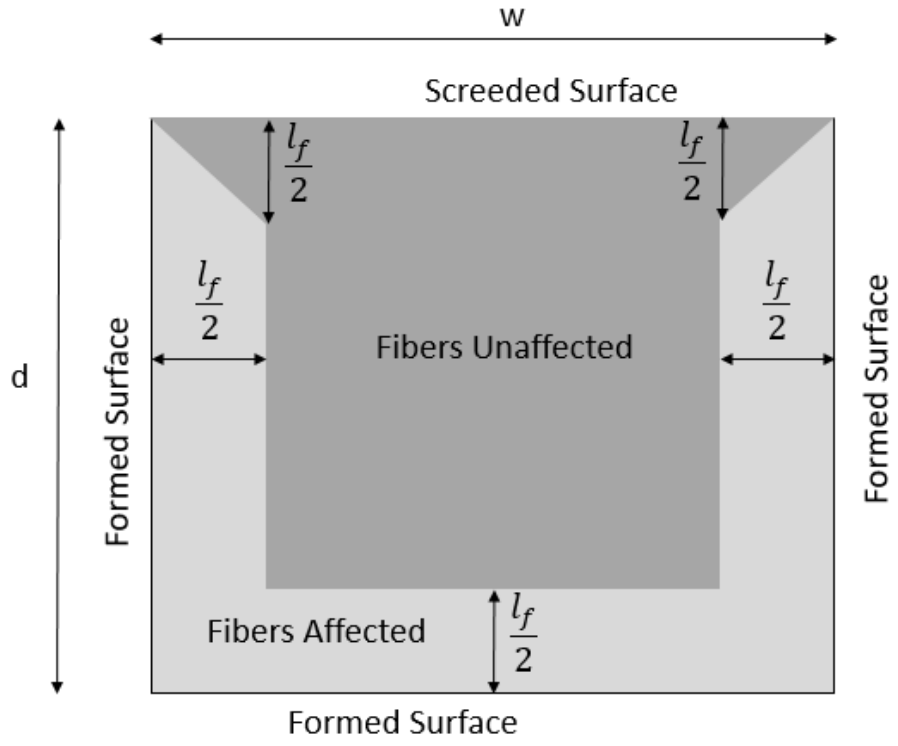

Figure 4-34: Schematic of areas affected by fiber alignment in molded specimens

Table 4-5: Direct tension tests average results after correcting for effective cross-sectional area from mold wall effect

	Placement Location	
Mean Results	Edge	Center
Peak Strength (psi)	1,240	1,220
Strength at 0.005 Strain (psi)	1,220	1,180

4.4 Summary

A comparison of the beam and direct tension results showed that the direct tension provided a lower coefficient of variation than the beam test, and more realistic and conservative peak strength results. The results showed that concrete placement in the center or end is acceptable; however, to be consistent with prism molding procedures for UHPC in ASTM C1856, it is recommended that the concrete should be placed from one end in one layer, without stopping the placement to avoid

lifts or areas without interpenetrating fibers in the samples. It is also recommended that the concrete should be placed through a large funnel that does not severely constrict the flow into the molds. Because the CT scan results showed a fiber preferential orientation near the sample edge where it was molded, a correction procedure has been proposed based on an equivalent area concept found in the French UHPC standard for flexural beams. Based on the research team's experience conducting the concrete direct tension test method and results, a recommendation for a Florida Direct Tension Method is described in Appendix A. The draft test method recommended is adapted from the test method proposed by the Federal Highway Administration (Graybeal and Baby 2013). Some of the language proposed has been reproduced verbatim from the FHWA proposed method in order to simplify adoption of the method and build on the knowledge base developed in the engineering and testing industries. For example, the language used in the definitions section of the test method was preserved from the FHWA draft method to prevent confusion over terminology.

CHAPTER 5. SPECIFICATION RECOMMENDATIONS

5.1 Introduction

The Florida Department of Transportation is in need of a specification detailing requirements for the use of proprietary mixes of Ultra-High-Performance Concrete (UHPC). Draft specifications were written by the Florida Department of Transportation, and the University of Florida has provided suggestions for changes, as shown in the following report. These suggested changes are based on thorough research on the topic of UHPC and on results of a survey sent to states across the country. Specifications of other states and countries were compared thoroughly to find what current practices are regarding UHPC. Deleted items are noted with a strikethrough, and added items are underlined and in red text. Notes about the reasoning behind suggestions are marked as superscript numbers in the text and are explained in Section 3 of this document.

Note: The following sections contain suggested revisions to specifications that are an integral part of this Task Report and will remain in this as-revised state in the accepted Final Report.

5.2 Specifications

SECTION 349

ULTRA-HIGH-PERFORMANCE CONCRETE FOR JOINTS[1]

349-1 Description.

Use ultra-high-performance concrete (UHPC) composed of an optimized gradation of granular constituents, cementitious materials,[3] and reinforcing fibers with a water-to-cementitious materials ratio of less than 0.25.

Prior to casting UHPC field connection joints, construct a mockup of a typical UHPC joint to demonstrate the casting process meet Contract Document requirements.

Obtain the premixed/prebagged UHPC product from a manufacturer that is currently on the Department's Approved Products List (APL).

349-2 Materials.

349-2.1 General: Meet the following requirements:

Prepackaged Ultra-High-Performance Concrete .....Section 927
Water/Ice.....Section 923*

*Use potable water.

349-3 Personnel Prequalification: Meet the UHPC production personnel qualification requirements of Section 105.

349-4 Construction Work Plan

Submit a detailed work plan to the Engineer for review and approval prior to placement of UHPC. As a minimum, include the following items for submittal[3] in the work plan:

1. Proof of UHPC material prequalification as Department APL product.
2. Proposed QC Plan in accordance with Section 105.
3. Proposed UHPC mix design- including ~~information about~~[3] the mix ingredients, water-to-cementitious materials ratio, flow, set time, tensile strength properties[4], and compressive strength properties of the mix at ~~different~~ages of 4, 7, 14, and 28 days.[4]
4. Submit the qualification testing of the UHPC at least 60 days prior to the first anticipated UHPC placement ~~casting concrete~~[3]. ~~Perform the s~~Sampling and testing shall be performed[3] by a qualified testing laboratory meeting the laboratory qualification requirements of Section 105.
5. Storage ~~plan~~ requirements[3] of UHPC materials ~~ingredients~~[3] per manufacturer's recommendation.

6. Proposed forming materials and procedures[3].
7. Minimum acceptable quality and/or performance level ~~Details~~[3] of all equipment to be used to batch and place UHPC materials.
8. Proposed schedule and duration of traffic control required for completion of this work.
9. Procedures used to roughen all surfaces that will be in contact with UHPC[3]. These prepared surfaces shall have an ~~Exposed~~ exposed-aggregate finish~~: Ensure that all precast concrete surfaces in contact with UHPC have exposed aggregate finishes~~ with an average peak-to-valley surface roughness of at least 0.25-inch. ~~average amplitude.~~[3]
10. ~~Placement procedure: Include plan for~~ Provide a procedure for ~~preparation of existing~~ cleaning the roughened concrete surfaces and pre-wetting ~~of the existing concrete interface~~ them to a saturated, surface-dry (SSD) condition ~~before~~ prior to[3] placement ~~, spreading, finishing, and curing~~ of UHPC.[3]
11. Include provisions for:
    a. acceptable ambient temperature and relative humidity
    b. batch temperatures
    c. batch consistency
    d. batch times

    and corrective measures, if appropriate.[5]
12. The procedure ~~plan~~ for ~~casting~~ placement[3] of a demonstration mockup to demonstrate the ability to properly cast UHPC in accordance with the design plans and specifications.
13. Proposed schedule and procedure for watertight integrity testing of completed UHPC joint.

349-5 Storage: ~~Properly s~~Store[3] the premix including powder, admixtures, fibers, and additives, obtained from manufacturer, and as required by the manufacturer's specifications to ensure that the materials are protected from moisture and the subsequent ~~the~~ loss of ~~their~~ physical and mechanical properties[3]. Ensure that LOT numbers and ~~their~~ expiration dates on the ~~preblended~~ bags are visible.[3]

349-6 Presence of UHPC Manufacturer Representative.

Arrange for a representative of the UHPC manufacturer to attend ~~during~~ the pre-placement ~~pour~~[1]-meeting, the casting of the mockup, and the first concrete placement on site.

349-7 UHPC Pre-Pour Meeting.[6]

Hold the pre-pour meeting prior to the UHPC mockup demonstration.

349-8 UHPC Joint Mockup:

349- 8.1 General: Construct a~~n~~[3] UHPC joint mockup in accordance with the design plans, approved shop drawings, and as recommended by the UHPC manufacturer.

Cast a mockup ~~at the jobsite~~[7] that is a partial or full-scale representation of the proposed joint. Following placement and sufficient curing of the UHPC, cut the hardened mockup transversely at two locations to allow for visual inspection of the joint interface and material bond. Make the completed joint mockup cut sections available for review and approval by the Engineer 28 days prior to placement of UHPC. The joint mockup remains the property of the Contractor. Remove the mockup from project site prior to completion of construction activities. The approval of construction using ~~the field casting~~ UHPC ~~placement~~ [3]dependents on successful demonstration of the mockup.

349- 8.2 Mix Workability

Preform ~~the~~ flow loss tests during demonstration of joint mockup casting to determine the~~duration~~ working time ~~that of~~the ~~the~~ UHPC ~~will remain workable~~.[3] Perform the tests while the ambient temperature is not greater than 90°F and concrete temperature is maintained between 60°F and 85°F.

Perform the working time test ~~following workability~~[3] procedure during the casting of UHPC joint mockup:

1. Take initial samples prior to the start of the discharge of UHPC from the mixer[3] and perform the flow tests. Record the time of sampling and initial flow value.
2. Measure the concrete and ambient temperatures~~[3]~~.
3. Continue sampling at every 10-minute intervals and determine the flow of each sample, until flow measure is below 4 inches.
4. Plot the flow versus time for the duration of the test. From the plot of flow-time curve, determine the flow time at 7 inches, which is considered the mixture working ~~cutoff~~ [3]time.
5. For the production concrete, complete the placement of UHPC in less than working ~~cutoff~~[3] time.

349- 8.3 Time of Set ~~Times~~[3]:

Perform the Time of Setting of UHPC for submittal in section 349-4.3 according to[3] ASTM C191 (Using Modifications Described in ASTM C1856).

349- 9 Construction Methods and Requirements.

1. Perform forming, batching, placing, and curing in accordance with the detailed work plan and the UHPC manufacturer's recommendations, accepted by the Engineer.
2. Construct ~~coated~~ formwork from nonabsorbent or coated[3] materials that are properly sealed and capable of resisting the hydrostatic pressures of unhardened UHPC. Do not use formwork composed of aluminum or magnesium.[8] Do not

remove formwork until the UHPC ~~undergoes~~ achieves a minimum compressive strength of 10,000 psi ~~is achieved~~[3].

3. Provide the required number of portable high shear batching units for mixing of the UHPC. Ensure that the mixing equipment, which is not supplied by the UHPC manufacturer, must be reviewed by the UHPC manufacturer for adequacy.
4. Ensure that the fibers are fully distributed, without clumping.
5. During batching, keep the temperature of the UHPC below 85°F. Add ice to the mix as recommended by the UHPC manufacturer's representative, but not to exceed the allowable specified water-to-cementitious materials ratio. The temperature of UHPC at the completion of mixing shall not exceed 85°F.[3]
6. For ~~The~~ precast concrete surfaces that will be in contact with UHPC, pre-wet their surfaces ~~ahead~~ prior to ~~of the~~ UHPC placement. Thoroughly and continuously wet the concrete contact area with fresh water for at least 24 hours prior to the ~~placing~~ placement of UHPC[3].
7. Ensure the formwork is free of ~~Remove~~[3] all standing surface water ~~just~~[3] prior to UHPC placement.
8. Follow the batching sequence as specified in the approved UHPC detailed work[3] plan and approved by the Department. Fill the surface of the UHPC field joints to ~~plus~~[3] 1/4 inch above the surface of the adjacent bridge deck.[9]
9. Place UHPC in accordance with the approved placement plan. Internal vibration of UHPC is not allowed during placement. Rodding is allowed only at locations where successive placements meet.[10] ~~Keep~~The minimum temperature of UHPC must be maintained above ~~temperature above~~60°F[3]. Cover and cure UHPC[3] until it has achieved a minimum compressive strength of 10,000 psi.[9] On ~~the S~~short ~~B~~bridges, place the UHPC in a continuous manner, ~~non-stop pour,~~ unless otherwise approved by the Engineer. Short bridges are defined as bridges with a maximum length of 100'.[11] ~~No c~~Cold joints are not ~~will be~~[3] permitted between any individual length of UHPC joint. Cure the UHPC in the form according to UHPC manufacturer's recommendations to attain the required strength shown on the contract documents.
10. Ensure that the connection joints remain free from differential movement and rotation until the UHPC achieves the required compressive strength shown in the project plans for opening bridge to traffic.
11. Keep the connections free of any dirt, ~~or~~ debris, and oil[3].
12. ~~Cure and cover Joints until the compressive strength achievement of at least 10,000 psi~~[3]Ensure that all lifting lug pockets and any other deck protrusions are ~~water blast~~ cleaned via water or sandblasting[3] and filled with UHPC.
13. After the installation of the joints, perform water integrity test in accordance with 349-11.
14. The grinding of the UHPC surface can be performed when strength of 10,000 psi has been achieved. Suspend grinding~~,~~[3] if significant fiber pullout is observed during grinding operations. Take corrective action to prevent the recurrence of the problem and such action ~~is~~ shall be[3] approved by the Engineer prior to implementation[3].
15. The bridge can be opened to traffic when the required UHPC compressive strength, in accordance with project plans[3], has been achieved.

349-10: Sampling and Testing

349-10.1 UHPC Quality Control Sampling and Testing: Perform sampling and testing of UHPC at the frequencies provided in Tables 349-1 and 349-2 during field demonstration of mockup ~~demonstration~~[3] ~~-~~and during construction, respectively. Perform the following quality control sampling and testing during casting of the mockup and field casting of UHPC placement:

1. Measure the flow of each batch of UHPC.
2. In the quality control log, record the UHPC flows, ambient air temperatures[3], and mix temperatures for each batch. Include the time and date, amounts of water/ice and admixtures corresponding to the UHPC batch,[3] and Lot numbers for traceability. A Lot of UHPC is defined as 25 CY or one day's production, whichever comes first.

Table 349-1: UHPC- Sampling and Testing Frequencies During Field Demonstration of Mockup

Material Characteristic Description	Test Method	Minimum Sampling and Testing Frequency
Flow of UHPC	ASTM C1437 (Using Modifications Described in ASTM C1856)	Required number of tests per Sub-articled 349- 8.2 Mix Workability
Time of Setting of UHPC	ASTM C191 (Using Modifications Described in ASTM C1856)	One test during mix design verification or field demonstration
Temperature of Freshly Mixed Hydraulic Cement Concrete	Concrete ASTM C1064	One test per batch
Concrete Compressive Strength of Cylindrical Concrete Specimens	Make test specimens in accordance with ASTM C31 and test them in accordance with ASTM C39 (Using Modifications Described in ASTM C1856)	Cast 4 sets of three cylinders during field demonstration. Test them at the ages of 4, 7, 14, and 28 days
Chloride content	FM 5-516	One test during mix design verification or field demonstration

3. As part of the as-built records, track and show the placement locations of UHPC Lots on the contract plans. Submit a copy of the as-built records to the Engineer.
4. Cylinder Samples:
   From every Lot, take 4 sets of three cylinders, 3"x 6", for compressive strength testing ~~cylinders,~~ in accordance with ASTM C31 and ~~(~~using modifications described in ASTM C1856~~)~~[3]. One set will be taken at the beginning and one set at the end of the Lot. In an evenly distributed manner, take the two intermediate sets ~~form~~ from[3] the middle portion of the Lot. Cure all sets in an environment like that of[3] the placed UHPC. For traceability, track all sets to Lot numbers.

Table 349-2: UHPC- Sampling and Testing Frequencies During Construction		
Material Characteristic Description	**Test Method**	**Minimum Sampling and Testing Frequency**
Flow of UHPC	ASTM C1437 (Using Modifications Described in ASTM C1856)	One test per batch
Temperature of Freshly Mixed Hydraulic Cement Concrete	Concrete ASTM C1064	One test per batch
Concrete Compressive Strength of Cylindrical Concrete Specimens	Make test specimens in accordance with ASTM C31 and test them in accordance with ASTM C39 (Using Modifications Described in ASTM C1856)	4 sets of three cylinders per Lot of 25 CY or one day's production, whichever comes first
Chloride content	FM 5-516	One test per month of UHPC production
Water Integrity Test for Bridge Deck joints:	349-11.2	One[3] test per bridge deck

349-10.2 UHPC Quality Control Compressive Strength Testing:

For each Lot, test the compressive strength cylinders at the times that are described below. Compressive strength is measured using 3- x 6-in. cylindrical specimens made and tested in accordance with ASTM C31/C31M with the appropriate modifications as described in ASTM C1856. ~~A~~ The strength ~~test~~ at a designated age is the average of at least three 3- x 6-in. specimens.[3]

1. ~~Test three cylinders p~~Prior[3] to the removal of forms or grinding of joints, ~~to~~ensure that the[3] UHPC has achieved a[3] compressive strength of 10,000 psi.
2. ~~Test three cylinders to e~~Ensure[3] that the UHPC has achieved the required strength shown in the project plans prior to opening ~~of~~[3] the bridge to traffic.
3. ~~Test three cylinders~~ Perform a compressive strength testing[3] at 28 days to verify final strength.
4. ~~Maintain~~ Hold[3] the remaining three cylinders for resolution testing, if needed.

Ensure that the tests are performed by a ~~Department~~ Department-qualified[3] testing laboratory. Cure the cylinders on-site in a similar environment as the UHPC joint material and ship them to the ~~Department~~ Department-qualified[3] testing laboratory for testing.

349-10.3 UHPC Chloride Content Limits for Concrete Construction:

Perform the chloride content test at a frequency of one sample per month of UHPC production. The maximum allowable chloride content ~~is 0.40 lb/cy~~ is ≤ 0.06 lb per 100 lb of cementitious materials per cubic yard[12].

349-11 Quality Assurance Program

349-11.1: Verification Sampling and Testing: The Engineer will observe the UHPC placement~~,~~ and[3] take verification samples for~~,~~[3] concrete temperature, flow, and compressive strength tests at a frequency of one sample per four Lots. Inform the Engineer of the anticipated UHPC placement[3] 48 hours prior to the anticipated start ~~the anticipated UHPC placement~~[3]. Final acceptance will be based upon 28-day compressive strength. Field coring of UHPC for dispute resolution ~~will~~is not ~~be~~ allowed[3].

Meet the requirements of 346-9.1 related to the verification sampling, testing, and comparison of the results with ~~correspondence~~ corresponding[3] QC sample results.

The Contractor is responsible for providing an adequate location to place ~~acceptance~~[3] specimens for initial curing prior to transport to the laboratory. Equip the curing boxes with supplemental heating[3] or cooling as necessary to cure specimens in accordance with ASTM C31.

349-11.2 Water Integrity Test for Bridge Deck joints: After the UHPC bridge deck joints have been installed and the formwork has been removed[13], flood the entire deck with one-inch depth of water for a minimum duration of 30 minutes. Inspect the concrete surfaces under the joint during this minimum[3] 30-minute period,[3] and for a minimum of 45 minutes after the supply of water has stopped, to ensure that there is no evidence of dripping water or moisture. The surfaces on the underside of the joint are watertight when they are free from any sign of moisture. ~~Locate the place(s) of leakage and~~ If the joint system exhibits evidence of water leakage at any location, take remedial measures necessary to stop the leakage~~, if the joint system exhibit evidence of water~~

~~leakage at any place~~.[3] Perform the work at the Contractor's expense and with no time extensions to the project. A subsequent water integrity test may be required, subject to the same conditions and consequences as the original test, per the direction of the Engineer. If no evidence of water leakage occurs, the Contractor need not seal the joint.

349-12 Method of Measurement

The ~~quantities~~ quantity of concrete to be paid for will be the total volume of UHPC, in cubic yards, ~~in place, completed~~ placed and accepted. ~~Include in the measurement, t~~The volume of UHPC used in the joint mockup shall be included in the total. The concrete quantities shown on the plan~~, measured by the cubic yard,~~ are for the Contractor's information only[3].

349-13 Basis of Payment

Payment shall be based on ~~The~~ the quantity of UHPC accepted ~~will be paid at~~ and the contract unit price ~~per cubic yards~~. ~~Price and p~~Payment[3] will constitute full compensation for surface preparation, supplying, mixing, transporting, placing, finishing, curing, grinding, and for furnishing all equipment, tools, labor, and incidentals required to complete the work.

~~Additional~~ The volume ~~quantity~~ of ~~material~~ UHPC used for ~~in the determination of~~ material ~~properties~~ property and ~~for~~ acceptance testing as described herein will be furnished at no additional cost to the Department[3].

If the UHPC does not meet the minimal material properties as described herein, the UHPC will be removed and replaced, or remediated to the satisfaction of the Engineer at the Contractor's expense.

Bar reinforcement and reinforcement of mechanical connectors (where required), will be paid under its own items.

Payment will be made under:

Item No. 349 - 1 UHPC Closure Joint for Precast Deck Panel-per cubic yard.

SECTION 927
PREPACKAGED ULTRA-HIGH-PERFORMANCE CONCRETE

927-1 Description.

This Section covers Ultra-High-Performance Concrete (UHPC) products.

927-2 Approved Product List.

Only use UHPC products listed on the Department's Approved Product List (APL). Manufacturers seeking evaluation of their products must apply in accordance with Section 6 and include certified test reports from an independent laboratory audited by and meeting the requirements of ISO 9001,[3] or meeting the Laboratory Qualification Program requirements of Section 105 showing that the product meets the requirements of this Section.

Provide a certification to the Engineer from the manufacturer conforming to the requirements of Section 6 indicating that the product meets the requirements of this Section.

Any change of materials or material sources requires new testing and certification of conformance with this Specification.

927-3 General Requirements.

927-3.1 Prepackaged UHPC Materials: Materials shall be prepackaged in clearly-labeled[3] moisture-proof[3] containers. ~~Manufacturer~~ The manufacturer[3] shall provide information about the packaging, mix proportions, yield, delivery method, storage, and mixing procedure ~~of~~ for[3] UHPC,~~;~~[3] including:

1. **Premixed[3] materials:** Brief description of the dry[3] ingredients ~~of dry materials~~ in each bag, the weight of each bag, and the[3] number of bags in each pallet.
2. **Fibers**: The type, diameter, length, and tensile strength of the[3] fibers~~;~~,[3] including the percentage of the mix's dry volume. ~~The UHPC steel fiber reinforcement~~ Steel fibers[3] must comply with the Source of Supply-Steel requirements of Section 6.
3. **Admixtures:** The manufacturer's material data sheet shall indicate whether the admixtures are ~~part~~ of contained in[3] the preblended/premixed cementitious[3] component of UHPC or ~~they are delivered~~ contained[3] in separate bags/container. ~~Do not use admixtures~~ Admixtures[3] or additives containing calcium chloride (either in the raw materials or introduced during the manufacturing process) shall not be used[3].

927-3.2 Water: The mixing water shall meet the requirements of Section 923, as potable water.

927-4 Storage: The manufacturer's instructions[3] shall indicate the storage temperature, covering, and delivery method of the unopened bag materials to protect them from moisture ingress, seepage, corrosion, and UV exposure. The production date of the premixed materials shall be stamped on each bag and instructions shall indicate the shelf life of the products[3] in its original unopened packaging.

Table 1: Prepackaged[3] UHPC Mechanical Properties		
Material Characteristic Description	**Test Method**	**Acceptance Criteria**
Concrete Compressive Strength of Cylindrical Concrete Specimens (Non-Heat Treated)	ASTM C39 (Using Procedures Described in ASTM C1856).	≥ 14,000 psi at 4 days ≥ 21,000 psi at 28 days
~~Split Cylinder First Cracking Strength~~[14]	~~ASTM C496 (Mount LVDTs to the ends of the test cylinder for measuring the first cracking strength.)~~[14]	~~≥ 1,000 psi at 28 days~~[14]
Direct Tension Peak Effective Strength	Florida Direct Tension Test	≥ 1,200 psi at 28 days[15]
Direct Tension Effective Strength at 0.005 Strain	Florida Direct Tension Test	≥ 1,000 psi at 28 days[15]
~~First Peak Strength~~	~~ASTM C1609 (Using Modifications Described in ASTM C1856)~~	~~≥ 1,200 psi at 28 days~~[15]
Static Modulus of Elasticity of Concrete in Compression	ASTM C469 (Using Modifications Described in ASTM C1856)	Report value ~~≥ 6,500,000 psi at 28-day~~[16]
Length Change of Hardened Concrete	ASTM C157 (Using Modifications Described in ASTM C1856)	≤ 800 micro-strain at 28 days, initial reading after set[17]

927-5 Material Data Sheet:

The material data sheet shall include the[3] UHPC product name, ~~its~~ recommended[3] applications, and usage[3] instructions and recommendations~~;~~, ~~describing~~ including[3] the following:

1. Storage of product components at project site.

2. Types of forms.
3. Mix proportions and yield in cubic yards. For each product, the manufacturer shall provide a mix design with a maximum allowable water-to-cementitious materials ratio of less than 0.25
4. ~~Mixing procedure and its~~ ~~w~~Working time of the mix[18].
5. Ambient and mixture ~~temperatures~~ temperature ranges recommended for ~~during~~ [3]mixing, batching, and placement.
6. Preparation ~~of~~ procedure for[3] the prefabricated concrete surfaces that will be in contact with the UHPC product
7. Batching, mixing, transportation, placement, finishing, and curing ~~method of~~ procedures for[3] the UHPC.
8. Recommended[3] ~~T~~ types of mixers and placement equipment
9. ~~Provide product~~ Typical mechanical and durability[3] properties listed in Tables[3] 1 and 2
10. ~~Provide the t~~ Typical[3] fresh properties ~~of UHPC product~~,[3] including~~;~~ density, flow, working time, and set time of the mix.

Table 2: UHPC Durability Properties		
Material Characteristic Description	**Test Method**	**Acceptance Criteria**
Abrasion Resistance of Concrete by Rotator Cutting Method	ASTM C944 (Using Modifications Described in ASTM C1856)	≤ 0.026 oz loss
Concrete's Ability to Resist Chloride Ion Penetration (For nonmetallic fiber)	ASTM C1202 (Using Modifications Described in ASTM C1856) (1/2~~"~~ in.^{3} depth)	≤ 360 coulombs at 28-day test
Chloride content	FM 5-516	≤ 0.06 pounds per 100 lb of cementitious materials[12] ~~≤ 0.40 lb/yd^3~~
Chloride ion permeability	AASHTO T259 (1/5~~"~~ in.^{3} depth)	< 0.1 lb/yd^3
Surface Resistivity (For nonmetallic fiber)	AASHTO T358	≥ ~~29~~ 100 ~~KOhm~~ kΩ·cm^3 at 28-day test[19]
Scaling Resistance	ASTM C672	Y < 3
~~Freeze-Thaw Resistance~~	~~AASHTO T 161 / ASTM C666A (600 cycles)~~	~~Relative Dynamic Modulus of Elasticity ≥ 95%~~[20]
Alkali-Silica Reaction	ASTM ~~C1260~~ 1567[21]	Innocuous ~~(at 28 Day Test)~~[22]

927-7 The Production Supervision of UHPC

The manufacturer shall provide training to the Contractor's supervisor and other personnel involved in the field operations of the UHPC,[3] or have a field representative available at[3] all times during the UHPC operations on ~~the~~[3] Department projects. The representative shall be knowledgeable in the supply, mixing, delivery, placement, finishing, and curing of the UHPC.

5.3 Justifications for Suggested Changes

[1]Since this specification is only discussing joint construction, it should be specified in the title.

[2]Requiring each item to be a submittal is useful for contractors so they know exactly what needs to be presented to the Department of Transportation

[3]Editorial change

[4]Because tensile strength properties are an important characteristic for UHPC, the properties should be submitted. Specifying which ages to report will be helpful to the contractor. Four- and 28-day tests were recommended because these ages are required by Alabama, Idaho, New Jersey, New Mexico, New York, Texas, and Ontario, while 7- and 14-day values were selected to match the values required in Table 349-1.

[5]Reformatted as a list to make submission easier for contractor

[6]This heading was made bold to be consistent with the rest of the specification.

[7]It is probably unnecessary to perform this at the jobsite and would likely cause added hassle. New Mexico's UHPC specification states that, "the mock-up Pour shall take place at an off-site location proposed by the Contractor and agreed to by the Project Manager." Idaho, Delaware, West Virginia, and Iowa require mock-ups but do not specify a location.

[8]Aluminum and magnesium forms can react with UHPC and are prohibited in the Canadian UHPC specification (CSA A23.3 2018). Existing FDOT specifications do not prohibit use of magnesium forms currently, requiring inclusion in this section.

[9]This has been separated into two sections for clarity.

[10]Internal vibration should be prohibited as it can cause fiber segregation and preferential alignment (CSA A23.3 2018; Edington and Hannant 1972).

[11] "Short bridges" has been defined as to avoid confusion.

[12] Maximum chloride content should be determined as a percentage of cement, according to ACI 201.2R-16. While there is a disagreement among experts as to whether cement content or cementitious material content should govern chloride limits, UHPC's high cement content should

allow for a higher chloride limit. Thus, 0.06% by mass of concrete is used in Table 9.5.2.1.2 of ACI 201.2R-16 (2016). Cementitious materials are defined as the amount of material used to calculate the w/cm in the mix design. To make calculations easier, it may be preferable to calculate an acceptable chloride content for a UHPC mixture with a typical cement content.

[13] The removal of formwork was added as a requirement before watertight testing of the bridge deck to avoid the possibility of the deck being flooded before the concrete had set.

[14]It is recommended that this test be removed because it is redundant with the flexural strength test requirements, and provides less information than the flexural strength requirements. It may also significantly overestimate the tensile strength because the compression along the length of the crack helps to hold fibers in place, thus increasing the strength they can hold without being pulled out (Graybeal 2006). Because both peak strength and first cracking strength can be determined in the same flexural cracking test, it will reduce the testing burden if first cracking strength is determined by ASTM C1609 instead of ASTM C496.

[15] It is recommended to require direct tension effective strengths using the proposed Florida test method instead of flexural strength requirements. To ensure that the UHPC has some toughness, a direct tension effective strength of at least 1,000 psi at a strain of 0.005 in./in. is recommended. If the specification only contains a peak tension strength, it is possible that a UHPC mixture without fibers could have a very high tensile strength before failure, but would not perform as expected in a structure.

The University of Florida intends to develop a correlation between the tensile strength (using direct tension) and the flexural strength, which may require a change in the post-cracking factor (1.1) used to specify the flexural peak strength. After development of this relationship, the tensile strength can be specified by direct tension testing or converted from flexural testing. Specified strength values from other organizations are as follows: for flexural strength: 2 ksi by Idaho and 2.1 ksi from Ontario; for tensile strength: 1,100 psi from Switzerland, 580 psi from Canada, 800 psi from Colombia, and 870 psi from France.

[16]A minimum value for modulus may be unnecessary and difficult to control since modulus is typically determined by the strength and aggregate modulus. Canada, France, and Switzerland only

require that the value be reported, which would be helpful for structural calculations. No other states require a modulus value to be met or reported.

[17]Most of the shrinkage in UHPC occurs early in the curing process (Binard 2017), so measuring length change from set until 28 days will give more accurate results than the specified first measurement of 1 day after casting. Switzerland, Idaho, and New York also include this adjustment.

[18]Because "mixing procedure" is already defined in section 7 of this list, it has been removed from step 4.

[19]This is a low requirement for UHPC, and significantly lower than an equivalent concrete quality required by the ASTM C1202 limit specified. Since both surface resistivity and ASTM C1202 are in essence electrical resistivity tests, there is a strong correlation between the two that allows for theoretical conversion between the two values. Conversion calculations can be done to give an estimated relationship between chloride ion penetrability (ASTM C1202-17a 2017) and surface resistivity (Spragg et al. 2014). Assuming a pore solution conductivity of 0.1 Ω·m and a geometry correction factor (to account for the conversion between bulk and surface resistivity) of 1.9 (Spragg et al. 2013), it was calculated that a concrete with chloride ion penetrability of 360 Coulombs, as limited in this specification, would have a surface resistivity of 109 kΩ·cm. 100 kΩ·cm is used as a soft conversion in this specification.

[20]This test is probably not necessary for Florida. While there may be some parts of the state that undergo freeze-thaw cycles, performing this test would require specialized equipment. In addition, the specified scaling resistance test can give a good indication of a material's ability to resist any freezing found in Florida.

[21]ASTM C1260 is designed specifically for alkali-silica reaction with sand. ASTM C1567 is recommended because it includes testing for SCM reactivity, and UHPC often has high SCM contents. Among states specifying an ASR test, Delaware and Idaho use ASTM C1567, and New York, New Mexico, and Texas use C1260.

[22]Both ASTM C1260 and ASTM C1567 are designed to be 14-day tests. While some agencies have started to specify a 28-day criterion, the original limits for innocuous aggregates were

determined based on 14-day values. While Delaware, Idaho, and New York specify 28-day testing for ASR, New Mexico and Texas use a 14-day test.

CHAPTER 6. CONCLUSIONS AND RECOMMENDATIONS

6.1 Conclusions

Responses from 32 states, Washington, D.C., and Ontario, Canada showed differences in material and construction practices. Reasons for differences were also identified. Survey results were used to make recommendations for UHPC specifications.

A draft Florida Test Method for UHPC direct tension testing has been developed and is recommended for adoption. This test method was based on a recommended direct tension test method developed by the Federal Highway Administration. It was modified to help prevent premature specimen failure in the gripping area through application of a small compressive force in the tapered portion of the aluminum plate attached to the UHPC samples that is not gripped by the universal testing machine. A correction procedure to account for the effects of fiber preferential orientation in cast samples tested in direct tension was also developed.

6.2 Recommendations

A draft Florida Test method for direct tension measurement of UHPC was developed. This test method provides the complete tensile stress-strain curve of UHPC that is needed to design UHPC structural members. Equipment is available at the University of Florida (UF) to perform this test. Some modifications will be required to FDOT SMO equipment in order to perform this test. It is recommended that FDOT adopt the proposed test method and determine whether to work with UF to arrange for use of the test equipment or retrofit the current SMO universal testing machine to be able to perform the test. Recommendations have been made for changes to sections 349 and 927 of the FDOT specifications. It is recommended that FDOT adopt the specification recommendations made for prebagged UHPC materials for field structural use.

6.3 Future Work

Work performed under this contract focused on requirements for field use of proprietary UHPC in Florida structures, primarily in bridge joint and repair applications. This work recommends requiring UHPC for these applications to achieve 21,000 psi compressive strength at 28 days. UHPC could be made at lower strengths more cost-effectively for other applications with excellent performance. Future research should investigate requirements for UHPC made with locally

available materials for different applications such as prestressed concrete members. This should include requirements for mechanical properties, durability, and construction requirements for these other applications. This could result in different classes of concrete for different purposes, including different strength and durability classes. UHPC could be value-engineered for different purposes with significant cost savings over proprietary UHPC materials. Future research should also investigate non-destructive evaluation techniques and other test methods for measuring the quality of UHPC structural members, including fiber dispersion and orientation.

REFERENCES

AASHTO T 132. 1987. “Standard Method of Test for Tensile Strength of Hydraulic Cement Mortars.”

ACI 201.2R-16. 2016. “Guide to Durable Concrete.” American Concrete Institute, Farmington Hills, MI.

ACI 318-14. 2014. “Building Code Requirements for Structural Concrete and Commentary.” American Concrete Institute, Farmington Hills, MI.

ACI 408-03. 2003. “Bond and Development of Straight Reinforcing Bars in Tension.” American Concrete Institute, Farmington Hills, MI.

ACI 446.1R-91. 1991. "Fracture Mechanics of Concrete: Concepts, Models, and Determination of Material Properties." American Concrete Institute, Farmington Hills, MI.

ACI CT-16. 2016. "ACI Concrete Terminology.” American Concrete Institute. Farmington Hills, MI.

AFNOR NF P18-470. 2016. “Concrete -- Ultra-High Performance Fibre-Reinforced Concrete -- Specifications, Performance, Production, and Conformity.” Association Francaise de Normalisation (AFNOR), Saint-Denis, France.

Ahlborn, Theresa M., Donald L. Misson, Erron J. Peuse, and Christopher G. Gilbertson. 2008. “Durability and Strength Characterization of Ultra-High Performance Concrete under Variable Curing Regimes.” In *Proc. 2nd Int. Symp. on Ultra High Performance Concrete, Fehling, E., Schmidt, M., & Stürwald, S.(Eds.)* Kassel, Germany, 197–204.

Albarwary, Ismaeel H. Musa, Ziyad N. Shamsulddin Aldoski, and Lawend K. Askar. 2017. “Effect of Aggregate Maximum Size upon Compressive Strength of Concrete.” *The Journal of The University of Duhok* 20 (July): 790–97. https://doi.org/10.26682/sjuod.2017.20.1.67.

Aldea, C-M, Surendra P. Shah, and A. Karr. 1999. “Permeability of Cracked Concrete.” *Materials and Structures* 32 (5): 370–376.

Alkaysi, Mouhamed. 2016. “Strength and Durability of Ultra-High Performance Concrete Materials and Structures.” University of Michigan, Ann Arbor, MI.

Argos. n.d. “Advanced Concrete: Pure Innovation in One Product.”

Arora, Aashay, Matthew Aguayo, Hannah Hansen, Cesar Castro, Erin Federspiel, Barzin Mobasher, and Narayanan Neithalath. 2018. “Microstructural Packing- and Rheology-Based Binder Selection and Characterization for Ultra-High Performance Concrete (UHPC).” *Cement and Concrete Research* 103 (January): 179–90. https://doi.org/10.1016/j.cemconres.2017.10.013.

ASTM C39. 2018. “Standard Test Method for Compressive Strength of Cylindrical Concrete Specimens.” ASTM International, West Conshohocken, PA.

ASTM C78. 2018. “Standard Test Method for Flexural Strength of Concrete (Using Simple Beam with Third-Point Loading).” ASTM International, West Conshohocken, PA.

ASTM C157. 2017. “Standard Test Method for Length Change of Hardened Hydraulic-Cement Mortar and Concrete.” ASTM International, West Conshohocken, PA.

ASTM C230. 2014. “Standard Specification for Flow Table for Use in Tests of Hydraulic Cement.” ASTM International, West Conshohocken, PA.

ASTM C293. 2016. “Standard Test Method for Flexural Strength of Concrete (Using Simple Beam With Center-Point Loading).” ASTM International, West Conshohocken, PA.

ASTM C469. 2014. “Standard Test Method for Static Modulus of Elasticity and Poisson’s Ratio of Concrete in Compression.” ASTM International, West Conshohocken, PA.

ASTM C496. 2017. “Standard Test Method for Splitting Tensile Strength of Cylindrical Concrete Specimens.” ASTM International, West Conshohocken, PA.

ASTM C512. 2015. “Standard Test Method for Creep of Concrete in Compression.” ASTM International, West Conshohocken, PA.

ASTM C666/C666M - 15. 2015. “Standard Test Method for Resistance of Concrete to Rapid Freezing and Thawing.” ASTM International, West Conshohocken, PA.

ASTM C882. 2013. “Standard Test Method for Bond Strength of Epoxy-Resin Systems Used with Concrete By Slant Shear.” ASTM International, West Conshohocken, PA.

ASTM C944. 1999. “Standard Test Method For Abrasion Resistance of Concrete or Mortar Surfaces by The Rotating-Cutter Method.” ASTM International, West Conshohocken, PA.

ASTM C1018-97. 1997. “Standard Test Method for Flexural Toughness and First-Crack Strength of Fiber-Reinforced Concrete.” ASTM International, West Conshohocken, PA.

ASTM C1202-17a. 2017. “Standard Test Method for Electrical Indication of Concrete's Ability to Resist Chloride Ion Penetration.” ASTM International, West Conshohocken, PA.

ASTM C1437. 2015. “Standard Test Method for Flow of Hydraulic Cement Mortar.” West Conshohocken, PA, United States: ASTM International, West Conshohocken, PA.

ASTM C1556-11a (2016). 2016. “Standard Test Method for Determining the Apparent Chloride Diffusion Coefficient of Cementitious Mixtures by Bulk Diffusion.” ASTM International, West Conshohocken, PA.

ASTM C1581. 2018. “Standard Test Method for Determining Age at Cracking and Induced Tensile Stress Characteristics of Mortar and Concrete under Restrained Shrinkage.” ASTM International, West Conshohocken, PA.

ASTM C1583. 2013. “Standard Test Method for Tensile Strength of Concrete Surfaces and the Bond Strength of Concrete Repair and Overlay Materials by Direct Tension (Pull-off Method).” ASTM International, West Conshohocken, PA.

ASTM C1609. 2012. “Standard Test Method for Flexural Performance of Fiber-Reinforced Concrete (Using Beam With Third-Point Loading).” ASTM International, West Conshohocken, PA.

ASTM C1856. 2017. “Standard Practice for Fabricating and Testing Specimens of Ultra-High Performance Concrete.” ASTM International, West Conshohocken, PA.

ASTM E1012. 2014. “Standard Practice for Verification of Testing Frame and Specimen Alignment Under Tensile and Compressive Axial Force Application.” ASTM International, West Conshohocken, PA.

Austin, Simon, Peter Robins, and Youguang Pan. 1999. “Shear Bond Testing of Concrete Repairs.” *Cement and Concrete Research* 29 (7): 1067–76. https://doi.org/10.1016/S0008-8846(99)00088-5.

Baby, Florent, B Graybeal, Pierre Marchand, and François Toutlemonde. 2013. “Flexural Tension Test Methods for Determination of the Tensile Stress-Strain Response of Ultra-High Performance Fibre Reinforced Concrete.” In *FRAMCOS 08-VIII International Conference on Fracture Mechanics of Concrete and Concrete Structures*, pp–1072.

Baby, Florent, Benjamin Graybeal, Pierre Marchand, and François Toutlemonde. 2012. “Proposed Flexural Test Method and Associated Inverse Analysis for Ultra-High-Performance Fiber-Reinforced Concrete.” *ACI Materials Journal* 109 (5).

Binard, J P. 2017. “UHPC: A Game-Changing Material for PCI Bridge Producers.” *PCI Journal*, 13.

Brandt, Andrzej M. 2014. *Optimization Methods for Material Design of Cement-Based Composites*. CRC Press.

Brouwers, HJH, and HJ Radix. 2005. “Self-Compacting Concrete: The Role of the Particle Size Distribution.” In *First International Symposium on Design, Performance and Use of SCC, Hunan, China*, 109–118.

Brouwers, HJH. 2006. "The Role of Nanotechology for the Development of Sustainable Concrete." *Proceedings of ACI Session on "Nanotechnology of Concrete: Recent Developments and Future Perspectives."* Denver, USA. November 7, 2006.

Brühwiler, E. 2016. “Recommendation: Ultra-High Performance Fibre Reinforced Cement-Based Composites (UHPFRC).” *Construction Material, Dimensioning and Application. Lausanne, Switzerland*.

Brühwiler, Eugen. 2017. “Draft UHPFRC Specification - UHPFRC Layer for Bridge Deck Strengthening and Waterproofing.”

Calmetrix. n.d. “Pheso Rheometer: Examples of Applications.” Slides. http://downloads.calmetrix.com/Application/Pheso_Examples_of_Use.pdf.

Carbonell Muñoz, Miguel A., Harris, Devin K., Ahlborn, Theresa M., and Frostersil, David C. 2014. “Bond Performance between Ultrahigh-Performance Concrete and Normal-Strength Concrete.” *Journal of Materials in Civil Engineering* 26 (8): 04014031. https://doi.org/10.1061/(ASCE)MT.1943-5533.0000890.

Chao, Shih-Ho, Antoine E. Naaman, and Gustavo J. Parra-Montesinos. 2009. “Bond Behavior of Reinforcing Bars in Tensile Strain-Hardening Fiber-Reinforced Cement Composites.” *ACI Structural Journal; Farmington Hills* 106 (6): 897–906.

Choi, Myoung Sung, Jung Soo Lee, Keum Seong Ryu, Kyung-Taek Koh, and Seung Hee Kwon. 2016. “Estimation of Rheological Properties of UHPC Using Mini Slump Test.” *Construction and Building Materials* 106 (March): 632–39. https://doi.org/10.1016/j.conbuildmat.2015.12.106.

Coppola, L., R. Troli, A. Borsoi, and P. Zaffaroni and M. Collepardi. 1997. “Influence of Superplasticizer Type on the Compressive Strength of Reactive Powder Mortars.” *Special Publication* 173 (September): 537–58. https://doi.org/10.14359/6201.

CSA A23.3. 2018. “Design of Concrete Structures - Draft.” Canadian Standards Association.

Danish Technological Institute. n.d. IT-Tools for Concrete: “4C-Packing- The Software.”.

da Silva and Ricardo. n.d. “4C-Packing- The Software.” Danish Technological Institute: IT-Tools for Concrete.

de Larrard, Francois. 1999. *Concrete Mixture Proportioning: A Scientific Approach*. CRC Press.

de Larrard, François, and Thierry Sedran. 1994. “Optimization of Ultra-High-Performance Concrete by the Use of a Packing Model.” *Cement and Concrete Research* 24 (6): 997–1009.

de Larrard, Francois and Thierry Sedran. 2002. “Mixture-Proportioning of High-Performance Concrete.” *Cement and Concrete Research* 32 (11): 1699–1704. https://doi.org/10.1016/S0008-8846(02)00861-X.

Ductal. n.d. “Ductal: Mechanical Performances.” Accessed January 28, 2019. https://www.ductal.com/en/architecture/mechanical-performances.

Duque, Luis Felipe Maya, De la Varga, Igor, and Graybeal, Benjamin A.. 2016. “Fiber Reinforcement Influence on the Tensile Response of UHPFRC.” In *First International Interactive Symposium on UHPC-2016 (Des Moines, IOWA, Jul. 18–20)*.

Edington, J, and DJ Hannant. 1972. “Steel Fibre Reinforced Concrete. The Effect on Fibre Orientation of Compaction by Vibration.” *Mater Struct* 5 (25): 41–44.

Eide, Mari Bøhnsdalen, and Jorun-Marie Hisdal. 2012. “Ultra High Performance Fibre Reinforced Concrete (UHPFRC)–State of the Art: FA 2 Competitive Constructions: SP 2.2 Ductile High Strength Concrete.”

Faifer, Marco, Liberato Ferrara, Roberto Ottoboni, and Sergio Toscani. 2013. “Low Frequency Electrical and Magnetic Methods for Non-Destructive Analysis of Fiber Dispersion in Fiber Reinforced Cementitious Composites: An Overview.” *Sensors* 13 (1): 1300–1318. https://doi.org/10.3390/s130101300.

Fehling, Ekkehard, Michael Schmidt, and S. Stürwald. 2008. *Ultra High Performance Concrete (UHPC): Proceedings of the Second International Symposium on Ultra High Performance Concrete, Kassel, Germany, March 05-07, 2008*. Kassel University Press GmbH.

Ferdosian, Iman, and Aires Camões. 2016. “Effective Low-Energy Mixing Procedure to Develop High-Fluidity Cementitious Pastes.” *Matéria (Rio de Janeiro)* 21 (1): 11–17. https://doi.org/10.1590/S1517-707620160001.0002.

Ferrara, Liberato, Massimiliano Cremonesi, Marco Faifer, Sergio Toscani, Luca Sorelli, Marc-Antoine Baril, Julien Réthoré, Florent Baby, François Toutlemonde, and Sébastien Bernardi. 2017. “Structural Elements Made with Highly Flowable UHPFRC: Correlating

Computational Fluid Dynamics (CFD) Predictions and Non-Destructive Survey of Fiber Dispersion with Failure Modes." *Engineering Structures* 133 (February): 151–71. https://doi.org/10.1016/j.engstruct.2016.12.026.

Ferrara, Liberato, and Alberto Meda. 2006. "Relationships between Fibre Distribution, Workability and the Mechanical Properties of SFRC Applied to Precast Roof Elements." *Materials and Structures* 39 (4): 411–20. https://doi.org/10.1617/s11527-005-9017-4.

Ferraro, CC. 2008. "Investigation of Concrete Repair Materials." *Florida Department of Transportation, Gainesville*.

Ferron, Raissa Douglas, Surendra Shah, Elena Fuente, and Carlos Negro. 2013. "Aggregation and Breakage Kinetics of Fresh Cement Paste." *Cement and Concrete Research* 50: 1–10.

Funk, James E., and Dennis R. Dinger. 2013. *Predictive Process Control of Crowded Particulate Suspensions: Applied to Ceramic Manufacturing*. Springer Science & Business Media.

Giesler, Andrew J, Shannon Burl Applegate, and Brad D Weldon. 2016. "Implementing Nonproprietary, Ultra-High-Performance Concrete in a Precasting Plant." *PCI Journal*.

Gowripalan, N, and Ian R Gilbert. 2000. "Design Guidelines for Ductal Prestressed Concrete Beams." School of Civil and Environmental Engineering, The University of NSW.

Graybeal, Ben. 2014. "Design and Construction of Field-Cast UHPC Connections."

Graybeal, Benjamin. 2016. "Pairing Prefabricated Bridge Elements with UHPC Connections," 2.

Graybeal, Benjamin A. 2006. "Material Property Characterization of Ultra-High Performance Concrete."

Graybeal, Benjamin A, and Florent Baby. 2013. "Development of Direct Tension Test Method for Ultra-High-Performance Fiber-Reinforced Concrete." *ACI Materials Journal* 110 (2).

Graybeal, Ben and Mark Leonard. 2017. "Introduction to Ultra-High Performance Concrete for Prefabricated Bridge Element Connections." EDC-4 UHPC 2017 Webinar Series: Introduction to UHPC." presented at the FHWA Webinar, March 7.

https://www.fhwa.dot.gov/exit.cfm?link=https://connectdot.connectsolutions.com/p87bc0bzm99/?launcher=false&fcsContent=true&pbMode=normal.

Haber, Zachary B, Igor De la Varga, Benjamin A Graybeal, Brian Nakashoji, and Rafic El-Helou. 2018. “Properties and Behavior of UHPC-Class Materials.” *FHWA-HRT-18-036*.

Hoang, Kim Huy, Philipp Hadl, and Nguyen Viet Tue. 2016. “A New Mix Design Method for UHPC Based on Stepwise Optimization of Particle Packing Density.”

Hsu, Kung-Chung, Jih-Jen Chiu, Sheng-Da Chen, and Yuan-Cheng Tseng. 1999. “Effect of Addition Time of a Superplasticizer on Cement Adsorption and on Concrete Workability.” *Cement and Concrete Composites* 21 (5): 425–30. https://doi.org/10.1016/S0958-9465(99)00030-X.

Iowa Department of Transportation. 2000. “Method of Test for Determining the Shearing Strength of Bonded Concrete (Inactive).” Specification Iowa 408-C.

Jones, MR, Li Zheng, and MD Newlands. 2002. “Comparison of Particle Packing Models for Proportioning Concrete Constitutents for Minimum Voids Ratio.” *Materials and Structures* 35 (5): 301–309.

Kim, Haena. 2016. “Design and Field Construction of Hawkeye Bridge Using Ultra High Performance Concrete for Accelerated Bridge Construction.”

Kim, Jae Hong, Hong Jae Yim, and Raissa Douglas Ferron. 2016. “In Situ Measurement of the Rheological Properties and Agglomeration on Cementitious Pastes.” *Journal of Rheology* 60 (4): 695–704.

Kusumawardaningsih, Yuliarti, Ekkehard Fehling, Mohammed Ismail, and Attitou Amen Mohamed Aboubakr. 2015. “Tensile Strength Behavior of UHPC and UHPFRC.” *Procedia Engineering*, Civil Engineering Innovation for a Sustainable, 125 (January): 1081–86. https://doi.org/10.1016/j.proeng.2015.11.166.

LaFarge North America. 2015. “Ductal Premix Safety Data Sheet.”

Laskar, Aminul Islam. 2011. “Mix Design of High-Performance Concrete.” *Materials Research* 14 (4): 429–433.

Le Hoang, An, and Ekkehard Fehling. 2017a. “Influence of Steel Fiber Content and Aspect Ratio on the Uniaxial Tensile and Compressive Behavior of Ultra High Performance Concrete.” *Construction and Building Materials* 153 (October): 790–806. https://doi.org/10.1016/j.conbuildmat.2017.07.130.

Li, P. P., Q. L. Yu, and H. J. H. Brouwers. 2017. “Effect of PCE-Type Superplasticizer on Early-Age Behaviour of Ultra-High Performance Concrete (UHPC).” *Construction and Building Materials* 153 (October): 740–50. https://doi.org/10.1016/j.conbuildmat.2017.07.145.

Li, P, Q Yu, HJH Brouwers, and R Yu. 2016. “Fresh Behaviour of Ultra-High Performance Concrete (UHPC): An Investigation of the Effect of Superplasticizers and Steel Fibres.” In *Proceedings of the 9th International Concrete Conference 2016, Environment, Efficiency and Economic Challenges for Concrete,* 635–644.

Li, Wenting, Mohammad Pour-Ghaz, Javier Castro, and Jason Weiss. 2011. “Water Absorption and Critical Degree of Saturation Relating to Freeze-Thaw Damage in Concrete Pavement Joints.” *Journal of Materials in Civil Engineering* 24 (3): 299–307.

Li, Zhengqi. 2015. “Proportioning and Properties of Ultra-High Performance Concrete Mixtures for Application in Shear Keys of Precast Concrete Bridges.”

Ma, Jianxin, Frank Dehn, and Gert Koenig. 2003. “Autogenous Shrinkage of Self-Compacting Ultra-High Performance Concrete (UHPC).” In *International Conference on Advances in Concrete and Structures*, 255–262. RILEM Publications SARL.

Naaman, Antoine E, and Husamuddin Najm. 1991. “Bond-Slip Mechanisms of Steel Fibers in Concrete.” *Materials Journal* 88 (2): 135–145.

NT Build 492. 1999. “Concrete, Mortar and Cement-Based Repair Materials: Chloride Migration Coefficient from Non-Steady-State Migration Experiments.” Nordtest method.

Ozyurt, Nilufer, Leta Y. Woo, Thomas O. Mason, and Surendra P. Shah. 2006. "Monitoring Fiber Dispersion in Fiber-Reinforced Cementitious Materials: Comparison of AC-Impedance Spectroscopy and Image Analysis." *ACI Materials Journal; Farmington Hills* 103 (5): 340–47.

Ozyurt, Nilufer, Leta Y Woo, Bin Mu, Surendra P Shah, and Thomas O Mason. 2004. "Detection of Fiber Dispersion in Fresh and Hardened Cement Composites." In *Advances in Concrete Through Science and Engineering, An International Symposium During the RILEM Spring Meeting*.

Pade, Claus, Lars Nyholm Thrane, and Martin Kaasgaard. 2009. *4C-Packing - User's Manual*. Version 3.0. Danish Technological Institute.

Park, Seung Hun, Dong Joo Kim, Gum Sung Ryu, and Kyung Taek Koh. 2012. "Tensile Behavior of Ultra High Performance Hybrid Fiber Reinforced Concrete." *Cement and Concrete Composites* 34 (2): 172–84. https://doi.org/10.1016/j.cemconcomp.2011.09.009.

Perry, V. H. 2015. "Ultra-High-Performance-Concrete Advancements and Industrialization—The Need for Standard Testing." *Advances in Civil Engineering Materials*, January, 20140028. https://doi.org/10.1520/ACEM20140028.

Pichler, Bernhard, Christian Hellmich, Josef Eberhardsteiner, Jaromír Wasserbauer, Pipat Termkhajornkit, Rémi Barbarulo, and Gilles Chanvillard. 2013. "Effect of Gel–Space Ratio and Microstructure on Strength of Hydrating Cementitious Materials: An Engineering Micromechanics Approach." *Cement and Concrete Research* 45 (March): 55–68. https://doi.org/10.1016/j.cemconres.2012.10.019.

Piérard, Julie, Bram Dooms, and Niki Cauberg. 2012. "Evaluation of Durability Parameters of UHPC Using Accelerated Lab Tests." In *Proceedings of the 3rd International Symposium on UHPC and Nanotechnology for High Performance Construction Materials, Kassel, Germany*, 371–376.

Piérard, Julie, Bram Dooms, and Niki Cauberg. 2013. “Durability Evaluation of Different Types of UHPC.” In *Proceedings of the RILEM-Fib-AFGC International Symposium on Ultra-High Performance Fibre-Reinforced Concrete*, 275–284.

Plank, J., C. Schröfl, and M. Gruber. 2009. “Use of a Supplemental Agent to Improve Flowability of Ultra-High-Performance Concrete.” *Special Publication* 262 (October): 1–16. https://doi.org/10.14359/51663219.

Portland Cement Association. 2018. “Ultra-High Performance Concrete.” https://www.cement.org/learn/concrete-technology/concrete-design-production/ultra-high-performance-concrete

Powers, T. C. 1958. “Structure and Physical Properties of Hardened Portland Cement Paste.” *Journal of the American Ceramic Society* 41 (1): 1–6. https://doi.org/10.1111/j.1151-2916.1958.tb13494.x.

Rangaraju, Prasada Rao, Zhengqi Li, and Kaveh Afshinnia. 2016. “Influence of Alkali Content of Cement on Mechanical and Durability Performance of UHPC.” *15th International Conference on Alkali-Aggregate Reactions*, 94. http://ibracon.org.br/icaar/livreto/15ICAAR_2016/files/assets/basic-html/page96.html

Rapoport, Julie, Corina-Maria Aldea, Surendra P. Shah, Bruce Ankenman, and Alan Karr. 2002. “Permeability of Cracked Steel Fiber-Reinforced Concrete.” *Journal of Materials in Civil Engineering* 14 (4): 355–58. https://doi.org/10.1061/(ASCE)0899-1561(2002)14:4(355).

Reza, Farhad. 2018. “Flexural Toughness Measurements on High-Strength Steel Fiber-Reinforced Concrete.”

Rossi, Pierre. 2001. “Ultra-High Performance Fiber-Reinforced Concretes.” *Concrete International* 23 (12): 46–52.

Rougeau, Patrick, and Béatrice Borys. 2004. “Ultra High Performance Concrete with Ultrafine Particles Other than Silica Fume.” In *Proceedings of the International Symposium on Ultra High Performance Concrete*, 32:213–225.

Russell, Henry G, and Benjamin A. Graybeal. 2013. “Ultra-High Performance Concrete: A State-of-the-Art Report for the Bridge Community.”

Rust, Charles Karissa. 2009. “Role of Relative Humidity in Concrete Expansion Due to Alkali-Silica Reaction and Delayed Ettringite Formation: Relative Humidity Thresholds, Measurement Methods, and Coatings to Mitigate Expansion.” PhD Thesis.

Saleem, Muhammad Azhar, Mirmiran, Amir, Xia, Jun, and Mackie, Kevin. 2013. “Development Length of High-Strength Steel Rebar in Ultrahigh Performance Concrete.” *Journal of Materials in Civil Engineering* 25 (8): 991–98. https://doi.org/10.1061/(ASCE)MT.1943-5533.0000571.

Schießl, Peter, Oliver Mazanec, and Dirk Lowke. 2007. “SCC and UHPC — Effect of Mixing Technology on Fresh Concrete Properties.” In *Advances in Construction Materials 2007*, 513–22. Springer, Berlin, Heidelberg. https://doi.org/10.1007/978-3-540-72448-3_52.

Schydt, J, Gunther Herold, and Harald S Müller. 2008. “Long Term Behavior of Ultra High Performance Concrete under the Attack of Chlorides and Aggressive Waters.” In *Proceedings of the 2nd International Symposium on Ultra High Performance Concrete*, 231–238.

Shihada, S, and M Arafa. 2010. “Effects of Silica Fume, Ultrafine and Mixing Sequences on Properties of Ultra High Performance Concrete.” *Asian Journal of Materials Science* 2 (3): 137–146.

Sim, Jongsung, Cheolwoo Park, and Do Young Moon. 2005. “Characteristics of Basalt Fiber as a Strengthening Material for Concrete Structures.” *Composites Part B: Engineering* 36 (6): 504–12. https://doi.org/10.1016/j.compositesb.2005.02.002.

Spragg, Robert, Scott Z Jones, Chiara Villani, Kenneth A Snyder, Dale P Bentz, Amire Poursaee, and Jason Weiss. 2014. “Surface and Uniaxial Electrical Measurements on Layered Cementitious Composites Having Cylindrical and Prismatic Geometries.”

Spragg, Robert, Chiara Villani, Ken Snyder, Dale Bentz, Jeffrey Bullard, and Jason Weiss. 2013. “Factors That Influence Electrical Resistivity Measurements in Cementitious Systems.”

Transportation Research Record: Journal of the Transportation Research Board, no. 2342: 90–98.

Staquet, Stéphanie, and Bernard Espion. 2004. "Early Age Autogenous Shrinkage of UHPC Incorporating Very Fine Fly Ash or Metakaolin in Replacement of Silica Fume." In *International Symposium on Ultra High Performance Concrete, Kessel Germany*, 587–599.

Sugamata, T., T. Kinoshita, M. Yaguchi, and K. Harada. 2006. "Characteristics of Concrete Containing a Shrinkage-Reducing Superplasticizer for Ultra-High-Strength Concrete." *Special Publication* 239 (October): 51–66. https://doi.org/10.14359/18370.

Thomas, Michael, B Green, E O'Neal, V Perry, S Hayman, and A Hossack. 2012. "Marine Performance of UHPC at Treat Island." In *Proceedings of the 3rd International Symposium on UHPC and Nanotechnology for High Performance Construction Materials, Kassel, Germany*, 365–370.

Topçu, İlker Bekir, and Mehmet Canbaz. 2007. "Effect of Different Fibers on the Mechanical Properties of Concrete Containing Fly Ash." *Construction and Building Materials* 21 (7): 1486–91. https://doi.org/10.1016/j.conbuildmat.2006.06.026.

Vandewalle, Lucie, D Nemegeer, György Balázs, B Barr, Joaquim Barros, P Bartos, Nemkumar Banthia, et al. 2003. "RILEM TC 162-TDF: 'Test and Design Methods for Steel Fibre Reinforced Concrete' - Sigma-Epsilon-Design Method - Final Recommendation." *Materials and Structures* 36 (October): 560–67.

Walsh, KK, NJ Hicks, EP Steinberg, HH Hussein, and AA Semendary. 2018. "Fiber Orientation in Ultra-High-Performance Concrete Shear Keys of Adjacent-Box-Beam Bridges." *ACI Materials Journal* 115 (2): 227–238.

Wang, Xuhao, Kejin Wang, Peter Taylor, and George Morcous. 2014. "Assessing Particle Packing Based Self-Consolidating Concrete Mix Design Method." *Construction and Building Materials* 70: 439–452.

Wille, K., and Boisvert-Cotulio, C. 2013. “13100.Pdf.” Techbrief FHWA-HRT-13-100. https://www.fhwa.dot.gov/publications/research/infrastructure/structures/bridge/13100/13100.pdf.

Wille, Kay, and Christopher Boisvert-Cotulio. 2015. “Material Efficiency in the Design of Ultra-High Performance Concrete.” *Construction and Building Materials* 86 (July): 33–43. https://doi.org/10.1016/j.conbuildmat.2015.03.087.

Wille, Kay, and Gustavo J. Parra-Montesinos. 2012. “Effect of Beam Size, Casting Method, and Support Conditions on Flexural Behavior of Ultra-High-Performance Fiber-Reinforced Concrete.” *ACI Materials Journal* 109 (May): 379–88.

Wille, Kay, Dong Joo Kim, and Antoine E Naaman. 2011. “Strain-Hardening UHP-FRC with Low Fiber Contents.” *Materials and Structures* 44 (3): 583–598.

Xiao, Rui, Zong-cai Deng, and Chenliang Shen. 2014. “Properties of Ultra High Performance Concrete Containing Superfine Cement and without Silica Fume.” *Journal of Advanced Concrete Technology* 12 (2): 73–81.

Appendix A Survey Questions

Table A-1: Question 3: Has your state considered (or do you already have) multiple classes of high performance concrete? (For example: HPC: 8-15ksi, Very HPC 15-21ksi, Ultra HPC 21ksi+)

	Only HPC is defined	HPC and UHPC are defined without levels or tiers above or between	Multiple levels or tiers of HPC are defined	Other
Alabama				only UHPC defined
Colorado	x			
Delaware			x	
Florida				Considering multiple levels
Idaho				
Indiana				HPC by unique specification only
Iowa		x		
Maine			21 ksi	
Maryland		x		
Michigan				HPC is not labeled as high performance but we have several specifications for it. UHPC is labeled.
Montana				project specific special provision only
Nebraska			x	
Nevada	x			
New Jersey			HPC-1 and HPC-2	
New Mexico		x		
New York			x	
Ohio		x		
Oklahoma				Just UHPC
Oregon		x		
Texas	x			
Virginia	x			
Washington	x			
West Virginia		x		
Ontario		x		
Washington DC		x		

Table A-2: Question 4: How does your state specify UHPC? Please list a numerical value and/or specific tests used for approval/qualification of UHPC, if applicable.

	Compressive strength	Tensile strength	Flexural Strength	Modulus of Elasticity	Durability requirements	Other
Alabama	14 ksi at 4 days, 21 ksi at 28 days	1,000 psi at 28 days splitting tensile strength			chloride ion permeability 250 coulombs at 28 days	shrinkage 800 microstrain at 28 days
Delaware	22 ksi				2250 coulombs	ASTM C1567 0.08% at 28 days
Iowa	10 ksi 24 hour, 21 ksi 28 day		5 ksi 28 day			flow 20 drops 7-8.5 inches
Maine	21 ksi					
Maryland	4200*				permeability 2500 coulombs average of 3	1.5 # fibers, corrosion inhibitor 2 gal/yd^3, max cement 550 lb, min. cementitious factor 580
Michigan	15ksi at 7 days				x	7- to 12-inch slump flow
Nebraska	21 ksi					
New Jersey	x					
New Mexico	x	x	x	x	x	
New York	21 ksi		flexural toughness		freeze-thaw	
Oregon	x					
Texas	x			x	permeability, ASR resistance	toughness, shrinkage
Virginia	x				x	

Table A-2, continued

	Compressive strength	Tensile strength	Flexural Strength	Modulus of Elasticity	Durability requirements	Other
West Virginia	x					by name as a proprietary product
	Compressive strength	Tensile strength	Flexural Strength	Modulus of Elasticity	Durability requirements	Other
Ontario	130 MPa (28 days) - LS-426(MTO test method)		15MPa (28 days) - ASTM C1609			slump flow ASTM C109, within 15 mm of target identified by contractor, plastic temperature between 10 and 25 Celsius

*No units were specified for the value of 4200 reported by Maryland

Table A-3: Question 5: If your state has a written specification for the use of UHPC, or if there has been a DOT project with UHPC project specifications, please upload them below if possible. [file upload]

State	Uploaded file in survey	File found by other means
Alabama		
Delaware		
Idaho		
Iowa		
New Jersey		
New Mexico		
New York		
Texas		
West Virginia		
Ontario		

Table A-4: Question 6: Which of the following mix designs have been used?

	Proprietary, pre-bagged UHPC mix	Non-proprietary mix design
Delaware		
Iowa		
Maine		
Michigan		
Montana		
Nebraska		
New Jersey		
New Mexico		
New York		
Ohio		
Oregon		
Virginia		
Ontario		
Washington, D.C.		

Table A-5: Question 7: What tests were used for qualification of the mix?

	Compression test	Flexure test	Fiber dispersion test	Flow/spread test	Other
Delaware	■			■	Rapid Chloride Ion Penetrability
Florida	■	■		■	temperature
Iowa	■	■		■	
Maine	■			■	
Michigan	■			■	
Montana	■			■	
Nebraska	■				
New Jersey	■			■	
New Mexico	■	■			
New York	■	■			■
Ohio	■		■	■	
Oregon	■	■		■	
Virginia	■				
Ontario	■	■		■	temperature
Washington, D.C.	■				

Table A-6: Question 8: If known, what kind of mixer was used for UHPC mixing (size, horsepower, brand)?

Delaware	Lafarge supplied the mixers
Iowa	Lafarge mixer
Maine	Unknown but it was a small portable mixer. Possibly ½ cy but not sure
Michigan	IMER Mortarman 750G Mixer, 13HP gas motor
Montana	Supplied by proprietary mix contractor
New Mexico	unknown
New York	unknown
Ohio	Pan Mixer, 2 Cu. ft.
Oregon	2 pan mixers – manufacturer provided (Lafarge)
Virginia	For beams, double shaft mixer and for the connection the mortar mixer
Ontario	pan mixer on site

Table A-7: Question 9: What surface treatment (if any) was used between pours to eliminate cold joints?

Delaware	Connections between precast structural elements were an exposed agg surface and must be SSD moistened before pouring.
Iowa	no cold joints permitted
Maine	none
Michigan	n/a
Montana	unk
New Mexico	NA
New York	pours were continuous
Ohio	Plywood cover

Table A-8: Question 10: What, if anything, would you do differently in the future?

Delaware	If material is not mix to the correct slump flow for the application discard it to the side, correct what is still in the mixer.
Maine	no changes
Michigan	Our "lessons learned" have mostly been rolled into the specification and the biggest challenge is in execution. Many people prefer the proprietary approach to the non-proprietary approach.
Montana	unknown
New Mexico	nothing at this time
New York	We are considering reducing strength requirement
Ohio	Contractor safety in handling the dry material, (Contractor didn’t have full PPE)
Ontario	Not allow delivery by ready-mix truck (for filling joints between precast panels). Discharge is too slow.

Table A-9: Question 11: How has UHPC performed since the casting?

State	Structural Performance	Durability	Aesthetics
Delaware	much better	much better	equal
Iowa	much better	much better	equal
Maine	N/A	N/A	equal
Michigan	equal	equal	worse
Montana	N/A	N/A	N/A
Nebraska	much better	much better	equal
New Jersey	slightly better	slightly better	slightly better
New Mexico	much better	much better	N/A
New York	much better	N/A	equal
Ohio	N/A	N/A	equal
Oregon	much better	much better	N/A
Virginia	N/A	N/A	N/A
Ontario	much better	slightly better	equal
Washington, D.C.	much better	N/A	N/A

Appendix B Draft Florida Test Method for UHPC Direct Tension Test

Florida Method of Test for

DIRECT TENSION TEST OF ULTRA-HIGH-PERFORMANCE CONCRETE

1. Scope
    a. This test method is suitable for both field and laboratory use to determine the tensile strength of an ultra-high-performance concrete (UHPC) mix.
    b. This standard does not purport to address all the safety concerns associated with its use. It is the responsibility of the user of this standard to establish appropriate safety and health practices and determine the applicability of regulatory limitations prior to use.
2. Reference Documents
    a. ASTM Standards:
    C1856 Standard Practice for Fabricating and Testing Specimens for Ultra-High-Performance Concrete
    E1012 Standard Practice for Verification of Testing Frame and Specimen Alignment under Tensile and Compressive Axial Force Application
    b. FHWA Procedure and Testing Apparatus DRAFT: Uniaxial Tension Test Method For Ultra-High-Performance Concrete
3. Terminology
    a. **alignment**, n-the condition of a testing machine and load train (including the test specimen) that influences the introduction of bending moments into a specimen during a tensile loading.
    b. **compressive strength** [FL-2], n-the maximum compressive stress that a material is capable of sustaining. Compressive strength is calculated by dividing the maximum force during a compression tests by the original cross-sectional area of the specimen.
    c. **elongation**, El, n-the increase in gauge length of a body subjected to a tension force, referenced to a gauge length on the body. Usually elongation is expressed as a percentage of the original gauge length. Discussion- The term elongation, when

applied to quasi-brittle materials, generally means measurement at both strain localized and non-localized sections.

d. **extensometer**, n-a device for measuring the change in distance between two reference points on an object.

e. **force** [F], n-in mechanical testing, a vector quantity of fundamental nature characterized by a magnitude, a direction, a sense, and a discrete point of application, that acts externally upon a test object and creates stresses in it.

f. **gauge length**, n-the original length of that portion of the specimen over which strain, elongation, or change of length are determined.

g. **modulus of elasticity** [FL-2], n-the slope of the stress-strain curve within the linear portion of the diagram.

h. **strain,** n-the per unit change in the size or shape of a body referred to its original size or shape. Strain is a nondimensional quantity, but it is frequently expressed in meter per meter, in. per in., or percent. DISCUSSION- In this test guide, the term strain usually refers to the axial component of the six components that describe a strain.

i. **stress**, [FL-2], n-the intensity at a point in a body of the forces or components of force that act on a given plane through the point. Stress is expressed in force per unit of area.

j. **effective stress**, the concrete stress at a point adjusted to account for the effect of fiber alignment from different sample surface conditions

4. Summary of Test Method

   a. A UHPC tensile specimen is cast in accordance with the test method

   b. Aluminum plates are fabricated and adhered to the specimen to distribute gripping pressure

   c. An extensometer is attached to the specimen to measure elongation

   d. The specimen is placed in the test machine and fixed into place using hydraulic grips.

   e. A compressive force is applied to create a stress of 1.0 ksi. This step may be omitted if the test machine grips do not allow for compressive forces.

f. Tension is applied until the peak tension force and the force at a strain value of 0.005 in./in. are determined.

5. Significance and Use
    a. This test method determines the tensile strength of a UHPC mix.
    b. This test method determines the ductility of a UHPC mix.
6. Apparatus
    a. Tensile Testing Machine, with the capability to grip the ends of the specimens without causing local crushing failure or allowing slippage. Machine shall have tension loading capabilities of at least 8,000 lbf. Machine must be aligned properly to pass the ASTM E1012 test with below 10% curvature.
    b. Extensometer, with the ability to measure displacement at each of the four sides of the specimen. The measuring devices should have a strain range of at least 25,000 microstrain over a gauge length of 4 in. The extensometer should be able to attach to the specimen with a 4-in. distance between the top and bottom attachment points.
    c. Clamps, to provide constant gripping force while epoxy cures and during tension testing, if necessary.
7. Materials
    a. UHPC containing sufficient fiber reinforcement to provide tensile strength after cracking shall be used
    b. Aluminum for the fabrication of plates.

    Note: Stock aluminum purchased with a 3/16-in. thickness will make plate fabrication easier.

    c. High-strength, high-stiffness epoxy to attach plates to UHPC surface.
8. Test Specimens
    a. Rectangular prisms of UHPC with dimensions of 2 × 2 × 17 in. shall be fabricated.
        i. At least six specimens shall be made for each mix of UHPC to ensure reliable data.
        ii. Molded prisms shall be placed in one continuous flow of UHPC to avoid creating layers of concrete that have no interpenetrating fibers between them. The UHPC shall be placed into the prism molds from one end without

stopping or moving the placement location. One way to achieve this result is to place a funnel or container with an opening in the bottom in a stationary location and continuously pour concrete into it until the mold is full. The opening of the funnel or bucket shall be at least 4 times the length of the fibers. Wider holes will allow the UHPC to flow faster.

iii. No vibration or tamping rods shall be used.

iv. Specimens shall be covered within 1 minute of finishing the top surface to prevent evaporation and drying of the top surface.

b. Machined aluminum plates, with a width of 2 in. and length of 6.25 in. shall be fabricated. Thickness of plates should be 3/16 in. for the first 4.25 in. of length, followed by a linear taper to a thickness of 0.04 in. over the last 2 in. (Figure B-1).

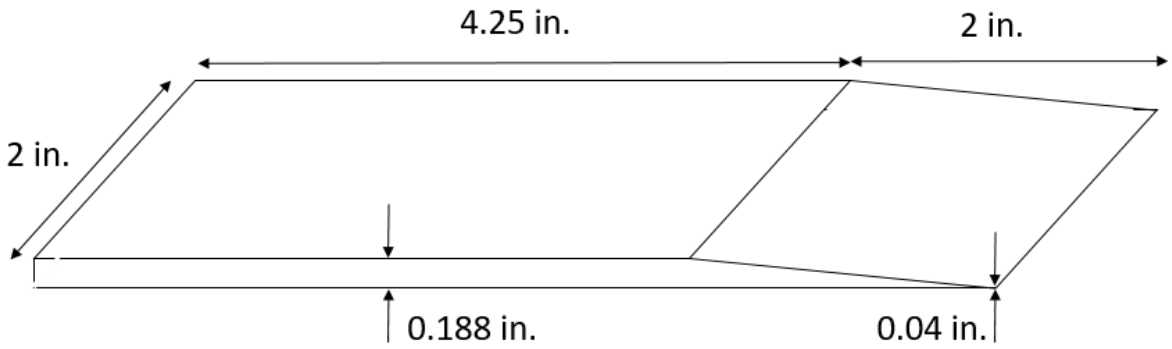

Figure B-1 Diagram of Aluminum Plate Dimensions

c. Aluminum plates shall be attached on the two opposing formed edges of the specimen. A layer of epoxy shall be used, and plates shall be clamped tightly during curing. Epoxy shall cure as specified by the manufacturer. The tapered edges of the plates shall point towards the middle of the specimen, as shown in Figure B-2.

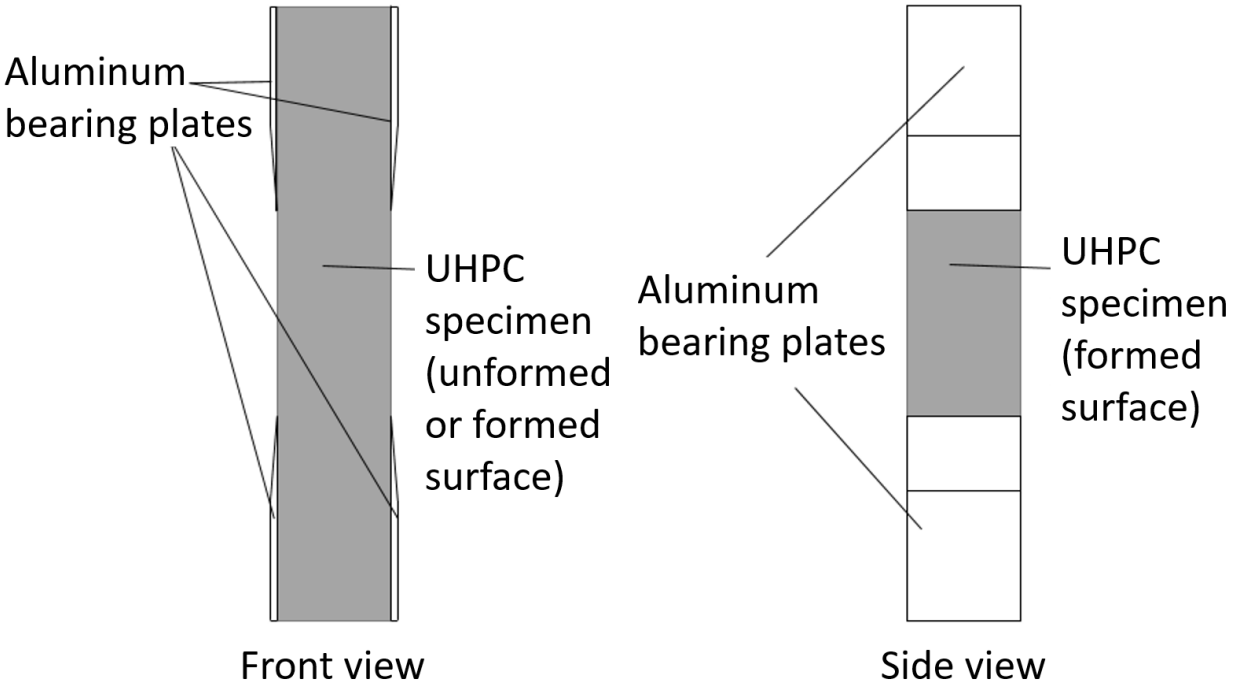

Figure B-2: Aluminum Plate Attachment Location

Note: Aluminum plates can be reused to save costs and time. After specimens have been tested, specimens may be placed in an oven to soften the epoxy and remove plates. Temperatures and heating times will vary based on epoxy type. Check safety data for specific epoxy type used and avoid heating specimen to a temperature that may soften the aluminum plates. Any epoxy remaining on the plates should be removed before plates are re-used.

9. Test Procedure
    a. Mark specimens to indicate grip location at 3.5 in. from each end as well as extensometer attachment locations at 6.5 in. from each end.
    b. Attach extensometer along the drawn lines. One method of attaching the extensometer is by using bearing screws on opposite faces that can be tightened
    c. Place specimen in the tension testing machine and grip the aluminum plates on the top or bottom, with the edge of the grips aligning with the mark 3.5 in. from the specimen's edge.
    d. Grip the aluminum plates on the opposite side of the specimen. This shall be done in a force-controlled setting so that the gripping force does not apply an axial load

to the specimen during this process. The top and bottom grips should have equal pressure applied before testing. The pressure should be high enough to prevent slippage during testing but low enough to avoid local crushing of the specimen.

e. Attach a C clamp to the tapered part of the aluminum plates on the top and bottom of the specimen to prevent the plates from delaminating from the aluminum plates during loading.

Note: During the development of this procedure, a gripping pressure of 3,000 psi was used. Pressure may depend on the machine used, grips used, and UHPC specimen strength.

f. Zero or tare all measuring devices on the extensometer and start data collection.
g. Load the specimen in compression at a constant crosshead displacement rate to give a stress rate of -1.5 ± 0.5 ksi/min. This step is meant to help seat the specimen. Apply the compressive load until the cross-section has a stress of 1.0 ksi. This step may be omitted if the testing machine grips do not allow for compressive loads.
h. Load the specimen in tension at a constant crosshead displacement rate to give a stress rate of 1.5 ± 0.5 ksi/min within the initial elastic portion of the tensile response. Continue the load test until the load drops below 50% of the maximum load obtained in the test.
i. Measure the depth and width of the tensile specimen above and below the main failure. Depth of the specimen shall be defined as the distance from the unformed surface to the formed surface that was on the bottom of the specimen when it was poured. The width of the specimen is defined as the distance between the faces of the specimen where the aluminum plates and grips were placed.

10. Data Analysis

a. The measurements of depth and width shall be used to calculate the effective cross-sectional area of the sample. **Error! Reference source not found.** gives correction factors for the zone near the edge of the sample to account for fiber alignment and development length for different sample surface preparation methods. The area within half the fiber length from each surface should be multiplied by the correction

factor to calculate the effective area, A_e of the specimen. Equation gives the effective area for the cross-section for the sample geometry shown in Figure B-2. This is done to account for fiber alignment effects that occur at the edges of the specimen, depending on how the specimen was shaped.

$$\mathrm{A}_e = wd + \frac{l_f}{2}\left[\left(w - \frac{l_f}{2}\right)\left(C_{fA} + C_{fC} - 2\right) + \left(d - \frac{l_f}{2}\right)\left(C_{fB} + C_{fD} - 2\right)\right] \qquad \text{Equation B-1}$$

Where w and d are sample dimensions (in.) as shown in Figure B-3, C_{fA}, C_{fB}, C_{fC}, and C_{fD} are the specimen side condition correction factors for the sides A, B, C, and D of the prism shown in Figure B-3 for the side condition described in **Error! Reference source not found.**, and l_f is the average fiber length (in.).

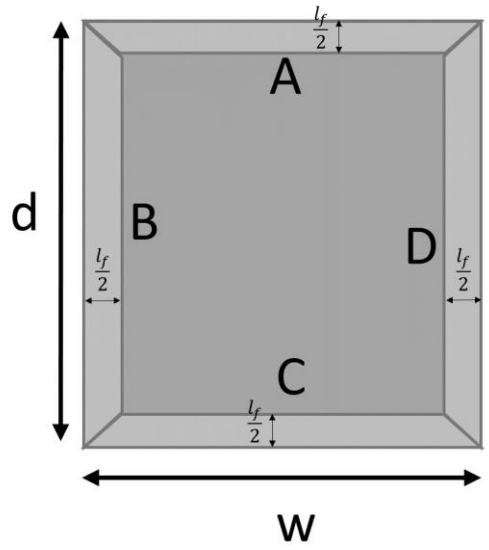

Figure B-3: Sample cross-section geometry and side definitions used in Equation B-1

Table B-1: Correction Factors for Edge effects in Flexure Specimens

Location	Correction Factor, C_f
Formed edges	1.2
Sawn edges	0.5
Edges not formed or sawn, and any portion of the cross-section farther than l_f from the edge	1

b. The specimen effective stress f_e (psi) shall be determined by dividing the load P (lbf) by the effective area as shown in Equation B-2. This value shall be plotted against the strain, ε, for each data point from the test, which is calculated using Equation B-3 using the average displacement δ (in.) from the displacement measuring devices divided by the gage length L (in.) over which the extensometer spanned. The concrete stress-strain plot shall be reported.

$$f_e = \frac{P}{A_e} \qquad \text{Equation B-2}$$

$$\varepsilon = \frac{\delta}{L} \qquad \text{Equation B-3}$$

c. The peak effective stress shall be reported, rounded to the nearest 10 psi.
d. The effective stress at a strain of 0.005 in./in. $f_{e0.005}$ shall be reported to the nearest 10 psi.
e. If required, the modulus of elasticity shall be reported. This can be done using regression analysis of the stress vs. strain data on the compressive and tensile loading curve before first cracking to find the slope. The UHPC sample gross area shall be used instead of the effective area to calculate the stress used in the elastic modulus calculation.